

Copyright
by
Brian Cuong Tieu
2008

**The Dissertation Committee for Brian Cuong Tieu certifies that this is
the approved version of the following dissertation:**

**Mechanism of local IL-6 production and its role in accelerating vascular
inflammation leading to aortic diseases**

Committee:

Allan R. Brasier, MD

Ronald G. Tilton, PhD

Steven A. Weinman, MD, PhD

Darrell H. Carney, PhD

Michael E. Boulton, PhD

Dianna M. Milewicz, MD, PhD

Dean, Graduate School

**Mechanism of local IL-6 production and its role in accelerating vascular
inflammation leading to aortic diseases**

by

Brian C. Tieu, BA

Dissertation

Presented to the Faculty of the Graduate School of

The University of Texas Medical Branch

in Partial Fulfillment

of the Requirements

for the Degree of

Doctor of Philosophy

The University of Texas Medical Branch

December 3, 2008

Dedication

This is dedicated to my parents Tom and Rose Tieu, who have constantly shown by example the value of hard work and reminded me daily to do my best; to my wife, Carolyn Cushing, MD, who has been by my side and made this a wonderful experience; to my family and friends for their unending care and motivation; and to my mentors Allan Brasier, MD and Ron Tilton, PhD for giving me an opportunity of a lifetime. Without their support and belief in me, I would not have been able to realize my dream. In addition, this is dedicated to my coworkers who have eagerly and pleasantly worked with me on my research and to the many people who have helped me along the way. To all of the people above, I owe them the greatest gratitude and utmost respect.

Acknowledgements

I would like to thank Dr. Allan Brasier, Dr. Ronald Tilton, and Dr. Adrian Recinos, III for their endless day-to-day supervision. Special thanks go to my committee members consisting of Dr. Allan Brasier, Dr. Ronald Tilton, Dr. Steven Weinman, Dr. Michael Boulton, Dr. Darrell Carney, and Dr. Dianna Milewicz (UTHSC-Houston) for their guidance over the years, support of the project, and helpful critique of this dissertation. Moreover, I would like to thank Mark Griffin and Warner Kaluarachchi from the UTMB Flow Cytometry Core for their assistance with flow cytometry; Linda Muehlberger and Kenneth Escobar from the UTMB Histopathology Core for help with histology; and Dr. Richard Hodge from the Synthetic Organic Chemistry Core for synthesizing Ang II. Thanks to Dr. Dongchuan Guo and Christina Papke from UTHSC-Houston for providing the human aortic dissection samples and IHC protocol. Finally, but certainly not least, I am extremely grateful for the unending assistance provided by Change Lee, Hong Sun, and Wanda LeJeune with the animal studies. Without their help and hard work, the research presented here would not be possible.

The following have supported the research presented here: The James W. McLaughlin Fellowship Fund (Brian C. Tieu, UTMB), NIEHS Predoctoral Fellowship T32ES007254 (Brian C. Tieu, UTMB), P50 HL083794 (Dr. Allan R. Brasier, UTMB), HL70925 (Dr. Allan R. Brasier, UTMB), DK079053 (Dr. Ronald G. Tilton, UTMB). Core laboratory support was from NIEHS grant P30 ES06676 (Dr. J. Halpert, UTMB) and BAA-HL-02-04 (Dr. A. Kurosky, UTMB).

Mechanism of local IL-6 production and its role in accelerating vascular inflammation leading to aortic diseases

Publication No. _____

Brian Cuong Tieu, PhD

The University of Texas Medical Branch, 2008

Supervisor: Allan R. Brasier, MD

Abstract: Vascular inflammation plays a significant role in aortic diseases and involves enhanced recruitment and local activation of circulating monocytes along with cytokine production, but the mechanisms responsible for these processes are unclear. The cytokine interleukin-6 (IL-6) is highly induced in aortic aneurysm and dissection and significantly increases the risk of aneurysm rupture and mortality due to cardiovascular diseases; however, it remains unknown where and how IL-6 is produced in the vascular wall and how it contributes to disease exacerbation. Using an Ang II-infusion mouse model, we found that 6 days of subcutaneous Ang II infusion into aged C57BL/6J mice induced aortic IL-6 and MCP-1 predominantly in the tunica adventitia. Likewise, IL-6 was detected mostly in the adventitia of sporadic aortic dissections in humans. There was concomitant macrophage recruitment, adventitial expansion, and development of thoracic and suprarenal aortic aneurysms and dissections in treated wild-type mice. In contrast, no dissections were produced with infusion into IL-6^{-/-} or CCR2^{-/-} mice over the same

time period along with significantly reduced inductions of aortic IL-6 and MCP-1. Using flow cytometric quantification of aortic cellular constituents, we found that Ang II induced CCR2⁺ macrophage accumulation of a specific CD14^{hi}CD11b^{hi}F4/80⁻ phenotype selectively in aortic dissections and not in aortas from IL-6^{-/-} mice, which were CD14^{lo}CD11b^{lo} F4/80⁺. Adoptive transfer of CCR2^{+/+} monocytes into CCR2^{-/-} mice resulted in selective monocyte uptake into the thoracic and suprarenal aorta with restoration of IL-6 and MCP-1 secretion and increased incidence of dissection. To elucidate a source of IL-6, we demonstrated that aortic adventitial fibroblasts (AoAFs) highly produce IL-6 and MCP-1 and Ang II treatment increased their expression. Ang II and monocytes stimulated AoAF proliferation also. In addition, coculture of monocytes and AoAFs strongly potentiated MCP-1 and IL-6, which differentiated monocytes to macrophages and up-regulated CD14 and CD11b as well as induced MCP-1 and MMP-9 expression. These results suggest that AoAFs are a source of IL-6 and that a leukocyte-fibroblast interaction in the aortic adventitia potentiates its production, leading to promotion of local monocyte recruitment and activation, thereby accelerating vascular inflammation, ECM remodeling and aortic destabilization.

Table of Contents

List of Tables	x
List of Figures	xi
List of Illustrations	xv
Chapter 1. Aortic Aneurysm, Dissection, and Vascular Inflammation	01
Aortic Aneurysm and Dissection	02
Vascular Inflammation in Aortic Aneurysm and Dissection	08
Inflammation in AAA	09
Inflammation in TAAD	12
Ang II and its Role in Vascular Inflammation	14
Role of MCP-1/CCR2 in Vascular Inflammation	21
Role of IL-6 in Vascular Inflammation	24
Adventitial Fibroblasts	29
Chapter 2. A Mouse Model of Vascular Inflammation Leading to Aortic Dissection	33
Ang II Infusion in Aged Wild-Type Mice Induces Thoracic and Abdominal Aortic Dissections	34
Cytokine and Chemokine Secretion Potentiated with Ang II infusion	40
Chapter 3. Aortic Macrophages	46
Identification of Aortic Macrophages	47
Aortic Macrophages in Sham- and Ang II-Treated Wild-Type Mice	53
Chapter 4. Role of CCR2 ⁺ Monocytes/Macrophages in Potentiating Vascular Inflammation and Aortic Dissection	60
CCR2 ^{-/-} Mice Develop Blunted Responses to Ang II Treatment	61
Adoptive Transfer of CCR2 ^{+/+} Monocytes Restores Vascular Inflammation and Aortic Dissection	65
Chapter 5. Role of IL-6 on MCP-1 Induction and Macrophage Differentiation	78
Blunted Aortic MCP-1 Secretion in IL-6 ^{-/-} vs. Wild-Type Mice in Response to Ang II	79

IL-6 ^{-/-} Mice Have Reduced Numbers of Aortic Macrophages with Different Phenotypes Compared to Wild-Type Mice.....	80
IL-6 Signaling is Active in Aortic Macrophages from Treated Wild-Type Mice, but Not in IL-6 ^{-/-} Mice	83
Chapter 6. Aortic Adventitial Fibroblasts and Their Interaction with Monocytes	88
Aortic Adventitial Fibroblasts Produce a Variety of Cytokines Including IL-6 and MCP-1	89
Ang II Stimulation Increases IL-6 and MCP-1 mRNA and Proliferation of Adventitial Fibroblasts.....	90
MCP-1 from AoAFs can Recruit Monocytes and Monocytes can Induce Proliferation of AoAFs	93
Coculture of Monocytes and AoAFs Induces IL-6 and MCP-1 as well as Monocyte to Macrophage Differentiation	98
Macrophage Differentiation and MCP-1 and MMP-9 Production is Dependent on IL-6	104
Chapter 7. Conclusion and Future Directions	114
Conclusion	114
Future Directions	124
Appendix A: Methods.....	130
Appendix B: Table 1. Aortic Macrophages.....	140
Appendix C: Table 2. Cytokines Secreted from Human AoAFs and Monocytes	141
References.....	142
Vita	179

List of Tables

Table 1:	Aortic Macrophages.....	140
Table 2:	Cytokines Secreted from Human AoAFs and Monocytes.....	141

List of Figures

Figure 1:	Sham- and Ang II-treated aorta with dissection	34
Figure 2:	Dissection in the suprarenal abdominal aorta	35
Figure 3:	Dissections in the thoracic and abdominal aorta.....	35
Figure 4:	Thoracic aorta from Ang II-infused mouse appeared thickened	36
Figure 5:	Adventitial remodeling in abdominal aorta with Ang II infusion.....	37
Figure 6:	Abdominal aortic cross-section after sham-treatment	37
Figure 7:	Abdominal aortic cross-section of a mouse with adventitial hematoma	38
Figure 8:	Dissection through the tunicas intima and media	39
Figure 9:	Macrophages in the aorta of mice	40
Figure 10:	IL-6 in aorta of mice	41
Figure 11:	MCP-1 in the aorta of mice.....	42
Figure 12:	Aortic adventitial fibroblasts in the aorta of mice	42
Figure 13:	Secreted aortic IL-6 levels from wild-type mice	43
Figure 14:	Secreted aortic MCP-1 levels from wild-type mice.....	44
Figure 15:	IL-6 in human type A aortic dissection.....	45
Figure 16:	CD14 ⁺ cells in the aorta	49
Figure 17:	CD14 ⁺ CD11b ⁺ and CD14 ⁺ CD11b ⁻ cell populations	49
Figure 18:	CD14 ⁺ CD11b ⁺ cells are F4/80 macrophages.....	50
Figure 19:	CD14 ⁺ CD11b ⁻ cells are not macrophages.....	50
Figure 20:	Backgating of CD14 ⁺ CD11b ⁺ F4/80 ⁺ cells.....	51
Figure 21:	Aortic macrophages from a sham-treated mouse.....	53
Figure 22:	Aortic macrophages from an Ang II-treated mouse	54

Figure 23:	Aortic macrophages from an aortic dissection.....	54
Figure 24:	Peripheral blood monocytes.....	55
Figure 25:	Peripheral blood monocytes compared to macrophages.....	56
Figure 26:	Comparison of expression levels of surface CD14, CD11b, and F4/80 on aortic macrophages	57
Figure 27:	Aortic macrophages are CCR2 ⁺	58
Figure 28:	Secreted aortic IL-6 levels from CCR2 ^{-/-} mice	62
Figure 29:	Secreted aortic MCP-1 levels from CCR2 ^{-/-} mice	63
Figure 30:	Aortic macrophages from sham-treated CCR2 ^{-/-} mice	63
Figure 31:	Aortic macrophages from Ang II-infused CCR2 ^{-/-} mice	64
Figure 32:	DiR800 and PKH26 labeled monocytes	67
Figure 33:	LI-COR imaging of CCR2 ^{-/-} mice injected with labeled wild-type monocytes	68
Figure 34:	<i>Ex vivo</i> imaging of abdominal contents on LI-COR Odyssey.....	69
Figure 35:	Imaging of DiR800-labeled CCR2 ^{+/+} monocytes in the aorta of CCR2 ^{-/-} mice.....	70
Figure 36:	Imaging of DiR800-labeled CCR2 ^{-/-} monocytes in the aorta of CCR2 ^{-/-} mice.....	71
Figure 37:	Secreted aortic IL-6 and MCP-1 from adoptive transfer experiments	73
Figure 38:	Staining for IL-6, MCP-1, and AoAF staining in the ascending aorta of Ang II-treated CCR2 ^{-/-} injected with wild-type monocytes.....	74
Figure 39:	Wild-type macrophages in the ascending aorta of Ang II- treated CCR2 ^{-/-} mice.....	75
Figure 40:	Aorta of CCR2 ^{-/-} mice receiving wild-type monocytes	76
Figure 41:	Secreted aortic MCP-1 levels from IL-6 ^{-/-} mice	80

Figure 42:	Aortic macrophages from sham-treated IL-6 ^{-/-} mice	81
Figure 43:	Aortic macrophages from Ang II-treated IL-6 ^{-/-} mice	81
Figure 44:	Comparison of CD14, CD11b, and F4/80 expression on aortic macrophages between treated IL-6 ^{-/-} and wild-type mice.....	83
Figure 45:	IL-6 signaling is not active in resident aortic macrophages of sham-treated wild-type mice.....	85
Figure 46:	IL-6 signaling is active in recruited macrophages of Ang II-infused wild-type mice	85
Figure 47:	IL-6 signaling is not active in resident aortic macrophages of sham-treated IL-6 ^{-/-} mice	86
Figure 48:	IL-6 signaling is not active in resident aortic macrophages of Ang II-infused IL-6 ^{-/-} mice	86
Figure 49:	ISH for IL-6 and MCP-1 mRNA in AoAFs.....	90
Figure 50:	Ang II induced IL-6 mRNA in AoAFs	91
Figure 51:	Ang II induced MCP-1 mRNA in AoAFs	91
Figure 52:	Ang II induced ³ H-Thymidine incorporation by AoAFs	92
Figure 53:	Ang II induced AoAF proliferation	93
Figure 54:	AoAFs can attract monocytes	94
Figure 55:	Quantification of migrated monocytes to AoAF-conditioned medium	94
Figure 56:	MCP-1 from AoAFs attracts monocytes.....	95
Figure 57:	PKH26 labeled AoAFs	96
Figure 58:	No transfer of PKH26 dye to THP-1 monocytes	97
Figure 59:	AoAFs counted by flow cytometry.....	97
Figure 60:	Quantification of AoAFs in monoculture vs. coculture.....	98

Figure 61: Concentration of IL-6 in monocultures and coculture of THP-1 monocytes and human AoAFs	100
Figure 62: THP-1 monocytes differentiated into macrophages	100
Figure 63: Comparison of surface CD14 expression on THP-1 cells in monoculture and derived macrophages.....	101
Figure 64: THP-1 cells differentiated into CD11c ⁺ CD11b ⁺ macrophages in coculture.....	102
Figure 65: Induction of IL-6 and MCP-1 levels in coculture with primary monocytes	103
Figure 66: Representative picture of iDC and macrophage	104
Figure 67: HLA-DR gating of primary monocytes/macrophages.....	105
Figure 68: IL-6 regulates the expression of surface CD14.....	106
Figure 69: IL-6 regulates the expression of surface CD11b.....	107
Figure 70: Comparison of surface CD14 and CD11b expression with inhibition of IL-6 signaling.....	108
Figure 71: IL-6 regulates surface expression of CD11b on THP-1 monocytes	109
Figure 72: Inhibition of IL-6 reduces MCP-1 levels in coculture.....	110
Figure 73: IL-6 controls the expression of MMP-9.....	111
Figure 74: IL-6 stimulation of THP-1 monocytes induces MCP-1 mRNA and MCP-1 protein	112

List of Illustrations

Illustration 1:	Normal aorta, aneurysm, and aortic dissection.....	08
Illustration 2:	IL-6-differentiated macrophages	118
Illustration 3:	Acceleration of vascular inflammation leading to aneurysm and dissection in response to Ang II.....	123

Chapter 1: Aortic Aneurysm, Dissection, and Vascular Inflammation

The aorta is a large, elastic artery of approximately 40 cm in length in adult humans that originates above the aortic valve in the heart and extends to the bifurcation of the two common iliac arteries (1). Its main function is to deliver the oxygen and nutrients in blood to the entire body via smaller branching arteries. It is the biggest and thickest artery in the human body.

The aorta consists of three layers, the tunica intima, tunica media, and tunica adventitia. The tunica intima consists of a thin, monolayer of endothelial cells that line the lumen of the aorta. The tunica media is the middle layer and consists of sheets of elastic tissue, the elastic lamellae, and vascular smooth muscle cells (VSMCs); it is the thickest layer. The media is separated from the intima by the internal elastic lamina. The outermost layer is the tunica adventitia, and it has long been considered just a support structure. It contains connective tissue, resident aortic adventitial fibroblasts (AoAF), nerve endings, and small vessels that nourish the aortic wall, the vasa vasorum (2;3). This layer is separated from the media by the external elastic lamina.

There are four main regions of the aorta; the ascending aorta, aortic arch, descending aorta, and abdominal aorta together create an appearance of a hook that gradually tapers toward the distal end. The ascending aorta is about 3 cm wide, 5 cm long, and contains the aortic root, which is composed of the three sinuses of Valsalva (also known as aortic sinuses, which are anatomic dilatations above the aortic valves), at its proximal end. It ends at the aortic arch, the bend in the hook, where the brachiocephalic arteries branch off. The aortic segment distal to those arteries is the descending aorta. It is about 2.5 cm in diameter and 20 cm long, ending at the diaphragm. Beyond the diaphragm is the abdominal aorta, which is 2 cm wide and 15 cm long. The ascending

and descending aortas are located in the thorax while the abdominal aorta, as its name implies, is located in the abdomen.

There are several diseases that affect the aorta. Takayasu's arteritis is a chronic inflammatory disease that causes fibrous thickening of the aortic arch and occlusion of the vessels arising from the arch leading to ocular disturbances and weakening of the pulses in the upper extremities(1;2). It is predominantly seen in women less than 40 years of age in Asia and Africa and its etiology is unknown. Giant cell arteritis is another disease that can affect the aorta; 15 % of all cases have disease in the aorta (giant cell aortitis) or branches off of the aortic arch (1). Unlike Takayasu's arteritis, it is an acute and chronic inflammatory disease, more common, and affects older individuals (2). Its cause is also unknown. These two diseases, however, account for a small portion of aortic diseases. The major diseases affecting the aorta are aortic aneurysm and aortic dissection and together, they account for 16,000 deaths annually in the United States (4;5).

AORTIC ANEURYSM AND DISSECTION

An aortic aneurysm is a localized, permanent dilatation of the aorta that can be fusiform or saccular in shape. A fusiform aneurysm is a symmetrical dilatation of the entire circumference of the aorta while a saccular aneurysm involves dilatation of only a portion of the vessel wall (2). Moreover, aneurysms can be described as either true or false. A true aneurysm is bound by all three layers of the aortic wall, which are usually attenuated due to the dilatation. A false aneurysm (also called pseudoaneurysm) is a blood-filled pseudo-vascular space or hematoma that communicates with the intravascular space through a breach in the vessel wall and is confined by only outer arterial layers or perivascular tissue (2). False aneurysms can develop after trauma to the thorax, a transmural rupture of the vascular wall that is contained, or dehiscence of

vessels such as those that may occur after vascular grafting. In addition, aneurysms usually occur in two areas, the abdominal aorta, also known as abdominal aortic aneurysms (AAAs), and the thoracic aorta, also known as thoracic aortic aneurysms (TAAs). Although rare, aneurysms can also develop in both the thorax and abdomen, called thoracoabdominal aneurysms.

AAAs occur three-times more frequently than TAAs and affect men more than women, with a ratio of 6:1, respectively (6). It has a prevalence of about 3 %-10 % in people older than 50 years (1;6). The most common site for AAA is in the infrarenal aorta, and atherosclerosis has long been considered to be its cause (1;2;7). In terms of risk factors for AAA, smoking is the strongest, followed by increasing age, hypertension, and hyperlipidemia (1;8). There is also a strong genetic predisposition to AAA (discussed below). The majority of AAA cases are asymptomatic, but when symptoms do appear, lower back pain that is usually gnawing and steady, lasting several hours to days, is the most common complaint (1). Definitive diagnosis is made by abdominal ultrasound or computed tomography (CT), with ultrasound being the most cost-effective (6). Treatment can consist of medical management of blood pressure with β -blockers, but that has been shown to not reduce the rate of expansion (1). When aneurysms increase in size to greater than 5 cm in diameter, their risk of rupture, which is the most feared consequence because it carries an 80 % mortality, increases to about 5 to 10 % per year (1). Therefore, it is recommended that those greater than 5 cm be repaired surgically by placement of prosthetic tube grafts (1). In addition, it is also worth noting that there are different variants of AAA. Inflammatory abdominal aneurysm (IAA) is one that has pronounced inflammatory infiltrates of macrophages and B- and T-lymphocytes along with fibrosis in the adventitia due to proliferation and differentiation of adventitial fibroblasts into myofibroblasts (9;10). Moreover, mycotic abdominal aneurysm is

another variant that results from an infection, particularly bacteremia due to *Salmonella gastroenteritis* (2).

Thoracic aneurysms are most commonly found in the ascending aorta, accounting for about 50 % of all cases, and the second most frequent site is the descending aorta, 40 % of all cases (6). Ten % occur at the arch. The age of onset is 65 years, 10 years younger than for AAA, and men are not greatly more affected than women with a 1.7:1 ratio, respectively (6). Twenty % of patients with TAAs have a first-degree relative with the disease and thus there can be a strong genetic component (5). TAAs are commonly due to *cystic medial necrosis* or medial degeneration with elastin degradation, smooth muscle cell apoptosis in the tunica media, and increased accumulation of proteoglycans instead of atherosclerosis (5). Compared to normal aortas, TAAs have thicker intima and adventitia and a thinner the media (5). Patients with TAAs have chest pain and vascular complications like aortic insufficiency or symptoms resulting from compression of adjacent tissue such as the lungs causing respiratory problems such as coughing and or compression of the esophagus to cause dysphagia. In diagnosing TAAs, a chest x-ray can reveal widening of the mediastinal silhouette and enlargement of the aortic knob while CT is good for detecting and monitoring the expansion of the aneurysm (1). Echocardiography is another imaging modality useful for detecting TAAs at the root and ascending aorta, the two common areas for aneurysms in patients with Marfan syndrome. Surgical repair is recommended in those patients with an ascending aortic aneurysm greater than 5.5 cm in diameter or greater than 5 cm in patients with Marfan or a bicuspid aortic value since they have high risk of rupture (6). It is also worth noting that patients infected with syphilis in the tertiary stage can develop aneurysm and dissection in the thorax.

Aortic dissection occurs when a tear in the wall of the aorta allows for blood flow into a layer of the aorta, usually in the media, resulting in formation of a false lumen that can communicate with the true lumen (1). Most cases usually start with a transverse or oblique tear in the intima of unknown cause, but medial degeneration is the most common predisposing factor (1). Sometimes dilatation is not seen. The tear is frequently within 10 cm of the aortic valve, and the blood pressure then rips the tissue of the weakened media apart (2). The tear occurs in the ascending aorta 66 % of the time and in the descending aorta 33 % (1). Aortic dissection can occur in the abdominal aorta also (11). There are two classification systems for aortic dissections based on the anatomy of the dissection. In the Stanford classification system, dissections are divided into Type A, which indicates involvement in the ascending aorta, or Type B, which indicates involvement of only the descending aorta only (12). The DeBakey system categorizes dissections into three types based on the location of the original intimal tear and the extent of disease (12). DeBakey Type I describes dissections originating in the ascending aorta that has affected both the ascending and descending aortas while Type II describes those that originate and are confined to the ascending aorta. Type II describes dissections originating in the descending aorta. These tears can extend proximally and or distally away from the heart, creating the false lumen (2). Aortic dissection is strongly associated with hypertension (70-90 % of patients) and connective tissue disorders like Marfan syndrome, which accounts for 5-9 % of all cases (1;2;13). It occurs twice as frequently in men than women, and the highest incidence is seen in aged individuals between 50-70 years old, except in patients with Marfan syndrome who develop it at a much younger age (25 years) (2;13). Dissections can occur in females during pregnancy, usually in the third trimester or early postpartum period (13). Other causes of, or predisposing factors for, aortic dissection are bicuspid aortic valve, chest trauma, iatrogenic trauma during

cardiac catheterization or angioplasty, open-heart surgery for aortic valve replacement, and enlargement of aortic aneurysms, particularly thoracic aneurysms in the absence of prophylactic surgical repair (1;12;14). Ninety-six % of patients with aortic dissection present with severe, sudden onset chest pain described as tearing or sharp stabbing in acute dissection (less than 2 weeks duration) (1). Tears in ascending aortas produce anterior chest pain while tears in the descending aorta produces intrascapular pain (11). The pain may migrate as the dissection extends down the aorta. The main cause of death is rupture of the dissection, leading to massive blood loss and consequences like cardiac tamponade (1;2). This risk increases over time in untreated dissections (11). Diagnosis of dissection is done with imaging modalities. Aortic angiography with contrast used to be the gold standard, but newer modalities like transesophageal echocardiography are being used increasingly due to its increased sensitivity, specificity, and rapidity (2;13). Since the risk of death is the highest in the first few hours after the dissection begins, immediate treatment to control blood pressure with nitroprusside and β -blockers or calcium channel blockers is generally started (13). If the dissection is located in the ascending aorta, immediate surgical repair is recommended. In uncomplicated, stable Type B aortic dissections, long-term medical management is preferred over surgery (13). A variant of aortic dissection called intramural hematoma is worth noting also. It arises from bleeding from the vasa vasorum causing a hematoma in the media and not due to an intimal tear; nevertheless, it is generally treated the same way as regular aortic dissections (1).

Progressive enlargement of type A TAAs can lead to aortic dissections (TAAD). Some researchers state that TAAs and thoracic aortic dissections are one disease (personal communication with Dr. Dianne Milewicz). TAADs can be inherited with genetic syndromes such as Marfan syndrome, Loeys-Dietz syndrome, Ehlers-Danlos, and

filamin A mutations or in isolation in an autosomal dominant manner (15). Familial TAAD is caused by mutations in the FBN1, TGFBR2, TGFBR1, MYH11, and ACTA2 genes and are responsible for 20 % of TAAD (15-17). The majority of cases are sporadic and highly associated with hypertension, weight lifting, and bicuspid aortic valve (15). However, the identification of those genes above and knowledge of the impact of hypertension on vascular wall suggests that overactive TGF- β signaling and or activation of stress and stretch pathways in smooth muscle cells may play a major role in the pathogenesis of TAADs in general (15). Of interest to the research presented here is the effect of the mutation of smooth muscle cell specific myosin heavy chain gene (MYH11) in patients with TAAD associated with patent ductus arteriosus (PDA). Smooth muscle cells from patients with this mutation and TAAD had increased expression of angiotensin-converting enzyme (ACE) and macrophage inflammatory protein-1 α and - β (MIP-1 α and MIP-1 β) (16). ACE cleaves angiotensin I to angiotensin II (Ang II), a peptide hormone that causes vasoconstriction of arteries and inflammatory signaling (18), and MIP-1 α and MIP-1 β are classically macrophage derived pro-inflammatory chemokines (19). Both of these genes and their products can induce, accelerate, and maintain inflammation and suggest that inflammation in the vessel wall plays an important role in TAADs.

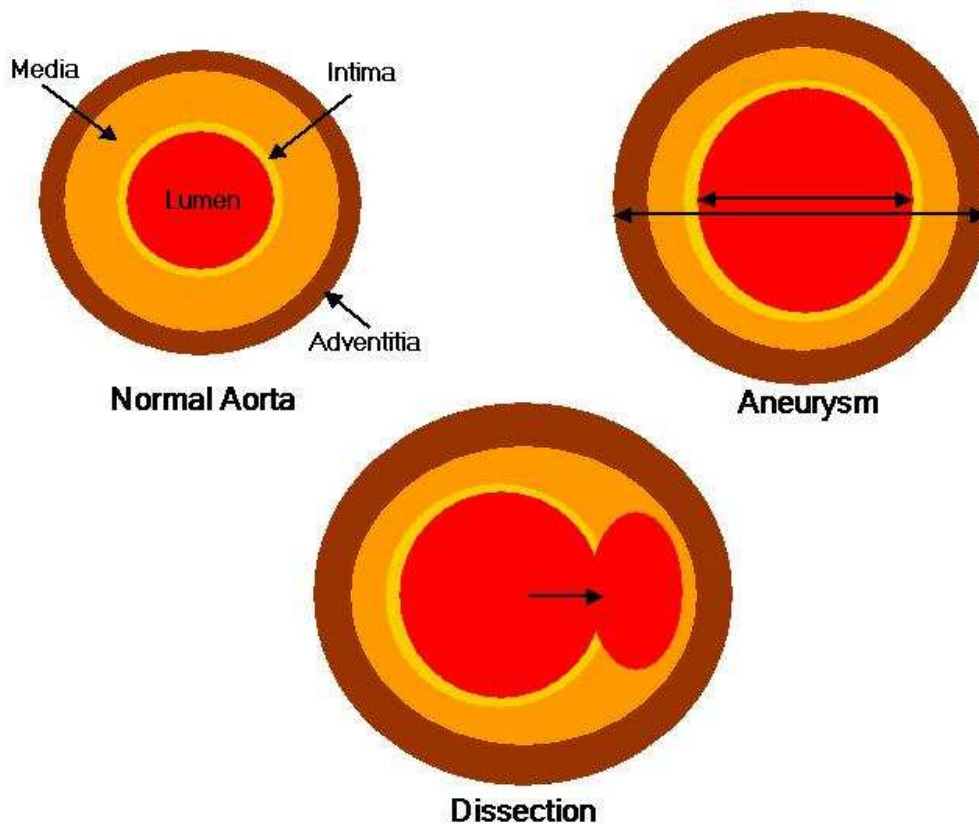


Illustration 1. Normal aorta, aneurysm, and aortic dissection.

VASCULAR INFLAMMATION IN AORTIC ANEURYSM AND DISSECTION

Vascular inflammation is a complex, multi-step process with the distinguishing characteristics of significant immune cell recruitment into the vessel wall and release of cytokines and proteins from the recruited leukocytes and native cells leading to pathological remodeling of the vascular wall. These processes have been well studied and have gained tremendous attention in atherosclerosis. In fact, atherosclerosis is now considered an inflammatory disease (20). The study of aortic aneurysms has not gained as much attention, but it also is now considered to be an immune disease (6;7). The vascular inflammatory process is well studied in AAA, but not in thoracic aneurysm

because TAs have long been considered a non-inflammatory disease of medial degeneration (5). However, recent studies have detected important signs of inflammation in TA and TAAD (4;21). Therefore, it is thought that vascular inflammation is an underlying component in common in these cardiovascular diseases and that they share similar features as well as some differences.

Inflammation in AAA

In AAA there is significant transmural infiltration of inflammatory cells (22;23). Infiltration is thought to occur either through the vasa vasorum in the adventitia or the intima into the media. Inflammatory cells are usually seen in the outer media and adventitia in aortic sections from patients with AAA (22;23). T- lymphocytes, B-lymphocytes/plasma cells, macrophages, neutrophils, natural killer cell (NK cells), and mast cells have all been detected in these regions and have been shown to contribute to AAA formation by causing destruction of extracellular matrix and apoptosis of VSMCs (24-27). The majority of inflammatory infiltrates are activated CD4⁺ T-cells (approximately 50 % or greater) and have a memory cell phenotype expressing a distinct pattern of cell surface markers including CD54, CD31, CD11a, CD27, CD44, CD95, and CD27 (27-32). Whether T cells are required for aneurysm development is a controversy since different experimental models produce conflicting results. In the elastase-induced AAA mouse model, larger aneurysms develop in CD4-deficient mice, suggesting that CD4⁺ T cells are not required for aneurysm formation (29); however, in the calcium chloride-induced mouse model of AAA, the absence of CD4⁺ T cells prevents aneurysms (33). B-cells or their antibody-producing form, plasma cells, are the second most abundant cell type found in AAA tissue, composing from 25-40 % of the infiltrates (27;30;32;34). Along with T cells, B-cells are thought to be important in a hypothesized autoimmune mechanism of AAA formation, where autoantibodies of the immunoglobulin

G (IgG) isotype, produced by plasma cells, react with aortic proteins normally present like aortic aneurysm-associated protein-40 (AAAP-40), elastin and elastin fragments, type I and III collagen, and oxidized low-density lipoprotein (ox-LDL) (6;35;36). NK cells are present in the media and adventitia and account for about 7 % of the infiltrates (32;37) Polymorphonuclear (PMN) cells, also known as neutrophils, have also been detected in AAA tissue, and in the elastase-infusion experimental model, L-Selectin deficient mice and infusion of anti-PMN antibodies (25;38). Recently, mast cells were found in the adventitia of aneurysms, and it was shown that the number of mast cells correlated positively with aneurysm diameter (26). Rats deficient in mast cells and treatment with the inhibitor of mast cell degranulation, tranilast, in the angiotensin II (Ang II)-infusion model of abdominal aneurysm in a hyperlipidemia background showed attenuated aneurysm formation (26). Another study using mast cell-deficient mice infused with elastase or subjected to aortic application of CaCl₂ found similar results (39). However, both of these studies have confounding factors that should not be overlooked and not all studies have detected PMNs in AAA (31). The other cell of interest is the macrophage. They have been shown to account for at least 2 % of all infiltrates in human AAA, but certainly much more in IAAA and experimental models (30;32;39). Most of these cells are located in the adventitia, particularly at the adventitia-media border, and also throughout the media (30;32;39). Interestingly, they are also seen in close proximity to T cells (30;36). Macrophages have long been known to contribute to aneurysm because they are the principle producers of the matrix metalloproteinases (MMPs), which degrade extracellular matrix proteins, found in AAA, particularly MMP-9 (also known as gelatinase) (40-42). Animal studies have shown that MMP-9 from monocytes and macrophages is necessary to induce AAA in response to CaCl₂ treatment (43;44). Macrophages are also known to secrete proinflammatory cytokines and produce

prostaglandin derivatives, leukotrienes, and reactive oxygen species (45-49). Some of their other roles in AAA may be to secrete chemokines to help recruit T- and B-cells along with other leukocytes and to present antigens to T cells (30).

Like the mix of inflammatory infiltrates, the expression of cytokines, chemokines, and growth factors are upregulated in AAA, but there is no clear pattern suggesting either a predominant Th1- or Th2-type response. The Th1-type response is also known as cellular immunity and results from the activity of activated CD4+ T-cells, CD8+ cytotoxic T-cells, and macrophages. It is associated with increases in the following cytokines: IL-1, IL-2, IL-12, IL-15, TNF- α , and IFN- γ and results in the induction of cell death and tissue destruction. The Th2-type response leading to humoral immunity results from the activity of activated CD4+ T-cells, B-cells, and plasma cells. It is associated with increases in IL-4, IL-10, and IL-5 and results in the production of antibodies. Some labs have detected Th1-type cytokines and not Th2-type cytokines and vice versa, while others have detected the presence of both types in AAA tissue. This discrepancy might be due to confounding factors like atherosclerosis, which is commonly found associated with AAA (2). IL-6 and IFN- γ , but not IL-2 or IL-4 have been reported to be increased in blood and aortic tissue of patients with atherosclerotic abdominal aneurysm (50). Increases in circulating IFN- γ is correlated with aneurysm size (51). Likewise, high levels of IFN- γ transcripts have been detected in AAA tissue (52;53). Moreover, mice lacking IFN- γ have been shown to be resistant to CaCl₂-induced aneurysms (33). In addition, TNF- α is also increased in AAA (32;45). On the other hand, Th2 cytokines have also been shown to be the predominant ones in AAA (24;54;55). IL-4, IL-5, and IL-10 were reported to be increased in AAA tissue as detected by western blotting compared to normal aortic tissue, and the receptor for IFN- γ was found to be absent despite the presence of that cytokine (54;55). Also, Schonbeck et al. could only detect

IL-2 or IL-15 weakly and not mature IFN- γ , IL-12, or IL-18 in AAA (54). Contrary to the findings mentioned above on IFN- γ , Shimizu et al. found that histocompatibility-mismatched aortas transplanted into IFN- γ receptor-deficient mice recipients developed large AAA with a strong immune response dominated by IL-4 and inhibition of the IL-4 with neutralizing antibodies prevented AAA formation (56). That suggested that IFN- γ prevents AAA formation while IL-4 causes it. Furthermore, there is a study that detected both Th1- and Th2-type cytokines in pure AAA samples that contained no contamination by atherosclerosis. IL-2, IFN- γ , TNF- α , IL-1 α , and IL-1 β transcripts, which are all Th1 gene, were present in addition to IL-4, IL-10, and IL-13 transcripts, which are Th2 genes. Out of that list, IL-2, IFN- γ , TNF- α , IL-1 β , IL-4, and IL-13 cytokines were detectable by multiplex ELISA. In addition, markers of general inflammation IL-6, MCP-1, MIP-1 β , TGF- β , IL-8 and MIF mRNA were detected. IL-6, MCP-1, MIP-1 β , G-CSF, GM-CSF, IL-7, IL-8, IL-12, and IL-17 proteins were measurable in AAA as well (34). Expression of these genes and their protein products were higher in AAA tissue than equivalent atherosclerotic aortic tissue. Koch et al. also saw enhanced expression of IL-8 and MCP-1 in human AAA (57).

Inflammation in TAAD

The inflammation occurring in TAAD has not been as well characterized mainly because these diseases have long been considered to have non-inflammatory lesions. Only recently has the inflammation been investigated. Similarly to AAA, significant increases in CD4⁺ and CD8⁺ T-cells were observed in TAAD aortas in the media and adventitia compared to control aortas (4;21). Some of these cells in the media, between smooth muscle cell layers, were actually flattened in shape and did not look like typical T cells (4). T-cells were the predominant cell type in the adventitia and appeared to surround the vasa vasorum (4;21). CD68⁺ Macrophages were the next most abundant

cell type detected and were found mostly in the media, being the predominant infiltrate type there (4;21). CD20⁺ B-cells were also detected in the adventitia in TAADs (21). Analysis of transcripts of cytokines from TAADs suggests that Th1-type cytokines predominate. mRNA levels of IFN- γ and IFN- γ -inducible chemokines IP-10 and Mig were significantly higher in TAAD aortas than control aortas while mRNA levels of Th2-type cytokines like IL-4, IL-5, and IL-13 were undetectable (21). The level of IFN- γ actually correlated with increased aneurysm size, increased intimal thickness, and decreased extracellular matrix proteins. In addition, RANTES and MIP-1 β as well as expression of CXCR3, a receptor for Mig and IP-10 expressed on T-cells, were increased in TAADS compared to non-aneurismal aortas (21). TAAs are also a major source of circulating IL-6; two reports by Dawson et al. actually show that TAAs produced more IL-6 than AAAs and control aortas (58;59). Moreover, apoptosis of SMCs was observed in the media of TAADs and that the T-cells expressed FasL, suggesting that T-cells were stimulating smooth muscle cell death in a Fas-FasL pathway (4).

Although AAA and TAAD are mostly like distinct diseases, there might be a possibility that they may share some common pathophysiological features including inflammation. The discrepancy between the inflammation seen between AAA and TAAD might reflect variations in sampling of patient tissue at different clinical stages, different human populations, and low power due to small patient numbers. It is possible that both of these diseases might start out as a Th1 response and then progress into a Th2 response or vice versa. Therefore, a relevant animal model of aneurysm and dissection is needed to study the pathogenesis of these diseases at fixed points in time. Several popular models exist to study abdominal aneurysms such as the elastase-perfusion and CaCl₂ treatment models briefly mentioned above. Although both models induce inflammatory lesions in the infrarenal aorta, both methods require very invasive and

artificial application of foreign substances to induce aneurysms. Thus, a less invasive, more physiologically relevant method would be better. Ang II infusion into hyperlipidemic or aged WT¹ mice would be a very good model to study aneurysm formation and vascular inflammation based on work supporting the relevance of Ang II to AAA and TAA/PDA. It has been shown that inhibition of angiotensin II binding to its receptor prevents ascending aortic aneurysm in a mouse model of Marfan syndrome (60) and that ACE inhibitors reduce aortic stiffness and aortic root dilatation in Marfan patients (61-63). Moreover, the angiotensin II type 1 receptor (AGTR1) 1166C allele, thought to exaggerate responses to Ang II, has been shown to be significantly associated with AAA (64). Furthermore, increased ACE and chymase enzymes with greater Ang II formation has been detected in aneurysmal aorta compared to normal (65-67), and angiotensin II type 1 receptor blocker (ARBs) has been shown to reduce oxidative stress in TAAs (68). Interestingly, Ang II infusion in mice produces both dilatory abdominal aneurysm formation and aortic dissection in different genetic backgrounds.

Ang II and its Role in Vascular Inflammation

Angiotensin II is a naturally occurring octapeptide hormone circulating in plasma (69). Its precursor is angiotensin I (Ang I), which comes from the cleavage of angiotensinogen by renin, and Ang I is converted to Ang II by ACE or a variety of other enzymes like cathepsin G, chymostatin-sensitive Ang-II-generating enzyme, and chymase found locally in different tissues (69). Ang II is the main effector hormone of the Renin-Angiotensin System (RAS) and is known to directly induce vasoconstriction to increase blood pressure, regulate water balance directly via stimulating thirst and modulating renal sodium and water reabsorption or indirectly via stimulating aldosterone release, and induce inflammatory cellular signaling through binding to the AT1 receptor.

¹ WT is the abbreviation for wild-type

Binding to AT2 seems to produce opposite effects (70;71). AT1 and AT2 are cell surface, G protein-coupled receptors capable of activating different intracellular signaling pathways. The AT1 receptor is the predominantly expressed angiotensin receptor in cardiovascular tissue and is upregulated in atherosclerosis while the AT2 receptor comprises only about 10 % of all angiotensin receptors (72). Both receptors have been found on endothelial cells, VSMCs, and macrophages to name a few.

As mentioned briefly above, production of Ang II can occur locally in tissue. All components of RAS or their equivalents are found in many tissues including the heart, vasculature, adipose tissue, and others (73-76). A variety of vascular tissues, particularly periaortic adipose tissue, fibroblastic cells, and VSMCs, can produce angiotensinogen (73;77;78). Also, renin-like enzymes such as cathepsin D have been identified on VSMCs and macrophages (79;80). In atherosclerotic plaques, ACE expression has been detected in macrophages, T lymphocytes, VSMCs, and endothelial cells (81-83). It has also been shown that during differentiation of monocytes to macrophages *in vitro*, angiotensin II receptors, ACE, and production of Ang II are all upregulated (84). Moreover, chymase and cathepsin G are capable of producing Ang II similarly to ACE in mast cells and monocytes, respectively (85;86). Thus, not only can Ang II come from the circulation, but also it can be made abundantly at the site of disease in the vessel wall where it can have autocrine and paracrine effects.

Ang II can stimulate inflammatory responses in the vessel wall including induction of reactive oxygen species leading to endothelial dysfunction (defined as impairment of acetylcholine-induced vasorelaxation with increased adhesiveness to leukocytes), leukocyte recruitment and adhesion molecules, LDL oxidation and uptake, inflammatory cytokine/chemokine expression, hypertrophy and proliferation of vascular cells such as VSMCs and adventitial fibroblasts, and even apoptosis (18;72;87;88). As

seen from this list, the roles of Ang II in atherosclerosis have been well studied. Many of them may be relevant to aneurysms since atherosclerosis is seen in many patients with AAA and features of vascular inflammation like leukocyte recruitment into the tunica adventitia are common to both diseases.

Ang II is known to stimulate NADH and NADPH oxidases in endothelial cells, VSMCs, and macrophages (89-92). *In vivo*, Ang II stimulates reactive oxygen species (ROS) production from NADPH oxidase primarily in endothelial cells and adventitial fibroblasts leading to VSMC growth (93). Ros production in the media has also been detected (90). The ROS generated in response to Ang II is thought to contribute to endothelial dysfunction by inactivating nitric oxide (NO) (90;94). Treatment with AT1-selective angiotensin receptor blockers normalizes ROS production and endothelial dysfunction in hypercholesterolemic animals and humans (95;96).

In terms of inflammation, Ang II is known to induce leukocyte recruitment via stimulating expression of chemokines and cell adhesion molecules and cytokine expression in many cells composing the vascular wall. Ang II augments recruitment of leukocytes via regulating the expression of multiple chemokines. MCP-1 is one of the most well known of those cytokines attracting cells such as monocytes and macrophages. Ang II increases MCP-1 expression in VSMCs and monocytes/macrophages, and inhibition of ACE reduces its expression in a rabbit model of atherosclerosis and decreases plasma levels in humans after myocardial infarction (97-102). Moreover, chemokines IL-8 and IP-10 are induced by Ang II in VSMCs (97;100;103). In addition to stimulating leukocyte recruitment, Ang II also facilitates cellular adhesion to the vascular wall. Ang II stimulates an increase in the vascular cell adhesion molecule VCAM-1 on the surface of cultured endothelial cells and VSMCs and in the aorta of Ang II-infused rats (104;105). Another intercellular adhesion molecule, ICAM-1, has also

been shown to be induced by Ang II on human umbilical vein endothelial cells and in humans via activation of the AT1 receptor (106). Moreover, an endothelial specific adhesion molecule, E-selectin, is upregulated by Ang II and results in increased leukocyte adhesion to human coronary endothelial cells (107). The expression of these adhesion molecules is thought to be partially ROS mediated. Furthermore, Ang II is known to be able to induce multiple cytokines. The most relevant to the research project presented subsequently is IL-6. Our lab has shown that direct stimulation of cultured rat VSMCs induces significant increases in IL-6 protein secretion and transcription via activation of NF- κ B by phosphorylation at Ser⁵³⁶(108;109). In monocytes, IL-6 is upregulated in response to Ang II, and Ang II has been shown to induce AT1 receptor cross-linking leading to greater potentiation of cytokine secretion like IL-1 β and adhesion to endothelial cells (110;111). The increased expression of some of these cytokines is also dependent on ROS. These features of vascular inflammation are also seen in the Ang II-infusion mouse model of aneurysm formation.

Ang II-infusion causes aneurysm formation and dissection in experimental animal models in the suprarenal aorta. Daugherty et al. were first to demonstrate that subcutaneous infusion of Angiotensin II at a dose of 500 or 1,000 ng/kg/min for 4 weeks into female hyperlipidemic mice caused accelerated atherosclerosis and aneurysm formation (112;113). The observed incidences of aneurysms were 20 % in LDLR^{-/-} mice and 33 % with apoE^{-/-} mice. In male apoE^{-/-} mice feed a high fat diet, the incidence can be almost 100 % (114-116). On average, male hyperlipidemic mice have a greater incidence than female mice of the same backgrounds receiving equal Ang II dosage (~80 % vs. ~50 %, male to female respectively) (114). Incidence does increase with Ang II dosage; higher dosing at 1,000 ng/kg/min produces almost twice the incidence as 500

ng/kg/min in male apoE^{-/-} mice. However, duration of treatment longer than 14 d² does not increase incidence (114). The average lumen of a suprarenal aneurysm in apoE^{-/-} mice infused with Ang II at a dosage of 1,000 ng/kg/min is around 1.8 mm, but it can enlarge to more than 4 mm, which is 5-times the size of the normal diameter of 0.8 mm (117). Analysis of the aortic dilatation by very high-frequency ultrasound showed that Ang II causes rapid expansion in the lumen within the first 5 dy of infusion followed by a more gradual increase in lumen diameter along with remodeling of the aorta consisting of adventitial thickening (112;118). The dilatation of the aorta stops with treatment and does not regress in male apoE^{-/-} mice (119). On the contrary, aneurysms in female mice are thought to regress after treatment because no aneurysms were scored at 14 wk³ post a 2-wk infusion, but a 30 % incidence was seen at the end of treatment (120). The induction of aneurysm was shown to be dependent on Ang II stimulation of the AT1 receptor since blockade of the AT1 receptor with losartan, an AT1-selective angiotensin II receptor blocker (ARB), completely prevented aneurysms while blockade at the AT2 receptor increased incidence and severity (121). Moreover, it is believed that the acceleration of atherosclerosis and aneurysm formation is caused by the pro-inflammatory actions of Ang II downstream of receptor binding and independent of hypertension since blood pressure increases mildly with treatment and elevating blood pressure with norepinephrine to a similar level as seen with Ang II did not produce the same pathologies (115;120;122;123). The development of aneurysm was first thought to be associated with hypercholesterolemia (112;113), but more recent studies have shown that C57BL/6 wild-type male mice can also develop suprarenal aneurysm, but at a reduced incidence of ~39 % (115). Ang II infusion in apoE^{-/-} mice has also been shown

² d is the abbreviation for day (s)

³ wk is the abbreviation for week (s)

to produce aortic dissection, with disruption of elastin fibers across the entire media, in the suprarenal aorta between 4-10 d of infusion prior to aneurysm formation (124). Continual treatment also leads to increased atherosclerosis starting after 28 d (124). Dissected aortas had grossly observable vascular hematoma/thrombi within the aortic wall, usually confined to the tunica adventitia. Moreover, approximately 7-10 % of treated mice also die due to AAA rupture (124;125). Analysis of the aortic cross sections from treated mice showed that the earliest cellular change detected (within 1 to 4 d of infusion) was macrophage recruitment into the media of the aneurysm-prone suprarenal area along with minimal elastin breaks. Further accumulation of macrophages into the adventitia occurred between 4-10 d and is followed by T-cells and B-cells recruitment into the same layer after 14 d (124). In terms of cytokine and chemokine production, Recinos et al. have shown that IL-6, G-CSF, GM-CSF, IL-10, TNF- α , IL-12(P40), MIP-1 α , IFN- γ , and IL-1 β were highly secreted from the entire aorta of LDLR^{-/-} mice infused with Ang II for 4 wk compared to sham-treated aortas (123). The significant increases were at least 1.4 fold for IL-1 β , and IL-6 was the most abundant, showing a 4.1 fold-change. This increase in IL-6 was shown by Wang and Deng et al. to be specifically coming mostly from the suprarenal aorta and the aortic arch of infused apoE^{-/-} and C57BL/6 mice (115;116). Elevated gene expression of aortic IL-6, TNF- α , MIP-1 α , IFN- γ , RANTES, and TGF- β has also been confirmed in treated apoE^{-/-} mice (126). Moreover, Ang II-infusion also significantly induced MCP-1 mRNA levels in the aorta of apoE^{-/-} and C57BL/6 mice early after infusion (126;127) and blockade of the AT1 receptor reduced its expression (128). The resulting cytokine profile and leukocyte recruitment are very similar to that seen in human AAA and TAAD as mentioned above.

Several studies using drug inhibitors and genetically modified mice have revealed significant insight into the mechanisms of Ang II-induced AAA. Inhibition of

cyclooxygenase-2 (COX-2) using a selective inhibitor, celecoxib, reduced AAA incidence and severity in response to Ang II-infusion in male apoE^{-/-} mice, and similar results were observed in COX-2^{-/-} mice (129;130). Moreover, deficiency of BLT-1, the G-protein-coupled receptor for leukotriene B4, also attenuated Ang II-induced AAA in apoE^{-/-} mice (131). However, deficiency and pharmacologic inhibition of 5-lipoxygenase, the enzyme that converts arachidonic acid into leukotrienes, did not have an effect on AngII-induced AAA in apoE^{-/-} mice (132). In addition, MMPs like MMP-2 and MMP-9, both of which can degrade elastin and collagen, have been detected in AAA of Ang II-infused mice (116;133), and their inhibition using a non-specific, general MMP inhibitor, doxycycline, attenuated AAA incidence in Ang II-treated LDLR^{-/-} mice (134). Similarly, the use of metacept, an inhibitor of histone deacetylase, which is also an indirect and non-specific inhibitor of MMP, reduced AAA in male apoE^{-/-} mice (135). Along those lines, deficiency of osteopontin was shown to be associated with reduced amounts and activity of aortic MMP-2 and MMP-9 and incidence of aneurysm (136). Furthermore, deficiency of NADPH oxidase subunits p47phox and NOX1 decreased AAA in treated hyperlipidemic male mice and C57BL/6 mice, respectively (125;137). Also, inhibition of two intracellular signaling pathways has been shown to interfere with AAA formation. Inhibiting the Rho-kinase pathway with fasudil decreased AAA in apoE^{-/-} mice by inhibiting apoptosis and proteolysis (138), and inhibition of JNK signaling with SP600125 was shown to cause regression of AAA induced by Ang II (139).

Taken together, these experiments show that some of the same agents thought to play significant roles in human aneurysms are duplicated in and have been shown to mechanistically cause abdominal aneurysms in the Ang II-infusion mouse model. Therefore, this model can provide relevant results that can be extrapolated back to

understanding the pathogenesis of AAA and TAAD in humans. One important marker induced in this mouse model is MCP-1.

Role of Monocyte Chemoattractant Protein-1 (MCP-1)/CCR2 in Vascular Inflammation

MCP-1 is a small (8-10 kDa) CC-type chemokine that specifically attracts cells that express its receptor, CCR2, which is 7-transmembrane G-protein coupled receptor, predominantly found on monocytes and T cells along with a variety of other cells such as basophils, B-cells, dendritic cells (DC), NK cells, VSMCs, fibroblasts, and endothelial cells (140-142). All of these cells can respond to and also express MCP-1 (143). Neutrophils do not express CCR2 or respond to MCP-1, but do recognize IL-8 (143). Since the study presented here primarily focuses on IL-6, with MCP-1 of secondary interest, only topics relevant to MCP-1 in vascular inflammation and aneurysm development are discussed.

In humans, MCP-1 has been consistently identified in atherosclerotic lesions along with macrophages, suggesting that macrophages and macrophage-derived foam cells are the major producers of this chemokine (102;144-146). This is also the case in AAA. Some studies also report detecting MCP-1 to a lesser extent in VSMCs and endothelial cells in both atherosclerosis and AAA (57;57;144-146). Moreover, MCP-1 levels have been shown to be elevated in plasma of patients with acute myocardial infarction or unstable angina, but not in patients with stable angina, suggesting that MCP-1 is associated with worsening disease severity (145).

Animal models reproduce these similar features. In rabbits, MCP-1 is normally detected in some endothelial cells and in the adventitia, but with cholesterol feeding MCP-1 is upregulated in macrophages recruited to the intima and smooth muscle cells (147). Moreover, in LDLR^{-/-} mice a high cholesterol diet rapidly induces aortic MCP-1

expression in macrophages along with macrophage recruitment (148). In apoE^{-/-} mice fed a normal diet, MCP-1 expression increases exponentially over time. This increase was significantly blunted by administration of an ARB (128;149). Along those lines, infusion of Ang II into rats induces MCP-1 expression by about 4-fold as well as with increase macrophage recruitment into the adventitia (150). In addition, monocyte accumulation in the apoE^{-/-} mouse has been shown to occur continuously during atheroma formation and proportionally to lesion size (151). Those monocytes have been identified as predominantly CCR2⁺Ly-6C^{hi} and not CCR2⁻Ly-6^{lo} (152;153).

More mechanistic animal studies have shown that MCP-1 and its receptor play important roles in atherosclerosis. Over expression of MCP-1 in the aorta was shown to be necessary for formation of atherosclerotic lesions in hypercholesterolemic rabbits while inhibition of local MCP-1 with a dominant negative mutant of MCP-1 limited progression of preexisting atherosclerosis and stabilized lesions in apoE^{-/-} mice with and without Ang II treatment (126;154;155). Likewise, MCP-1^{-/-}LDLR^{-/-} double knockout mice showed 83 % less lipid deposition throughout their aortas and fewer aortic macrophages as compared to LDLR^{-/-} mice (156). Furthermore, markedly decreased lesion formation was observed in CCR2^{-/-}apoE^{-/-} double knockout mice compared to apoE^{-/-} mice (157). In addition, CCR2⁺ bone marrow was shown to be critical for initiation of atherogenesis, but not during progression of established lesions in apoE^{-/-} mice (158;159).

The role of CCR2 has also been studied in aneurysm formation using CCR2^{-/-} mice. These mice have significantly impaired recruitment of macrophages into areas of inflammation, produce dramatically less IFN- γ in response to protein from *Mycobacterium bovis*, and are not able to clear infections by *Listeria monocytogenes*, which is thought to mainly require the work of macrophages (160;161). In the CaCl₂

model of AAA, CCR2^{-/-} mice were shown to be resistant to aneurysms as determined by an increase in aortic diameter of 100 %, but CCR5^{-/-} mice (RANTES receptor deficient) and CXCR3^{-/-} mice (IFN- γ -inducible chemokines receptor deficient) were not, suggesting that CCR2 is involved directly in AAA formation (162). Furthermore, CCR2 was shown to be very important for macrophage infiltration into the aorta in response to Ang II and for associated vascular remodeling such as aortic wall thickening, adventitial thickening/fibrosis, and vascular inflammation (127;163). More importantly, using the bone marrow transplant technique, Ishibashi et al. demonstrated that transplanting CCR2-deficient bone marrow into irradiated apoE^{-/-} mice led to blunted induction of aortic IL-6 expression and attenuated development of Ang II-induced aneurysm by 9-fold as compared to apoE^{-/-} receiving CCR2^{+/+} (WT) bone marrow (the incidence decreased from 90 % to 10 %) (164). From that study, the authors concluded that CCR2⁺ monocytes play a critical role in accelerating atherosclerosis and aneurysm formation; however, that conclusion is misleading due to the technique. In bone marrow transplantation, all cells in the bone marrow from one mouse will be injected into a recipient mouse. Thus mice receiving CCR2^{-/-} bone marrow will also have T-cells, B-cells, dendritic cells, NK cells, and basophils lacking CCR2. Although they can conclude that CCR2⁺ cells recruited into the aorta are responsible for the IL-6 induction and aneurysm incidence of 90 %, the monocytes cannot be singled out as the pathogenic cell. Therefore, it still is not clear which leukocyte is responsible for these two important phenomena. Another problem with Ishibashi's study is that bone marrow transplantation is harsh on the animals. For example, in another study done by Ishibashi (127), transplanting CCR2^{-/-} bone marrow into WT mice recipients unexpectedly produced the same induction of aortic MCP-1 expression, around 2-fold, as transplanting CCR2^{+/+} WT bone marrow into the WT mice in response to Ang II. Transplant of WT bone marrow into WT mice was expected to

produce the same 7.5-fold induction as seen in unaltered WT mice infused with Ang II, but that did not happen, suggesting that the irradiation and repopulation procedure influenced vascular inflammation (127). This confounding issue has been noted by Daugherty (119).

In the study presented here, we attempt to identify the most important leukocyte and its role in Ang II-induced vascular inflammation and aortic diseases. We hypothesize that CCR2⁺ monocytes and macrophages are responsible for full potentiation of aortic MCP-1, IL-6, and aneurysm formation in the mouse model of Ang II-infusion. For this purpose, we performed adoptive transfer of purified WT monocytes or CCR2^{-/-} monocytes, at a physiological relevant number, into CCR2^{-/-} mice recipients undergoing sham- or Ang II-treatment. This technique is better than bone marrow transplantation because it allows us to directly study the role of CCR2⁺ monocytes in vascular inflammation without the confounding effects of irradiation. We also labeled the monocytes *in vitro* and were able to track their recruitment throughout the body and particularly into the aorta to determine if these cells actually home specifically to areas where lesions develop. Moreover, the resulting effect on aortic MCP-1 and IL-6 secretion and incidence of aortic dissection were measured. Together, these results will provide much needed insight into the role of monocytes/macrophages in vascular inflammation, especially IL-6 potentiation.

Role of Interleukin-6 in Vascular Inflammation

IL-6 is a 21-28 kDa glycoprotein that is produced and secreted by activated monocytes/macrophages, lymphocytes, endothelial cells, VSMCs, fibroblasts, and a host of other cells (165-167). There are two ways IL-6 initiates intracellular signaling. The classic pathway starts with binding of IL-6 to its receptor α -subunit, IL-6R α , on cell membranes and subsequent recruitment of gp130, a separate transmembrane protein, to

form an active hexameric signaling complex. The second mechanism, called the trans-signaling pathway, allows for cells not expressing the IL-6 receptor to respond to IL-6. In the trans-signaling pathway, IL-6 binds to its soluble receptor, sIL-6R α , which is a cleavage product of the membrane bound IL-6R α , and that complex then associates with gp130. Downstream of both pathways, gp130-associated tyrosine kinases (JAKs-1 and Tyk 2 kinases) are then recruited to tyrosine-phosphorylate gp130. That leads to recruitment of cytoplasmic transcription factors Signal Transducer and Activator of Transcription (STAT1 and STAT3) that bind to gp130 via their src homology-2 (SH2) domains. The STATs are then phosphorylated at Tyr⁷⁰⁵ by the JAK/Tyk kinases, allowing them to homo- or hetero-dimerize and translocate into the nucleus where STATs bind to target genes like C-reactive protein (CRP), fibrinogen, and angiotensinogen to enhance their transcription (168;169). Although the Ras-ERK-MAPK pathway also can be initiated by IL-6, that pathway plays a minor role compared to the Jak/STAT pathway. Since gp130 is ubiquitously expressed, almost any cell can respond to IL-6 via the trans-signaling pathway (168).

IL-6 has multiple biological activities. It can induce differentiation of B-cells and growth of plasma cells, activate T-cells, stimulate production of platelets and acute-phase response proteins in the liver, cause proliferation of VSMCs in conjunction with platelet-derived growth factor (PDGF), and help recruit leukocytes into areas of inflammation (18;72;170). *In vitro*, IL-6 can directly induce monocytes to differentiate into macrophages and upregulate CD36 on their surface (168). Moreover, MCP-1 is induced by the IL-6 Jak/STAT pathway in cultured peripheral blood mononuclear cells and VSMCs (171;172). Endothelial cells do not express IL-6R, but studies have shown that they can be stimulated *in vitro* by IL-6 via the trans-signaling pathway to upregulate proteins such as ICAM-1 to help leukocytes such as monocyte and T-cells that express

the surface $\alpha_m\beta_2$ integrin Mac-1 (CD11b/CD18) to bind (170;173). Recent studies have shown that trans-signaling is required for Ang II-dependent hypertension and for recruitment of mononuclear cells into sites of inflammation (174;175). Recruitment of T-lymphocytes into the vascular wall has been shown to cause Ang II-dependent hypertension (176). Together these results suggest that Ang II-induced IL-6, via trans-signaling, mediates T-cell recruitment leading to hypertension. Moreover, they suggest that MCP-1 might be the chemokine induced by IL-6 that actually recruits T-cells.

IL-6 is highly upregulated in patients with atherosclerotic cardiovascular diseases. There is increased IL-6 in atherosclerotic tissue, primarily in macrophages and, to a lesser degree, VSMCs (177;178). IL-6 also has been shown to colocalize with AT1, ACE, and Ang II in macrophages around the site of plaque rupture in coronary arteries from patients with myocardial infarction (179). Multiple clinical studies have shown that patients with unstable angina have high levels of plasma IL-6 and are at increased risk for plaque rupture leading to an acute myocardial infarction (MI) (180-182). People without clinical evidence of heart disease, but with IL-6 levels in the upper quartile of the normal range are at increased risk of future MI and cardiovascular mortality as well as all-cause mortality (183-185). Furthermore, elevated IL-6 has been associated with increased mortality regardless of cardiovascular disease severity (185). There are similar findings with CRP, which is produced by cells such as hepatocytes following IL-6 stimulation (183;186;187).

Patients with AAA have consistently been shown to have higher venous and arterial IL-6 concentrations compared to control patient populations without AAA (51;58;59;188-190). Moreover, explanted AAA tissue actively secretes IL-6 (46;50;191). Dawson et al. have further shown that aneurysms were the source of high IL-6 in circulation *in vivo* based on the facts that IL-6 concentrations in arterial blood increased

downstream of aneurysms in a linear trend and no significant difference was seen in CRP levels, suggesting that systemic inflammation did not influence the IL-6 levels measured (58;59). Interestingly, patients with TAA had four times the circulating level of IL-6 than controls and more than two times the concentration compared to patients with AAA. The latter correlated with the 2-fold greater aneurysm surface area in TAA patients than AAA patients, but not with aortic diameter, indicating that larger-volume aneurysms secrete more IL-6 (58;59). It is worth noting that IL-6 plasma levels correlate positively with aneurysm rupture, but not significantly with aneurysm size or expansion in patients with AAA although non-significant increases with enlarging diameters have been reported (51;58;188;190;191). In patients without dilatation, elevated serum IL-6 is positively correlated with aortic diameter, suggesting that IL-6 may likely play a role in aneurysm formation (189). In addition, AAA patients with the -174 G→C polymorphism in the IL-6 promoter have higher circulating levels of IL-6 and are at increased risk for all-cause and cardiovascular mortality (190).

It should also be recognized that most patients with AAA have concurrent atherosclerotic disease and two-thirds of all patients with AAA die from cardiovascular causes not related to their aneurysm (192). Thus, it is becoming clear that IL-6 might not only be contributing to the development and exacerbation of AAA, but that the IL-6 coming from aneurysms may also be increasing risk of cardiovascular mortality at all stages of disease. Therefore, it is of extreme importance to understand the mechanisms of how IL-6 is produced and its contribution to AAA formation/exacerbation because that knowledge may shed light on its roles in worsening atherosclerotic disease leading to cardiovascular mortality in patients with AAA.

Studies have been performed to study the actions of IL-6 relevant to cardiovascular diseases, but they have not looked at the local roles IL-6 in the vascular

wall where the aortic diseases occur. Most were performed *in vitro* with direct stimulation of IL-6 on cultured cells such as endothelial cells, VSMCs, and monocytes in isolation. Although these studies give valuable knowledge on how these cells respond to IL-6 and their molecular mechanisms, they are performed in very defined conditions with one large dose stimulation. Those results do not necessarily translate *in vivo* where there is a mixture of interactions between different cell types and multiple cytokines and agents inducing a variety of signaling pathways, ultimately giving rise to a net effect. Only a few animal studies have attempted to directly study the role of IL-6. In the study of IL-6 in atherosclerosis, a short-term administration of exogenous IL-6 led to enhanced plaque development in apoE^{-/-} mice (193), but a lifetime deficiency of IL-6 in that background also caused enhanced lesion formation despite reduced recruitment of inflammatory cells and decreased expression of MMP-9 transcripts (194). Moreover, in LDLR^{-/-} mice, IL-6 deficiency only reduced plaque lesion area modestly, without significance (195). In contrast to the studies on atherosclerosis, there are no published research studying the role of IL-6 in aneurysm formation *in vivo*, but there was a brief mention of unpublished data that IL-6 deficiency and IL-6 inhibition with neutralizing antibodies suppressed aneurysm formation in the elastase-infusion model of AAA (196). Because IL-6 is such a relevant marker to aneurysms and because it has broad implications for inflammation, work is needed to better understanding its role in aneurysm formation.

In this research, we aim to understand where and how IL-6 is upregulated locally in the aorta and the effects of local IL-6 on aortic macrophage differentiation as well as their recruitment into the aorta in response to Ang II. We focus on macrophages because their recruitment into the tunica media of the aorta precedes aneurysm, dissection and atherosclerosis, which suggest that they play a significant early role in those aortic diseases. In addition, they are well known to produce MMPs which have been shown to

be crucial to aneurysm development (41;124). In addition, studies on aortic macrophages specifically are lacking besides their detection in aneurysms, not to mention how they are affected by local IL-6. Keidar et al. have shown that peritoneal macrophages increase expression and levels of CD36, a macrophage receptor for oxidized LDL, in response to IL-6 with Ang II-infusion in apoE^{-/-} mice, but it is not clear if local aortic macrophages respond similarly because these two macrophages can behave quite differently (197).

To specifically study aortic macrophages we developed a new method to isolate them from the aorta and compare their phenotype in the wild-type and IL-6 deficient backgrounds in response to Ang II. In addition, we determined whether IL-6 regulates aortic MCP-1 production. From these data we propose a plausible cell-to-cell interaction that could be responsible for the induction of these cytokines *in vivo*. Studies presented here, therefore, provide valuable understanding of the local actions of IL-6 in aortic diseases and in other cardiovascular diseases.

Adventitial Fibroblasts

As mentioned above, inflammatory cell infiltration and cytokine expression have been documented in the tunica adventitia for AAA, TAA, and atherosclerosis. Research has shown that in some cases, the earliest events occur in the adventitia, and that it is the predominant location of inflammation. Furthermore, increased adventitial inflammation has been strongly correlated with atherosclerotic plaque rupture, the final step in the progression of an atheroma that triggers the acute myocardial infarction (198;199). These observations have led to an “outside-in” hypothesis for cardiovascular diseases, in which vascular inflammation is initiated or exacerbated in the adventitia and then progress inward into the vascular wall toward the intima (200). This has already been suggested as a pathway in the pathogenesis AAA and TAA (4;5). One important cell

type that has recently emerged as central to adventitial inflammation is the adventitial fibroblast.

Adventitial fibroblasts can originate from two distinct cell types depending on their location. In the coronary arteries, they come from mesenchymal cells derived from proepicardial cells through an epithelial-to-mesenchymal transition (201). However, adventitial fibroblasts in the aortic and pulmonary trunks, aortic and pulmonary arch arteries, and brachiocephalic and carotid arteries come from neural crest cells (202). Adventitial fibroblasts in the pulmonary arteries and descending aorta most likely are not neural crest cell derived (202) and their origins along with those in the abdominal aorta remain unknown (203).

Although this cell type has long been ignored, it is being increasingly apparent that adventitial fibroblasts are the first to react to vascular injury and possess many characteristics that allow it to contribute to the pathogenesis of cardiovascular diseases (204). They are known to proliferate in response to Ang II both *in vitro* and *in vivo* (123;205-207). In apoE^{-/-} mice, Ang II treatment causes severe adventitial thickening seen along with aneurysms that is mostly composed of adventitial fibroblasts (113;124). Ang II is also known to induce adventitial fibroblast differentiation to myofibroblasts that express α -smooth muscle actin dependent on ROS produced by NADPH oxidase and downstream p38 and JNK stress signaling pathways (208). This phenotype switch has also been observed in IAA (9). Differentiation to myofibroblasts is associated with increased proliferative and migratory activities (203). In response to arterial balloon angioplasty, restenosis of the lumen by intimal hyperplasia is a major problem. In animal models of endoluminal injury, adventitial fibroblasts have been shown to proliferate and migrate from the adventitia into the intima where they contribute to the intimal hyperplasia, narrowing the lumen (209-211). Studies labeling

the adventitial fibroblasts *in vitro* and directly *in vivo* with LacZ have shown that the labeled adventitial fibroblasts migrate into the intima after vascular injury, but not in the uninjured state (212;213). The ability of mice and rat aortic adventitial fibroblasts to induce MMP-2 expression, protein, and activity in response to different stimuli may help these cells migrate into aortic tissue (214;215). Moreover, adventitial fibroblasts are a tremendous source of ROS, particularly superoxide. The major site of superoxide production was found to be the adventitia in rabbit aortas, and further analysis showed that the adventitial fibroblasts were its source (216;217). These cells have constitutively active NADPH oxidase that can be induced further by Ang II to enhance production of ROS (217). The major component of that oxidase was found to be p67^{phox} since specifically inhibiting that protein resulted in loss of NADPH oxidase activity. Furthermore, only limited information is known about the ability of adventitial fibroblasts to produce cytokines. One study has detected MCP-1 in the adventitia of apoE^{-/-} mice before presence of atherosclerotic lesions, but its source was only assumed and not directly identified (218). Moreover, adventitial fibroblasts harvested from AAA tissue were shown have much greater gene expression of MCP-1, IL-8, VEGF, and TNF- α compared to normal dermal fibroblasts by gene chip analysis, but it is unclear whether those findings translate into cytokine production (219). Thus it has become increasingly clear that the adventitia is no longer just a passive structure, but that it can actually play an integral role in mediating vascular diseases.

In this study, we further characterize human aortic adventitial fibroblasts (AoAFs) based on their cytokine profile, response to Ang II stimulation, and interaction with monocytes to potentiate inflammation. The full extent of cytokines these adventitial fibroblasts are capable of producing and the extent to which Ang II can potentiate their expression is currently not known. Moreover, although Ang II has been shown to induce

cultured primary rat aortic adventitial fibroblasts to proliferate and cause murine adventitial fibroblasts to proliferate *in vivo* (93;205;206;220), it remains unclear if human AoAFs will respond similarly. In addition, since monocytes/macrophages are recruited into the adventitia in human aneurysms as well as in animal models of aortic diseases, especially with Ang II infusion, they are in close proximity to adventitial fibroblasts, which in some cases are also increasing in number. Therefore, we explore potential interactions between these two cell types and how they might further potentiate vascular inflammation. Collectively, this knowledge will provide a better understanding of how events in the tunica adventitia may contribute to initiation and exacerbation of many cardiovascular diseases.

The aims in this study are to create a reliable and relevant animal model to study aortic diseases and vascular inflammation, to determine how the vascular inflammation develops, to understand some of its effects *in vivo*, and to dissect *in vitro* the cellular and molecular mechanisms contributing to vascular inflammation. In Chapter 2, we characterize a short-term Ang II-infusion model, with WT mice, of aortic aneurysm and dissection based on histology and cytokine production, and in Chapter 3, we present a new technique to isolate, phenotype, and quantitate aortic macrophages. In the following chapter, we use the model with *CCR2*^{-/-} mice to demonstrate how vascular inflammation, with an emphasis on IL-6 and MCP-1, and dissections are accelerated. In Chapter 5, the effects of IL-6 on aortic macrophage differentiation and regulation of MCP-1 *in vivo* are elucidated. Based on our observations from all of those studies, we next present in Chapter 6 a highly plausible cell-to-cell interaction *in vitro* that supports our findings *in vivo*. Overall, these findings provide valuable insight into the role of IL-6 that is applicable not only to aneurysm and aortic dissection, but to a broad spectrum of inflammatory diseases including atherosclerosis.

Chapter 2: A Mouse Model of Vascular Inflammation Leading to Aortic Dissection

The first aim was to establish a mouse model to study acute vascular inflammation leading to cardiovascular disease. It is known that Ang II-infusion for 4 wk in hyperlipidemic apoE^{-/-} mice leads to increased macrophage recruitment to the aorta, accelerates atherosclerosis, and promotes aortic abdominal aneurysms (AAA) (113;122). Moreover, our laboratory has recently shown that Ang II-infusion for 4 wk in LDLR^{-/-} mice fed a high fat diet potentiates vascular cytokine/chemokine production, especially IL-6, along with profound atherosclerosis (123). Thus, Ang II infusion could be used to induce vascular inflammation and cardiovascular diseases *in vivo* with relevance to humans (18); however, using these hyperlipidemic knockout mice would cause confounding influences due to dyslipidemia, which is well known to promote inflammation (221) and to increase the incidence of AAA (115). In a study that excludes the contribution of dyslipidemia, Deng et al reported that 7-11 mo⁴ old C57BL/6J WT mice, the background strain for both apoE^{-/-} and LDLR^{-/-} mice, can develop AAA with an incidence of 39 % and have increased aortic expression of IL-6 in the aortic arch and abdominal aorta after 1 mo of Ang II treatment (115). This is in contrast to a previous study performed by Daugherty et al. in 1999 that reported that C57BL/7J WT mice were resistant to Ang II-induced AAA (112), but this discrepancy might be due to the higher dose of Ang II used by Deng of 1.44 mg/kg/d vs. the 0.72 mg/kg/d used by Daugherty. Although all models mentioned above developed vascular disease, the disadvantage to Deng's and the hyperlipidemic models was the 1 mo or longer duration of study, a time frame that precludes examination of early events in the development of vascular inflammation. To clarify whether Ang II can induce aneurysm formation in WT mice

⁴ mo is the abbreviation for month (s)

and develop a model that will quickly develop inflammation in the aorta, 7-12 mo old WT mice were infused with Ang II at a dosage of 2,500 ng/kg/min over 6 and 10 d.

ANG II INFUSION IN AGED WILD-TYPE MICE INDUCES THORACIC AND ABDOMINAL AORTIC DISSECTIONS

At 6 d of treatment, sacrifice of some of the animals clearly showed a hematoma confined to the tissue of the aorta whereas sham-infused mice did not (Figure 1). PBS was infused through the left ventricle to remove blood from the aortic lumen, leaving the trapped hematoma. The hematoma shown in Figure 1 extends from the ascending aorta to the suprarenal abdominal aorta. Hematomas have been observed confined to the suprarenal abdominal aorta also (Figure 2) or the thoracic aorta (not shown).

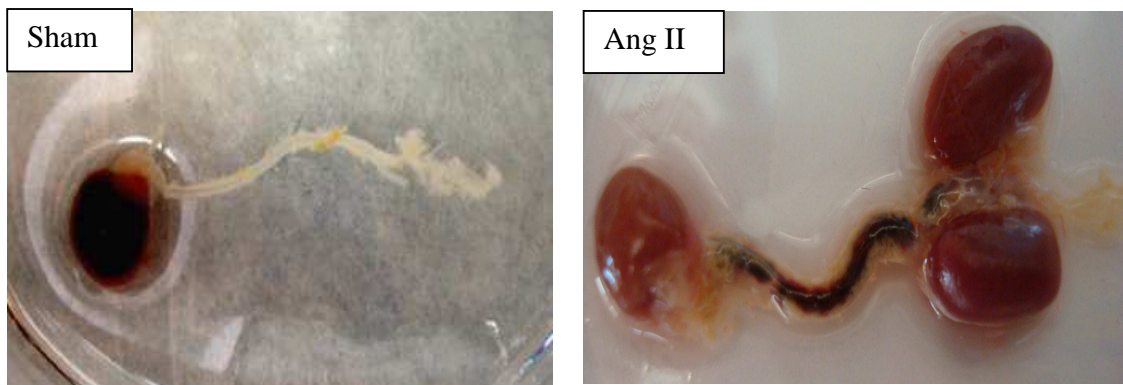


Figure 1. Visual hematoma throughout aorta



Figure 2. Hematoma confined to the suprarenal abdominal aorta

Figure 3 shows two separate hematomas, one confined to the thoracic aorta and the other to the abdominal aorta. Interestingly, no pathology was seen in the infrarenal aorta, where AAA in humans is frequently located (6).



Figure 3. Hematomas localized to the thoracic aorta and the abdominal aorta, separated by a non-affected region.

The incidence of hematomas was 35 % (8/23) at 6 d. In animals that did not develop hematomas with treatment, the aortas appeared thickened (Figure 4) compared to

sham-treated aortas (Figure 1) but it was not noticeable until transverse sections of the aortas were analyzed.



Figure 4. Thoracic aorta from Ang II-infused mouse appeared thickened.

Upon examination of cross-sections of the aortas by Movats pentachrome staining, six main observations were made. First, Ang II induced extensive adventitial remodeling in both the thoracic and abdominal aorta regions, which mainly appeared to be due to increasing numbers of cells, as seen by the light red staining representing cellular cytoplasm in adventitia. The cells are most likely aortic adventitial fibroblasts because the remodeling resembles fibrosis of the tunica adventitia (Figure 5). Fibrosis in the adventitia has been reported with Ang II infusion in WT mice (127). A cross-section from a sham-treated WT mouse is shown in Figure 6 as comparison. Second, along with adventitial remodeling, medial hypertrophy can be seen after Ang II treatment (Figure 5, as compared to sham treatment in Figure 6). Third, there was increased production of mucopolysaccharide/proteoglycans as seen by blue staining (Figures 5&6). Fourth, in animals with aortic hematomas, a pseudo-lumen filled with clotted blood was obvious in the adventitia, Figure 7. All mice with aortic hematomas had the pseudo-lumen localized to the adventitia throughout the aorta.

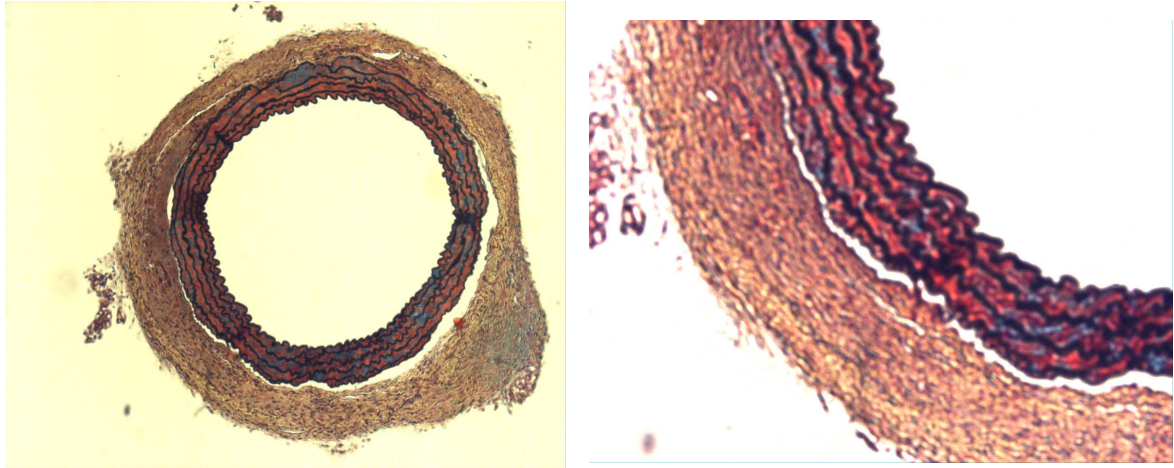


Figure 5. Adventitial remodeling in abdominal aorta with Ang II infusion as seen by Movats staining, 4x (left) and 10x (right).



Figure 6. Abdominal aortic cross-section after sham-treatment as seen by Movats staining, 4x (left) and 10x (right)

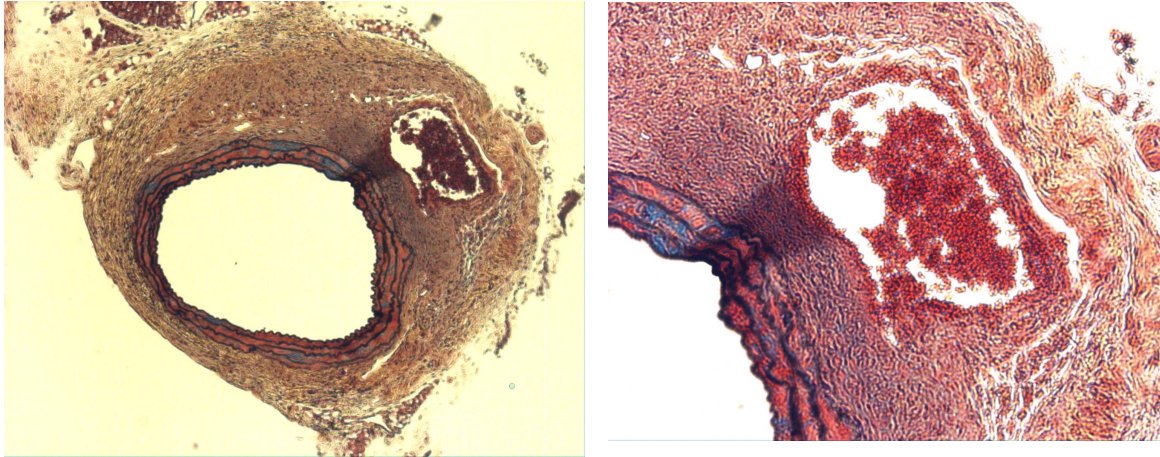


Figure 7. Abdominal aortic cross-section of a mouse with adventitial hematoma showing a pseudo-lumen filled with clotted blood as seen by Movats staining, 4x (left) and 10x (right)

Fifth, a channel as seen in the indentation that spans all three aortic tunics in Figure 7 at 10x magnification, was observed, most likely allowing for communication between the lumen and the pseudo-lumen. These channels were observed in both the ascending and suprarenal abdominal aortas, corresponding to the two main locations where hematomas were observed in the aorta. Finally, in some sections, a complete tear from the tunica intima, through the tunica media, to the pseudo-lumen in the tunica adventitia was observed (Figure 8).

Based on the data above, Ang II-infusion caused aortic dissection after just 6 d of treatment. Aortic dissections have been detected originating in the ascending aorta and propagating down towards the abdominal aorta or more frequently in the suprarenal aorta. There was clearly a pseudo-lumen that developed, which communicated with the real aortic lumen, as seen by the appearance of RBCs in the pseudo-lumen.

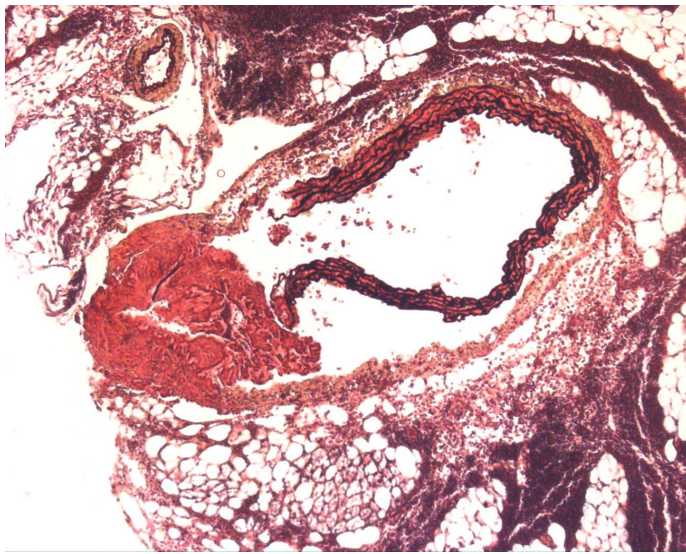


Figure 8. Dissection through the tunica intima and media of the suprarenal aorta. A false lumen was created in the adventitia that communicated with the true lumen.

Tears in the intima that extended into the media were also observed. Furthermore, adventitial remodeling was apparent in dissected aortas.

Although Ang II-infusion induced aortic dissections in mice, there were several differences compared to human dissections. The main difference was that the dissection tore through all layers of the aorta creating a channel that communicated with a false lumen in the adventitia. In human aortic dissections, a tear occurs in the intima through to the media creating a communicating channel with a pseudo-lumen in the media (2). Moreover, the mice had abdominal dissections, which are not common in humans, and they are found in the infrarenal aorta of humans and not the suprarenal aorta (222). In addition, the adventitial remodeling that occurs in mice is much more extensive than in humans. It actually is very similar to the adventitial thickening that occurs in IAA. Nevertheless, this mouse model replicated the main features of aortic dissection indicating its utility for studying vascular inflammation over a short time period.

CYTOKINE AND CHEMOKINE SECRETION WERE POTENTIATED WITH ANG II INFUSION

Although the pathology that occurred was slightly different than that seen in humans, the short-term infusion model gave us a valuable tool to study accelerated vascular inflammation leading to aortic dissection. Ang II is known to induce leukocyte recruitment and expression of cytokines and chemokines in aortas of experimental models independent of its effects on constricting arteries to increase blood pressure (223). Of all the leukocytes that home to the aorta, macrophages are recruited to the adventitia and media of the suprarenal aorta where aneurysms are observed as soon as 1 to 4 d after Ang II infusion in apoE^{-/-} mice (124). In WT mice infused with Ang II for 6 d, staining for MOMA-2 revealed macrophage accumulation in the adventitia of the ascending aorta and suprarenal aorta (Figure 9). In comparison, sham-treated mice had far fewer macrophages in their aortas if any were seen (Figure 9)

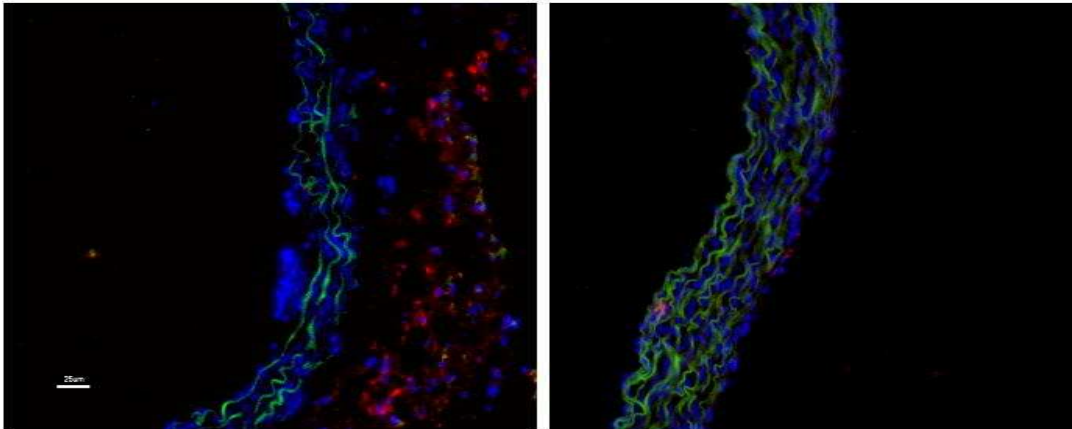


Figure 9. Macrophages in the aorta of mice. Positive red fluorescence was localized to the tunica adventitia of aortas in Ang II-treated mice (left) and sham-treated mice (right). Green is autofluorescence of medial elastic lamellae and blue is DAPI. 20x.

Moreover, expression of IL-6 was predominantly seen in the adventitia of aortas from treated mice, but not clearly noticeable in the aortas from sham-treated mice (Figure 10).

Staining in the intima was also noticed, but did not seem to be as uniform as in the adventitia.

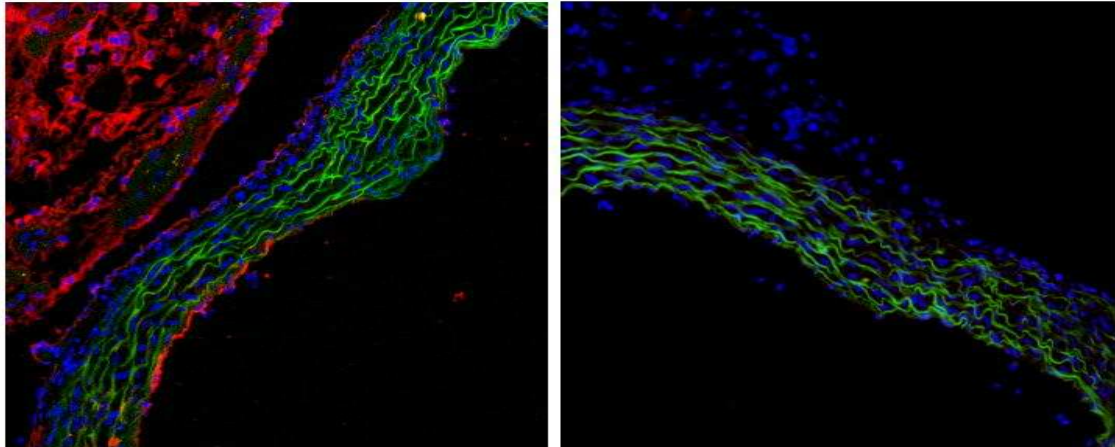


Figure 10. IL-6 in aorta of mice. Positive red fluorescence was seen in the tunica adventitia and less in the intima of Ang II-treated mice (left). Representative section from sham-treated (right). 20x

In addition, staining for MCP-1 was clearly noticeable at the adventitial-medial border and extending into the media, but did not appear uniform in the media. In the adventitia, there seemed to be uniform staining throughout, but it appeared to be less intense, suggesting a low level of expression in the tunica adventitia (Figure 11). Since most of the staining for IL-6 and MCP-1 were in the adventitia and specifically at the adventitial-medial border where adventitial fibroblasts normally reside, it was hypothesized that these cells could contribute to the cytokines/chemokines expressed in vascular inflammation. Staining for aortic adventitial fibroblasts with an anti-fibroblast antibody clone ER-TR7 revealed that this antibody could detect aortic adventitial fibroblasts at the adventitial-medial border in aortic sections from sham-treated mice (Figure 12).

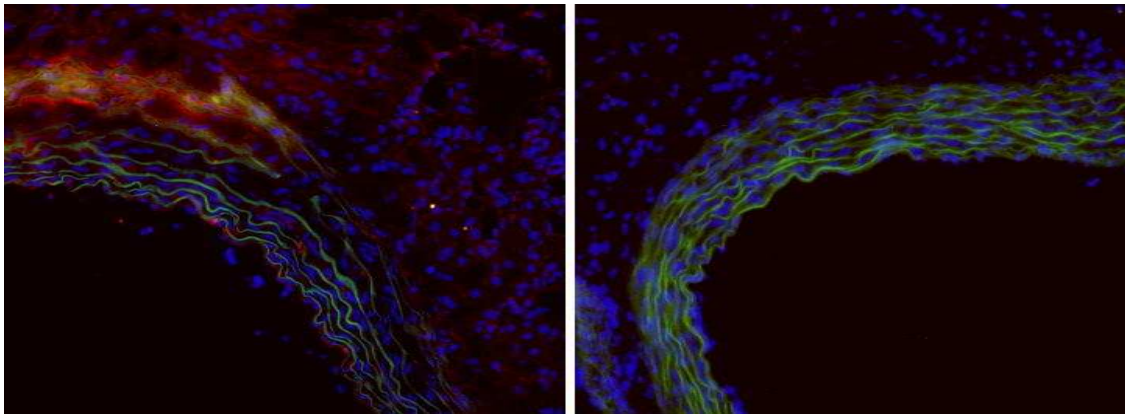


Figure 11. MCP-1 in the aorta of mice. Positive red fluorescence was seen mostly at the adventitial-medial border and extending into the media in Ang II-treated mice (left). Representative section from sham-treated (right). 20x

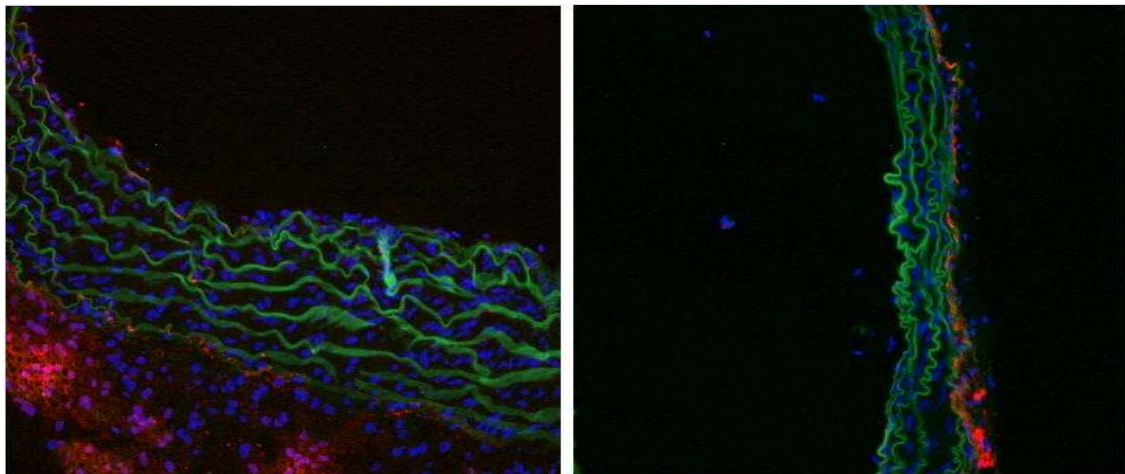


Figure 12. Aortic adventitial fibroblasts in the aorta of mice. AoAFs (red fluorescence) can be seen at the adventitial-medial border in sections from sham-treated mice (left). An increase in signal area was seen in sections from Ang II-treated mice (right). 20x

In Ang II-infused mice, there seemed to be more staining in the adventitia, suggesting that an increase in fibroblasts may be responsible for most of the adventitial remodeling seen with movats staining above. Proliferation and differentiation of adventitial fibroblasts into myofibroblasts have been shown to occur in inflammatory abdominal

aneurysm and contribute mostly to the adventitial thickening, which is called the “mantle sign” on computed tomography scans (9).

Besides staining for IL-6 and MCP-1 to determine their location in aortic cross-sections, aortas from the aortic root to the iliac bifurcation were explanted in culture medium to measure the amount of these cytokines secreted after 4 h. Multiplex ELISA analysis was performed on the culture medium and revealed that the medium of aortas from sham-treated animals ($n=6$) had an IL-6 concentration of $7,994 \pm 3,528$ pg/mL. Medium of aortas from Ang II-treated animals for 6 d had an IL-6 concentration of $28,808 \pm 1,300$ pg/mL ($n=7$) while at 10 d of infusion ($n=7$), the concentration was $25,745 \pm 2,232$ (Figure 13). This represented an increase of 3.6-fold at 6 d and 3.2-fold at 10 d.

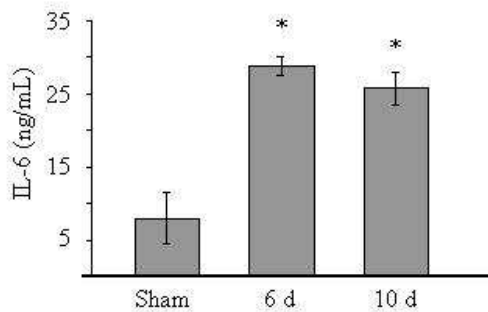


Figure 13. Secreted aortic IL-6 levels in culture medium containing aortas from sham- or Ang II-infused mice after 6 d and 10 d. *, $P < 0.05$ vs. sham treatment. Data are expressed as mean \pm SEM

Simultaneously on the same samples used to measure IL-6, MCP-1 levels were quantified also. Medium containing aortas from sham-treated animals had a MCP-1 concentration of 293 ± 141 pg/mL. Medium from aortas from treated animals for 6 d had a MCP-1 concentration of $1,918 \pm 174$ pg/mL while at 10 d of infusion, the concentration was

2,011 ± 440 pg/mL (Figure 14). This represented an increase of 6.5-fold at 6 d and 6.9-fold at 10 d.

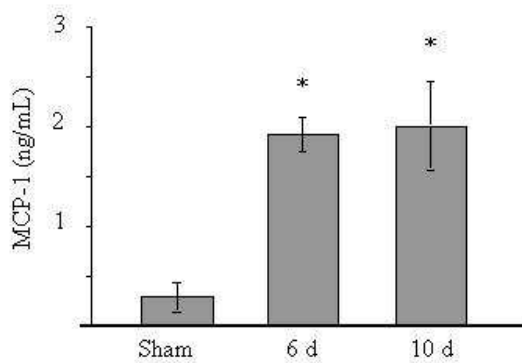


Figure 14. Secreted aortic MCP-1 levels in culture medium containing aortas from sham- or Ang II-infused mice after 6 d and 10 d. *, $P < 0.05$ vs. sham treatment. Data are expressed as mean ± SEM

Because IL-6 was the main focus of study, it was important to determine the localization of IL-6 in aortas of humans with sporadic type A aortic dissection. Using immunofluorescence, IL-6 was detected mainly in the tunica adventitia of diseased aortas also (Figure 15). Little to no staining for IL-6 was detected in stable ascending aneurysms or normal control samples. This confirms the finding in the Ang II-infusion mouse model and supports its use as a good model to study the role of IL-6 in vascular inflammation leading to aortic dissection.

In summary, 6 d of Ang II infusion into aged WT mice produced the main features of aortic dissection including a visible hematoma in the aorta, dissection of the layers of the aorta creating a false lumen that communicates with the true lumen, adventitial remodeling, and vascular inflammation. Specifically, macrophage recruitment was predominantly in the adventitia along with IL-6, MCP-1, and adventitial fibroblasts. However, the biggest difference between this model and aortic dissection in humans was that all three layers of the aorta were dissected instead of just the intima and media and

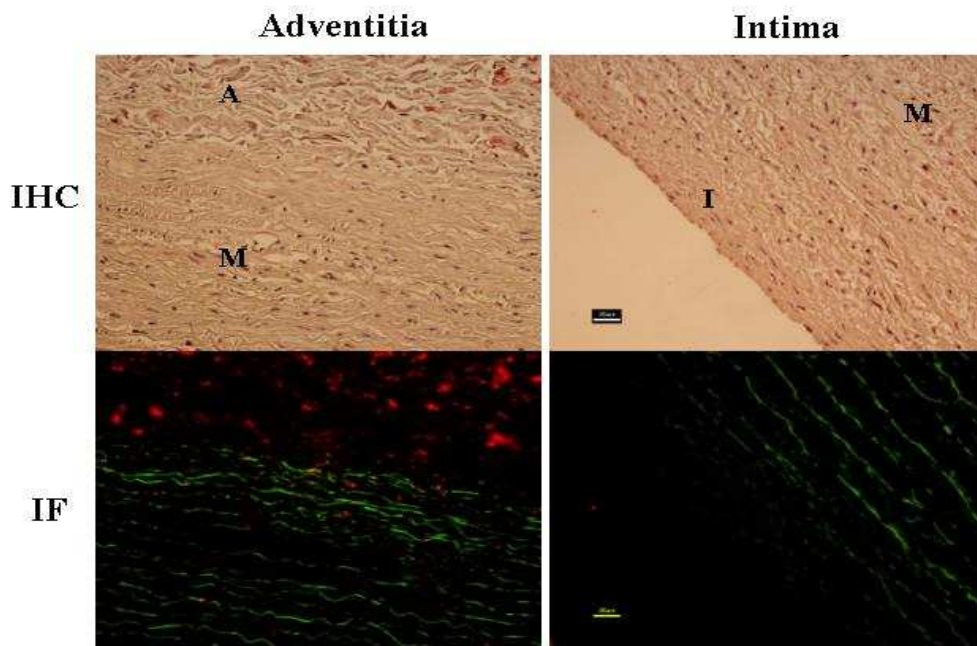


Figure 15. IL-6 in human type A aortic dissection. Left panels show staining for IL-6 in the adventitia (A) as seen with red substrate (top) and red fluorescence (bottom). Right panels the intima (I) and media (M). 20x

the resulting false lumen was in the adventitia and not the media. In spite of these discrepancies, this mouse model can still be used to study the role of Ang II in aortic dissection, which has been implicated in human studies (16;63). Furthermore, this model can also be valuable in studying the contribution of cytokines and major cell types like macrophages in vascular inflammation and disease.

Chapter 3: Aortic Macrophages

The hypothesis we are pursuing in this thesis is that aortic macrophages play a pivotal role in initiating, promoting, and sustaining vascular inflammation. Previous studies have been incomplete using simple detection with one marker or morphology for identification. In addition, proper immunohistochemical analysis requires that many thin tissue sections be analyzed because of regional heterogeneity in macrophage accumulation. For a typical mouse aorta from the root to the iliac bifurcation, which is approximately 50,000 μm in length, 8,333-10,000 sections at 5-6 μm thickness would have to be studied to fully know what is occurring in the entire aorta. Typically a small portion of the aorta is actually studied because there is only a certain region of interest, some samples are lost during sectioning, or the sections are divided among several experiments for multiple end-points. Thus, this limited analysis or regional bias can overestimate or totally miss important information, leading to type I or type II errors. The person (s) performing the analysis of sections can unintentionally introduce observational bias. Moreover, it is sometimes hard for that person to judge between a positive or negative event because results from immunohistochemical or histological staining are not usually obvious, but “gray”, making any quantification difficult and observer-specific. Along with the fact that only a representative section that clearly supports the point of argument is presented by authors in publications, there can be substantial bias introduced when using immunohistochemistry or histology. Although targets of interest can be counted and normalized to area/volume of aortic tissue to make immunohistochemistry “quantitative”, there has to be the assumption that every section of tissue was analyzed and that is usually not the case. These shortcomings of immunohistochemistry and histology make results qualitative at best.

Some studies have also utilized non-aortic macrophages such as peritoneal macrophages as a model to determine the effect of various treatments with cardiovascular significance and extrapolate these findings to macrophages in the aorta or coronary arteries, where the diseases manifest (197). It is well known that macrophages in different tissue function differently and are often given a distinct name (224). For example, peritoneal macrophages have a specific marker that tells them to home to the peritoneum while Kupffer cells go to the liver. Furthermore, characterization of aortic macrophages based on several parameters and how these features collectively contribute to cardiovascular diseases and vascular inflammation has not been attempted. Along these lines, there have been no direct studies on how aortic macrophages change with treatment over time.

In Chapter three, an aortic digestion technique utilizing a combination of collagenase and elastase is described that allows for isolation of intact, single-cell, macrophages for direct study using flow cytometry. This method has proven to be useful for the study of changes to multiple surface or intracellular antigens apart of cellular signaling events, which infer signaling pathway activation. It also overcomes the disadvantages mentioned above for immunohistochemistry by allowing for a complete picture of activities occurring throughout the aorta and providing results that can be presented in a quantitative, unbiased manner.

IDENTIFICATION OF AORTIC MACROPHAGES

Macrophages are derived from peripheral blood monocytes (225). Once monocytes leave the blood stream and enter tissue, the cells become macrophages (225). Macrophages and monocytes express many surface proteins in common so distinguishing these two cell types based on the presence or absence of those markers is impossible. There are generic markers for tissue macrophages such as F4/80, but the actual identity of

the proteins, their functions, and roles in vascular inflammation are unknown. Thus, they can only provide info on the presence of macrophages and nothing more. Although some surface proteins such as scavenger receptors and CD36 are known to be upregulated on macrophages and have been used to distinguish monocytes from macrophages, they are only relevant to environments of hyperlipidemia and oxidized lipids in humans and experimental animal with atherosclerosis. Their expression independent of these environments is not likely and so would be irrelevant to pure aneurysm formation and aortic dissection. Therefore, it was necessary to monitor how markers change in expression as monocytes differentiate into macrophages and use generic markers to confirm differentiation to macrophages along with the technical definition that all monocytes homing into tissue are macrophages. CD14, CD11b, and F4/80 were used to detect aortic macrophages.

Since all monocytes and macrophages express CD14, CD14 was used to first distinguish aortic macrophages from the other cells comprising the aorta, mainly endothelial cells, smooth muscle cells, and adventitial fibroblasts, which all do not express CD14. As seen in Figure 16, there are two distinct populations in the SSC-A (side scatter- infers cell cytoplasmic characteristics) vs. CD14 zebra plot (which displays a mix of contour and cellular density information). This CD14 positive population represented only 0.72 % of all cells in the aorta. This positive population is confirmed in the histogram as determined by comparison to the isotype control.

The gated CD14⁺ population was viewed on a CD11b vs. CD14 zebra graph (Figure 17). There were two populations seen, one CD14⁺CD11b⁺ and one CD14⁺CD11b⁻. The CD14⁺CD11b⁺ population was confirmed to be CD11b⁺ compared to isotype control staining (Figure 17).

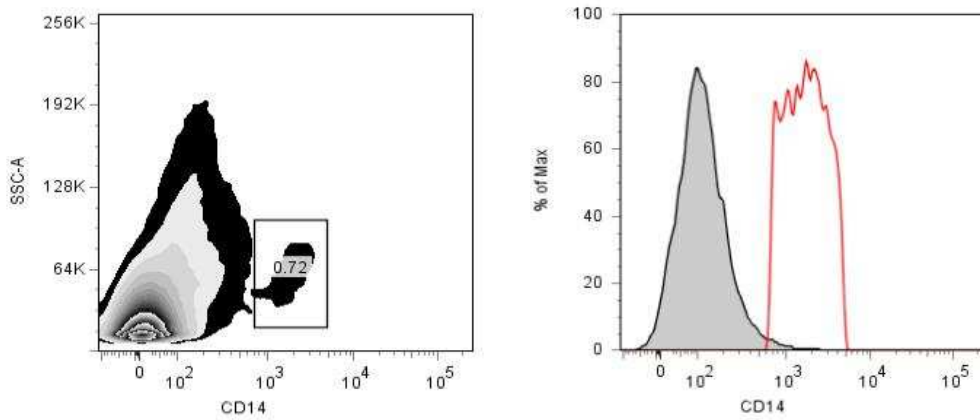


Figure 16. CD14⁺ cells in the aorta. CD14 cells are gated (left- box). Histogram confirming CD14 positive population (red curve) as compared to isotype control (right).

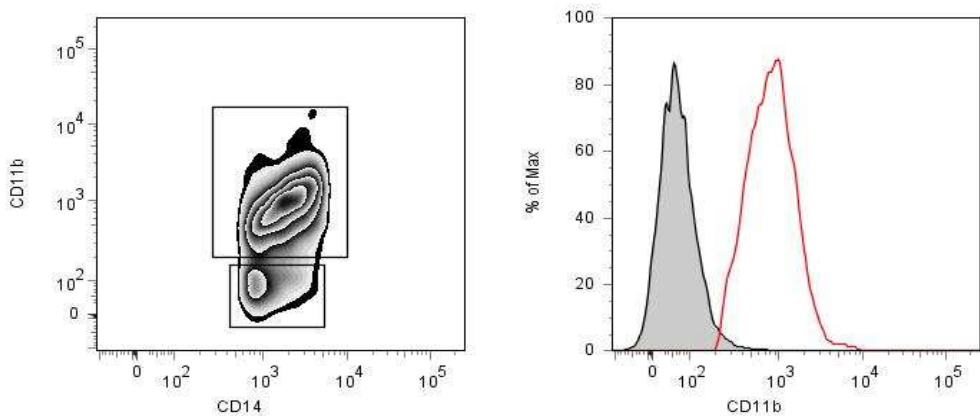


Figure 17. CD14⁺CD11b⁺ and CD14⁺CD11b⁻ cell populations. Left, CD14⁺ cells were found to be positive (larger box) and negative for CD11b (smaller box). CD11b positive cells were confirmed to be positive in comparison to isotype control, right histogram.

Staining for F4/80 was used to confirm that CD14⁺CD11b⁺ cells were macrophages. The double positive population was also positive for F4/80 as seen in Figure 18.

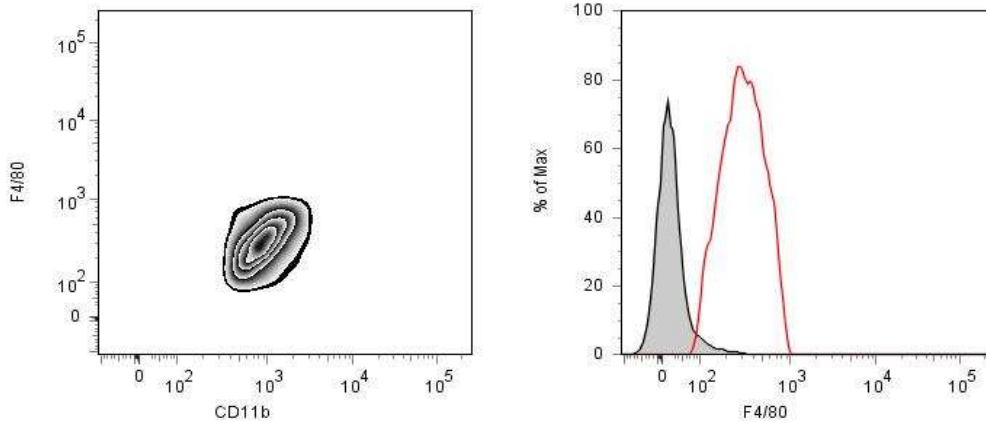


Figure 18. CD14⁺CD11b⁺ cells are F4/80 positive macrophages. The CD14⁺CD11b⁺ population was view in the F4/80 vs. CD11b zebra graph, left, and the histogram confirmed that the population was positive for F4/80, right.

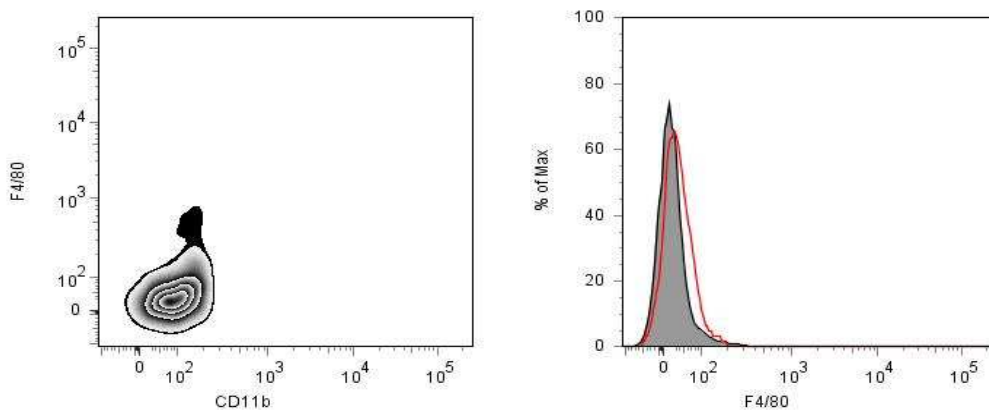


Figure 19. CD14⁺CD11b⁻ cells are not macrophages. The CD14⁺CD11b⁻ population was viewed in the F4/80 vs. CD11b zebra graph, left, and the histogram confirmed the population was negative for F4/80, right.

The CD14⁺CD11b⁻ cells were F4/80 negative, suggesting that they are not macrophages (Figure 19).

The CD14⁺CD11b⁺F4/80⁺ population was backgated to find the location of macrophages in a FSC-H (forward scatter- infers cell size) vs. SSC-A plot as seen by red contour circles outlining the triple positive macrophages (Figure 20). Immunofluorescence staining for CD11b showed the presence of macrophages in the tunica adventitia, similar to the MOMA-2 staining for macrophages in Figure 9. This CD14⁺CD11b⁺F4/80⁺ gate was used for all subsequent aortic digestion samples to locate aortic macrophages for analysis.

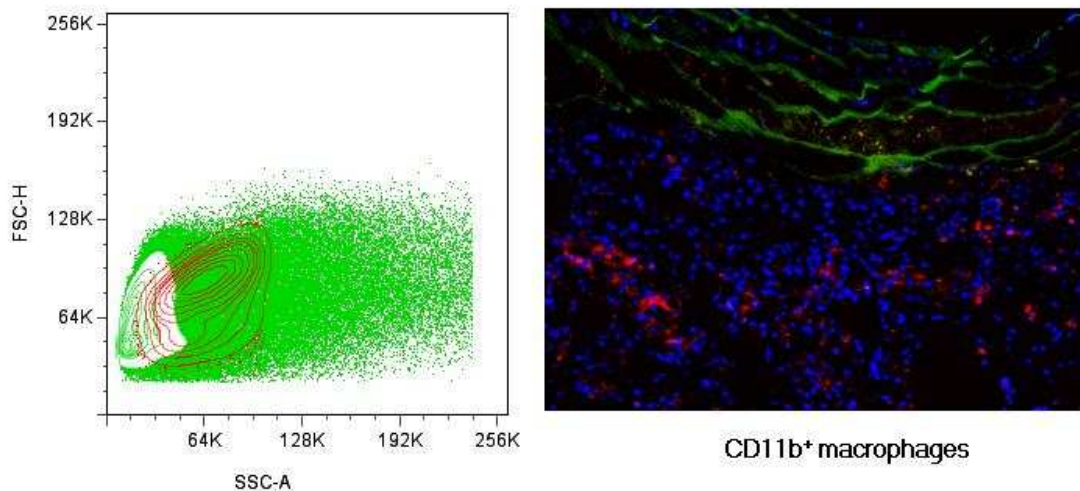


Figure 20. Backgating of CD14⁺CD11b⁺F4/80⁺ cells to determine the gate for macrophages. The triple positive cells in figure 18 were backgated using FlowJo to locate the macrophage population in a FSC-H vs. SSA-A plot, left. Contour plotting in red shows the macrophage population. The CD11b⁺ macrophages (red) were localized to the adventitia by immunofluorescence, right.

There are several pieces of evidence that strongly support aortic CD14⁺CD11b⁺ cells as aortic macrophages. First, these cells are positive for a pan-macrophage marker in mice, F4/80. Second, the position of this population in a FSC vs. SSC plot has been

shown to be the same position where monocytes/macrophages are located in humans and mice (226;227). In comparison to other major leukocytes, monocytes/macrophages have a greater FSC and SSC than lymphocytes, but a similar degree of FSC as neutrophils; however, neutrophils have a greater SSC due to the numerous granules in their cytoplasm (226). Third, surface expression of CD14 is found primarily on monocytes and macrophages at high levels (228-230). A small portion of neutrophils can express CD14, but they express it at low levels on the plasma membrane and most of the CD14 proteins are actually contained intracellularly in azurophilic granules, not on the surface (227;230). In general, neutrophils are classically considered to be CD14⁻ cells (231). Although mRNA for CD14 has been detected in a variety of extramyeloid cells such as epithelial cells by *in situ* hybridization, it is only clearly observable after stimulation with LPS; furthermore, the surface expression of CD14 proteins on those cells was not detected (228). Fourth, high expression of CD11b is primarily found consistently on the surfaces of monocytes and macrophages and not other leukocytes in peripheral blood, spleen, and bone marrow of mice (232). Other leukocytes like neutrophils can express CD11b also, but monocytes and macrophages are the major ones (233-235). Moreover, CD11b is highly accepted as an established marker for activation of monocytes and macrophages (236). Thus, based on the detection of F4/80, FSC and SSC characteristics with flow cytometry, and the fact that these cells are positive for both CD14 and CD11b, it is reasonable to conclude that the cells identified here are macrophages in the aorta. Figure 21 shows the presence of the double positive macrophage population that is also positive for F4/80. There is also a CD14⁻CD11b⁺ population that is not positive for F4/80. The identity of that cell population is not known, but the cells are certainly not mature macrophages. They might be neutrophils.

AORTIC MACROPHAGES IN SHAM- AND ANG II-TREATED WILD-TYPE MICE

Using the optimized parameters for aortic digestion and gating described above, aortic macrophages from sham- and Ang II-treated mice with and without aortic dissection were analyzed. In sham-treated aortas ($n = 15$), $CD14^+CD11b^+F4/80^+$ macrophages composed 0.46 ± 0.08 % (or $1,840 \pm 314$ macrophages) of all cells from the aorta obtained after digestion (Appendix B, Table 1). Figure 21 shows a contour graph of aortic macrophages from a sham-treated mouse. The quadrants in Figure 21 were based on isotype control staining and kept consistent in subsequent figures.

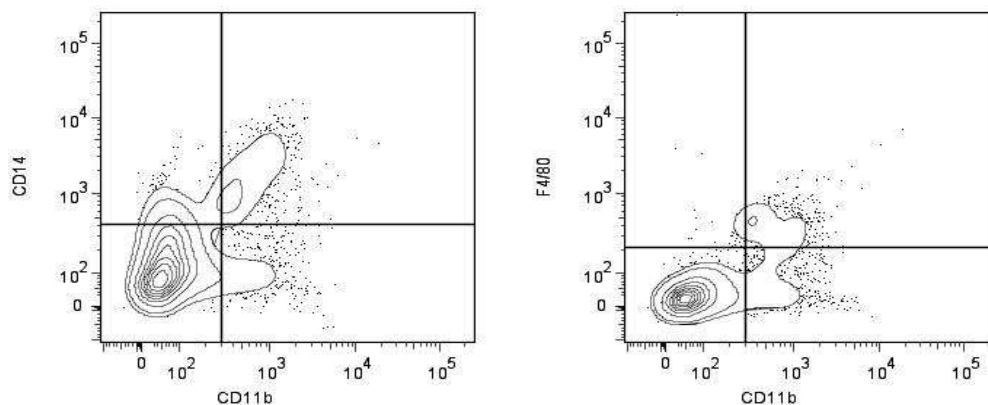


Figure 21. Aortic macrophages from a sham-treated mouse. $CD14^+CD11b^+$ macrophages (left) are also F4/80 positive (right).

Figure 22 shows a contour graph of macrophages from a mouse infused with Ang II. The macrophage population has increased to compose 2.44 ± 0.55 % of all cells in the aorta (or $9,750 \pm 2,218$ cells, $n = 11$) and CD14 and CD11b expression levels are higher. Figure 23 shows a contour graph of macrophages from a treated mouse with aortic dissection. 31.87 ± 2.39 % of all aortic cells are macrophages (or $127,452 \pm 9,575$ cells, $n = 4$).

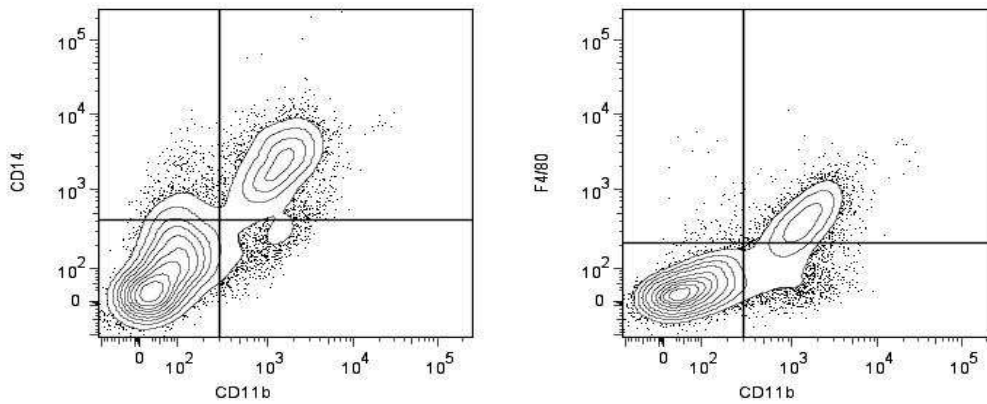


Figure 22. Aortic macrophages from an Ang II-treated mouse. $CD14^+CD11b^+$ macrophages (left) are also F4/80 positive (right).

Surface expressions of CD14 and CD11b on these macrophages are even greater than on macrophages from a mouse that did not develop aortic dissection. Interestingly, these macrophages are F4/80 negative. Although this may seem unexpected, it is supported by previous studies that show that activated macrophages lose expression of F4/80 (237-239).

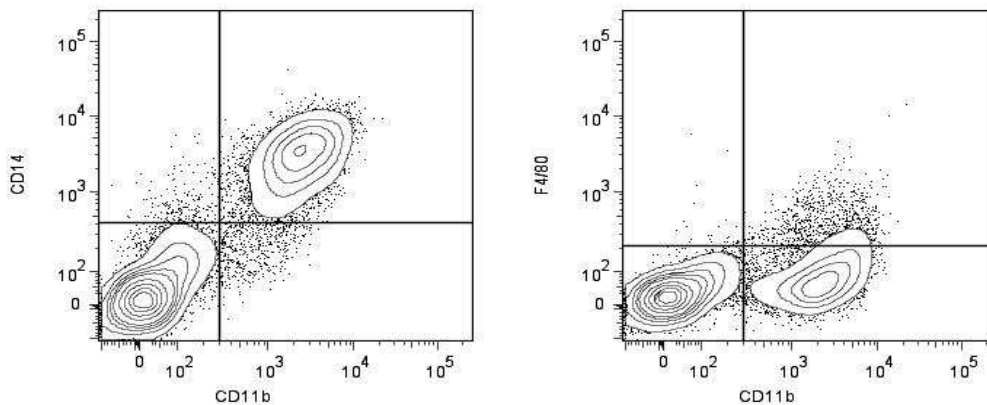


Figure 23. Aortic macrophages from an aortic dissection. $CD14^+CD11b^+$ macrophages (left) are not F4/80 positive (right).

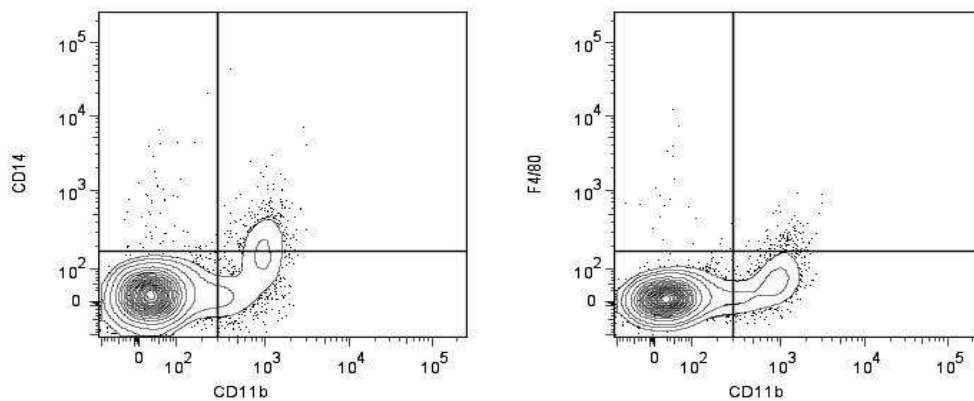


Figure 24. Peripheral blood monocytes. CD14⁺CD11b⁺ monocytes (left) are not F4/80 positive (right). Quadrants are based on isotype controls using peripheral blood samples.

Although the cells found in aortic dissections do not express F4/80, they are most likely not resting monocytes for several reasons. Compared to macrophages, peripheral blood monocytes do not express such high levels of CD14 or CD11b (Figure 24). The level of surface CD14 is much lower on monocytes than the macrophages from aortic dissections and produces a clearly distinct histogram (Figure 25A). The level of surface CD11b expression on monocytes was also less than macrophages from dissection, but there was some overlap as seen by histogram (Figure 25B). In addition, the CD14⁺CD11b⁺ cells from aortic dissections were digested from aortic tissue and did not come from peripheral blood since PBS was infused systemically to flush out blood. Any dead monocytes trapped in the hematoma of aortic dissections were removed with the washing steps during antibody staining and also were excluded based on low FSC properties. Therefore, these cells are most likely tissue macrophages.

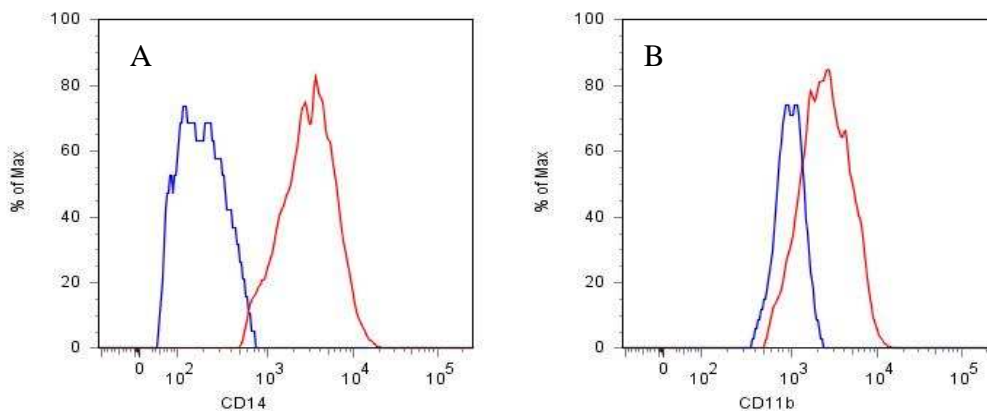


Figure 25. Peripheral blood monocytes compared to macrophages from aortic dissection. Monocytes (blue) have much less surface CD14 (left) and surface CD11b (right) than macrophages (red).

Of the aortic macrophages from the three groups, macrophages isolated from aortic dissection express the highest level of CD14 and CD11b (red curves in Figure 26A and 26B). Those from Ang II-treated animals without dissection had similar CD14 surface expression to macrophages from dissections, but their expression of CD11b was noticeably less (green curves in Figure 26A and 26B). Resident aortic macrophages from sham-treated animals had the lowest level of CD14 and CD11b (blue curves in Figure 26A and 26B). In terms of F4/80, aortic macrophages from sham- and Ang II-treated animals were positive for this marker, but those from dissections were negative or expressed it at low levels (Figure 26C).

Since MCP-1 levels increased with Ang II treatment (Figure 14), the aortic macrophages were stained for CCR2, the receptor of MCP-1, to determine whether MCP-1 could be contributing to the recruitment of monocytes to the aorta. Staining with an antibody against CCR2 revealed that resident aortic macrophages in sham-treated mice and the macrophages recruited with Ang II treatment were CCR2⁺ (Figure 27). Thus, aortic macrophages in sham- and Ang II-infused mice were CD14⁺CD11b⁺F4/80⁺CCR2⁺.

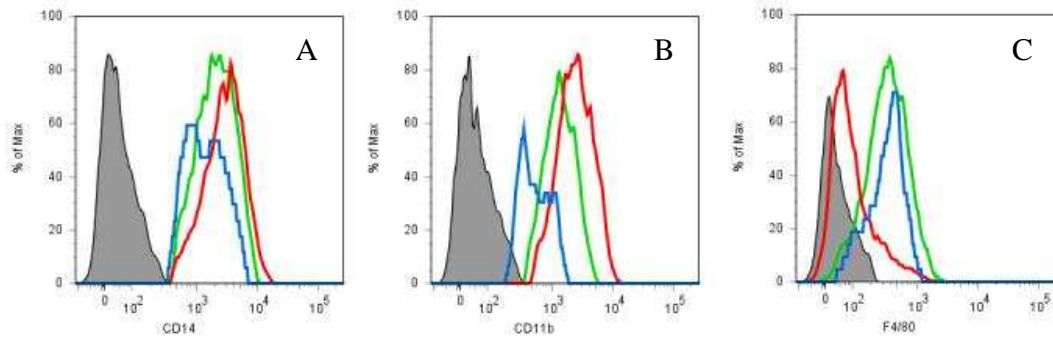


Figure 26. Comparison of expression levels of surface CD14, CD11b, and F4/80 on aortic macrophages from sham-treated (blue) and Ang II-treated mice (green) and mice with Ang II-induced aortic dissection (red)

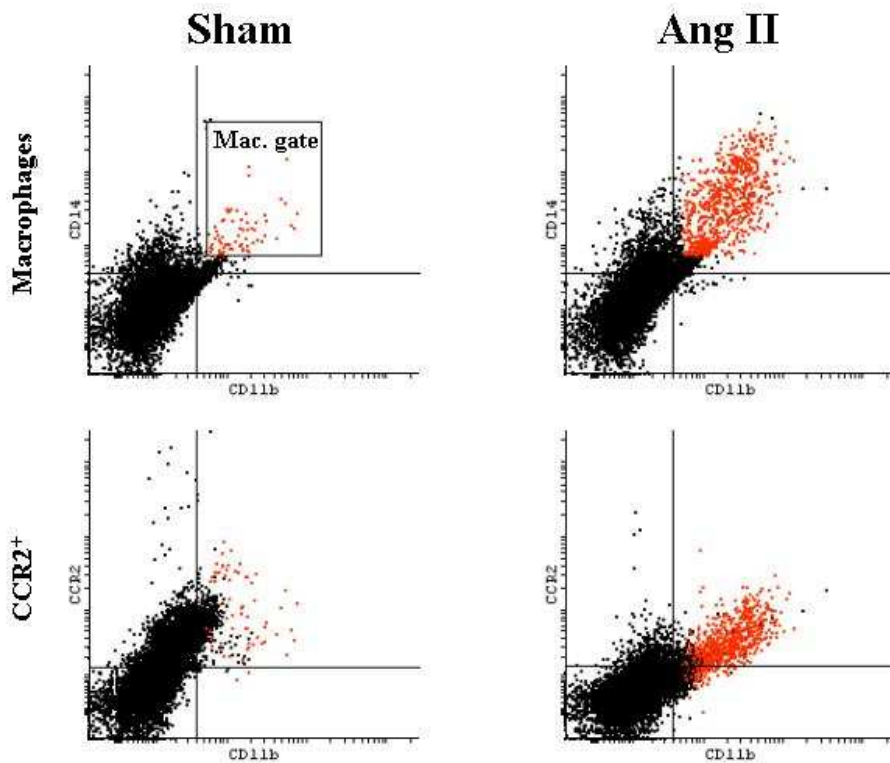


Figure 27. Aortic macrophages are CCR2⁺. CD14⁺CD11b⁺ macrophages were identified in sham-infused (top left) and Ang II-infused mice (top right) and gated (Mac. gate). Those gated macrophages appeared positive for CCR2 (red dots) in sham-treated (bottom left) and Ang II-treated mice (bottom right). Quadrants were determined by isotype controls.

In summary, a method of digesting the aorta was developed based on elastase and collagenase enzymes that allowed for the detection and characterization of aortic macrophages. This is the first report of using such technique to directly quantify and characterize aortic macrophages on several parameters including CD14, CD11b, F4/80, and CCR2. This technique gives the advantages of monitoring changes in the expression of relevant surface markers with treatment and disease and of changes that occur as monocytes differentiate into macrophages. These events give valuable insight into the

initiation and progression of vascular inflammation and aortic dissection. Using the technique, a significant increase in number of CD14⁺CD11b⁺ macrophages were observed with Ang II treatment, with the most seen in aortic dissections. In addition, there was a trend towards increased expression of cell-surface CD14 and CD11b with treatment and disease. That suggests that the increase in CD11b may be contributing to the ability of the macrophages to bind and migrate into the aorta and throughout aortic tissue. The modest increase in CD14 might also contribute to these processes because it has been shown that ligand binding to this protein can facilitate the ability of monocytes/macrophages to attach to substrate (240). Moreover, the loss of F4/80 on macrophages in aortas with dissection was unexpected, but the phenomenon was supported by literature showing that F4/80 is downregulated in activated macrophages *in vivo* (237;238). This finding clearly demonstrates the ability of this technique to isolate and characterize aortic macrophages and understand how they change with treatment and disease status. In addition, the increase in aortic macrophage number with Ang II infusion was most likely due to monocyte recruitment from peripheral blood into the aorta by MCP-1 since the macrophages were positive for the MCP-1 receptor and aortic MCP-1 was demonstrated to increase by 6.5-fold with treatment as described in Chapter 2. Taken together, we conclude that aortic macrophages are contributing significantly to Ang II-induced vascular inflammation and most likely play a role leading to aortic dissection.

Chapter 4: Role of CCR2⁺ Monocytes/Macrophages in Potentiating Vascular Inflammation and Aortic Dissection

The large increase in macrophages in aortas of Ang II-treated animals suggests that these cells may significantly contribute to Ang II-induced inflammation and aortic dissection, but their role has not been clearly delineated. Whether they are involved in inducing or potentiating the increases in cytokines described in Chapter 2 or in causing aortic dissection remains to be elucidated. Knowing the answers to these unknowns will shed valuable light into better understanding how vascular inflammation comes about in this model and can possibly be generalized to the process that occurs in cardiovascular diseases in humans.

The best way to study the role of macrophages is to use a model in which macrophages are selectively depleted while other conditions remain unaffected. Although this is not currently possible, at the current time, the closest option is the CCR2^{-/-} mouse model that has been used to study monocytes and macrophages in cardiovascular diseases. These mice lack the receptor for MCP-1 and cannot respond to this chemokine (160;161). Moreover, this model has significantly reduced numbers of circulating monocytes in peripheral blood, which leads to fewer macrophages present in areas of inflammation (160;161). This reduction has been hypothesized to be due to the important role that MCP-1 plays in monocyte migration from bone marrow to blood. The few monocytes that are circulating do not express CCR2; however, many published findings using this model cannot be totally attributed specifically to the lack of response to MCP-1 by monocytes. Decreased recruitment of T-lymphocytes, B-lymphocytes, Natural Killer cells (NK cells), dendritic cells, and others are expected to play a factor in the results also. An excellent way to overcome this confounding factor(s) would be to restore a pure

population of a single cell type into this knockout mouse and observe the effects of changing this one defined parameter. Of interest here would be the transfer of CCR2^{+/+} monocytes (also known as WT monocytes) into CCR2^{-/-} mice. This is relevant because macrophages recruited to the aorta express this receptor in WT mice and because aortic MCP-1 is highly induced by Ang II. Since there are no endogenous cells to compete with the adoptive cells, the role of CCR2 positive monocytes and macrophages can be directly studied. The results obtained can be directly attributed to the transferred monocytes when compared to the knockout background without adoptive transfer. Another advantage is that this approach can allow for the observations of events that would not normally occur in this knockout background, and direct tracking of the adoptive CCR2^{+/+} monocytes can be performed. In this chapter, the responses to Ang II treatment in CCR2^{-/-} mice are first characterized and then adoptive transfer experiments are presented to demonstrate the role of CCR2⁺ monocytes and macrophages in vascular inflammation and aortic dissection formation.

CCR2^{-/-} MICE DEVELOP BLUNTED RESPONSES TO ANG II TREATMENT

Previously, it has been shown that compared to Ang II-treated CCR2^{+/+} mice, Ang II infusion into dyslipidemic CCR2^{-/-} mice lead to reduced atherosclerotic lesion area in the aorta and decreased incidence of abdominal aortic aneurysm (10 %) along with blunted vascular remodeling (127;164). Bone marrow transplant studies have shown that transfer of bone marrow from CCR2^{-/-} mice into apoE^{-/-} mice reduces atherosclerotic lesion area, but not after lesions were already established (159). Therefore, it seems that CCR2⁺ leukocytes accelerate the initiation of vascular inflammation leading to atherosclerosis and aneurysms, but these cells may not be necessary for maintenance of those diseases. Moreover, CCR2^{-/-} mice also develop reduced adventitial remodeling compared to WT mice in response to Ang II. There is decreased fibrosis of the tunica

adventitia and significantly fewer macrophages present in the aortic wall (127). However, all of these studies cannot prove that CCR2⁺ monocytes are solely responsible for these events and their role in Ang II-induced aortic dissection is not known.

In response to a short-term, high-dose infusion of Ang II, CCR2^{-/-} mice do not secrete the same level of aortic cytokines as WT mice (Figure 28). Measurement of IL-6 secreted from explanted aortas of treated CCR2^{-/-} showed a concentration of 12,917 ± 2,088 pg/mL (*n*=7) in incubation medium while medium from sham-treated animals had a concentration of 6,323 ± 1,618 (*n*=6) (Figure 28). Although the 2-fold increase with treatment was statistically significant compared to sham-treatment, *P*<0.02, this level was well less than that observed for Ang II-treated WT mice (IL-6 concentration of 28,808 ± 1,300 pg/mL), which was more than 2-fold greater.

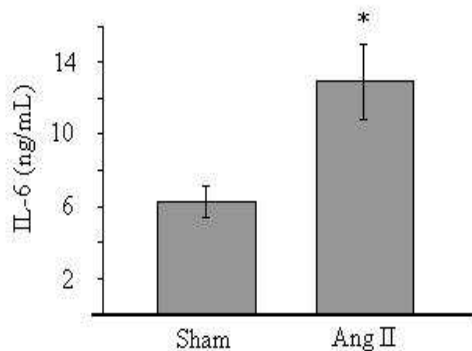


Figure 28. Secreted aortic IL-6 levels in culture medium containing aortas from sham- or Ang II-infused CCR2^{-/-} mice after 6 d. *, *P*<0.02 vs. sham-treatment. Data are expressed as mean ± SEM

Measurement of MCP-1 secreted from explanted aortas of treated CCR2^{-/-} showed a concentration of 907 ± 210 pg/mL in incubation medium while medium from sham-treated animals had a concentration of 380 ± 169, Figure 29. Although the increase with treatment was statistically significant compared to sham-treatment, *P*<0.05, this level was well less than that observed for WT mice (MCP-1 concentration of 1,918 ± 174 pg/mL) which was more than 2-fold greater.

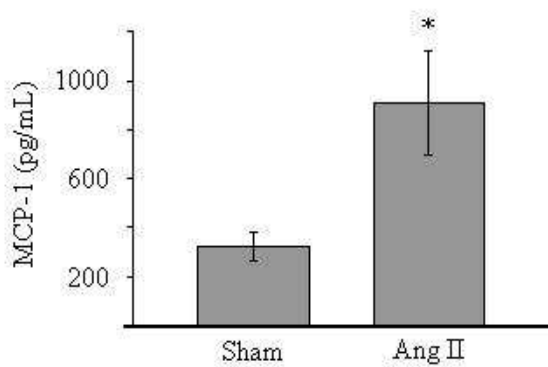


Figure 29. Secreted aortic MCP-1 levels in culture medium containing aortas from sham- or Ang II-infused CCR2^{-/-} mice after 6 d. *, $P < 0.05$ vs. sham-treatment. Data are expressed as mean \pm SEM

The amount of macrophages in the aorta was quantified using the aortic digestion technique described above (Chapter 3). CD14⁺CD11b⁺F4/80⁺ aortic macrophages in sham-treated mice were identified using flow cytometry (Figure 30). Figure 31 shows a representative flow cytometry graph of aortic macrophages from an Ang II-treated mouse.

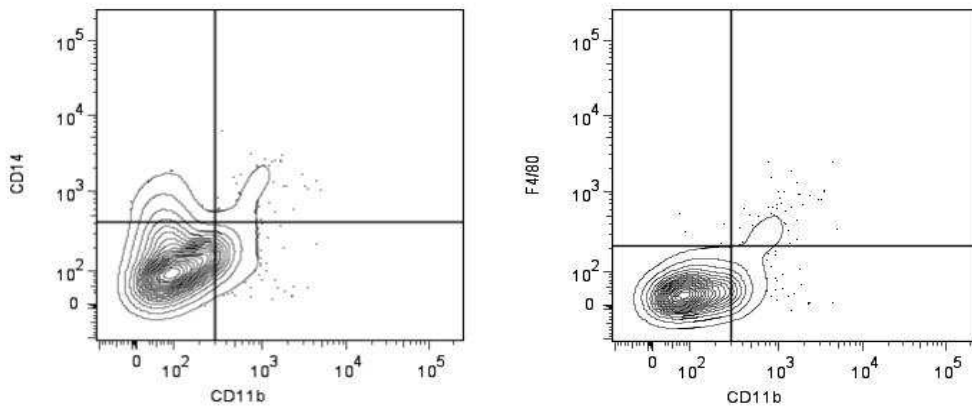


Figure 30. Aortic macrophages from sham-treated CCR2^{-/-} mice. CD14⁺CD11b⁺ macrophages were identified (left) and confirmed to be F4/80⁺ (right)

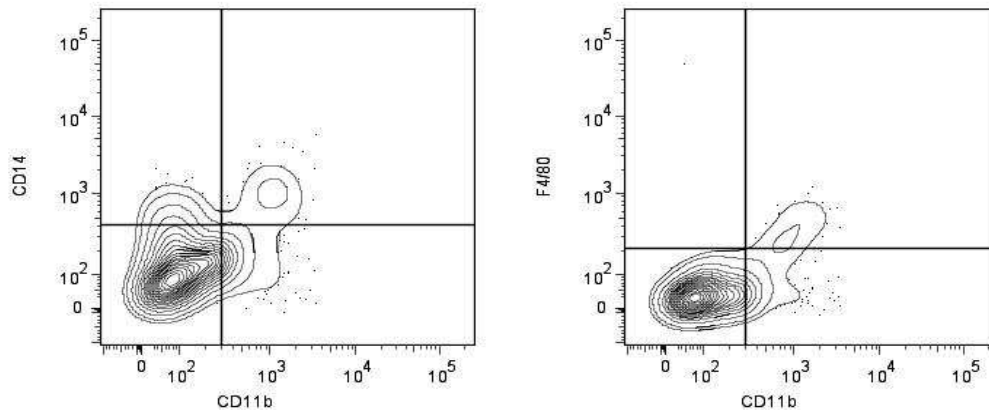


Figure 31. Aortic macrophages from Ang II-infused $CCR2^{-/-}$ mice. $CD14^{+}CD11b^{+}$ macrophages were identified (left) and confirmed to be $F4/80^{+}$ (right)

There were $2,626 \pm 106$ $CD14^{+}CD11b^{+}$ aortic macrophages ($n=7$) in Ang II-treated mice while the aortas from sham-treated mice had 942 ± 102 macrophages ($n=7$), appendix B, Table 1. Although there was a 2.8-fold increase in the number of macrophages, it was still well less than the 5.3-fold increase seen in treated WT mice without dissection and less than the 69-fold increase seen in WT mice with dissection. Moreover, the percentage of cells that were macrophages in the aorta was less compared to WT animals in both the sham-treated and treated groups (0.24 ± 0.03 % in sham-treated $CCR2^{-/-}$ aorta vs. 0.46 ± 0.08 % in sham-treated WT aorta and 0.66 ± 0.03 % in treated $CCR2^{-/-}$ aorta vs. 2.44 ± 0.55 % in treated WT aorta without dissection). The numbers of resident aortic macrophages in $CCR2^{-/-}$ mice were significantly fewer than resident aortic macrophages in WT mice ($P<0.006$), and the numbers of recruited macrophages in treated aortas were significantly less also ($P<0.004$). Although immunohistochemistry on aortic cross sections spanning a short length of aorta have shown reduced macrophage recruitment in $CCR2^{-/-}$ mice, this is the first report of

systematic quantitation of aortic macrophages from the entire aorta. In addition, no dissections were observed in CCR2^{-/-} infused with Ang II after 6 d.

ADOPTIVE TRANSFER OF CCR2^{+/+} MONOCYTES RESTORED VASCULAR INFLAMMATION AND AORTIC DISSECTION

Since CCR2^{-/-} mice lack CCR2⁺ monocytes, have reduced numbers of macrophages, and based on the fact that macrophages are known to play an integral role in vascular inflammation and cardiovascular diseases, we hypothesized that adoptive transfer of CCR2^{+/+} monocytes into CCR2^{-/-} mice could rescue the cytokine induction and aortic dissection to levels observed in WT mice. Previously, it has been shown that Ang II treatment of irradiated WT mice receiving bone marrow of CCR2^{-/-} mice produces blunted vascular inflammation and remodeling, similar to Ang II-treatment of CCR2^{-/-} mice (127). Although that study claimed that monocytes/macrophages were the critical cells inducing vascular inflammation and remodeling, there was insufficient data to support this conclusion. The technique used does not allow for studying the role of a single cell type. Only a correlation between the lack of CCR2⁺ monocytes/decreased presence of macrophages in aortic tissue and the blunted effects to Ang II treatment could be made from the previous work. Other cell types coming from the bone marrow that expresses CCR2 can be playing a role in vascular inflammation and cannot be ruled out with bone marrow transplant experiments. Thus, the role of CCR2⁺ monocytes/macrophages in contributing to the full responses to Ang II remains to be proven. To do so, we performed adoptive transfer of CCR2^{+/+} monocytes into CCR2^{-/-} mice was performed.

Monocytes were isolated from peripheral blood obtained by heart puncture from WT C57BL/6J mice. Approximately 0.7-1.0 mL of blood was obtained per mouse with an average of 0.8 mL per mouse. Blood was collected into sterile EDTA coated tubes

chilled on ice. Red blood cells (RBCs) were lysed prior to isolation of monocytes using a negative selection process where monocytes were purified based on exclusion from antibody binding. This method was chosen to keep monocytes in the inactive state and to prevent antibody masking of antigens of interest. This procedure was performed using a custom murine monocyte isolation kit from StemCell Technologies according to the manufacturer's protocol. Briefly, the antibody cocktail included antibodies against CD2, CD5, CD45R, and F4/80 and bound to cells in peripheral blood except for monocytes. The antibodies were then tagged with dense particles creating a complex of cell-antibody-dense particle that could be separated based on its greater density compared to untagged monocytes with a separation medium. The average yield was approximately 234,000 monocytes per mL of blood, and 1.5×10^6 monocytes were planned for injection into each recipient mouse; this number has been reported to be in the physiological range for mice (241). Therefore, eight WT mice were sacrificed to harvest the appropriate amount of blood to give enough monocytes to inject into each $CCR2^{-/-}$ mouse. Analysis using flow cytometry showed that >95 % of the cells isolated were positive for CD14 (not shown). After isolation, the cells were doubled-labeled with DiR800, an infrared dye that emits signal at 800 nm and PKH26, a dye fluorescing similarly to Texas Red. The DiR800 label allows for detection of the adoptive monocytes *in vivo* with imaging on the LI-COR Odyssey machine while the PKH26 allows for detection of the same monocytes in thin tissue sections by fluorescence microscopy using a rhodamine filter (Figure 32). The main purpose of labeling these cells was to determine whether $CCR2^{+/+}$ monocytes homed to the aorta where vascular inflammation and aortic dissections are observed.

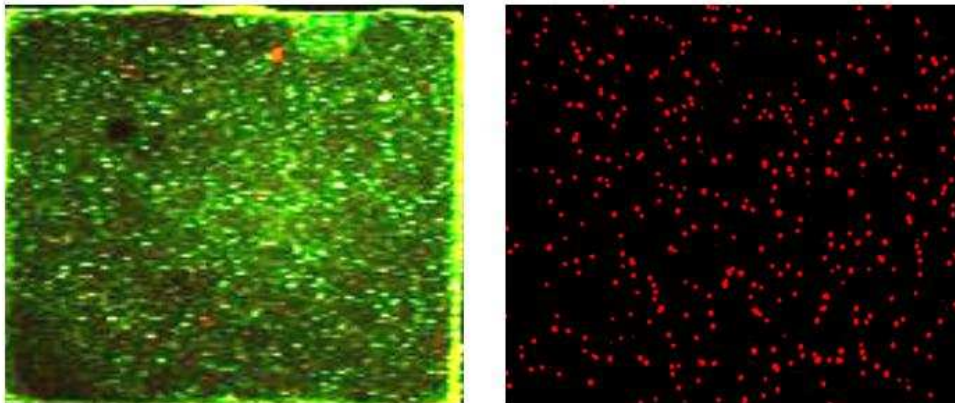


Figure 32. DiR800 and PKH26 labeled monocytes. WT monocytes were labeled with DiR800 and detected on the LI-COR Odyssey in the 800 nm channel (left-green cells). The same cells were labeled with PKH26 and detected by fluorescence microscopy (right-red cells at 20x magnification).

Injections of the labeled monocytes were performed into tail veins on day six after infusion with Ang II or saline for sham-treated animals, and the animals were sacrificed at day ten, allowing four days for the monocytes to circulate. The mice were imaged with the LI-COR Odyssey while anesthetized, and subsequently, the hearts and aortas were harvested after perfusion with PBS to flush out blood and imaged. Representative images of treated and non-treated mice injected with labeled monocytes are shown in Figure 33.

As seen in Figure 33, LI-COR imaging allowed for detailed visualization of the entire mouse body on the ventral and dorsal sides along with the location of the injected monocytes. Images of the backs clearly show the ears, head, body, hind feet, and tail. On the ventral side, the nose, mouth, front feet/hands, thorax, abdomen, and tail can be seen. The green color shows the location of adoptive transferred monocytes predominantly in the spleen as seen on the dorsum and in the liver as seen on the ventrum. Organ localization was confirmed by removing abdominal contents (Figure 34). Green can also be seen in the tail, where the monocytes were injected.

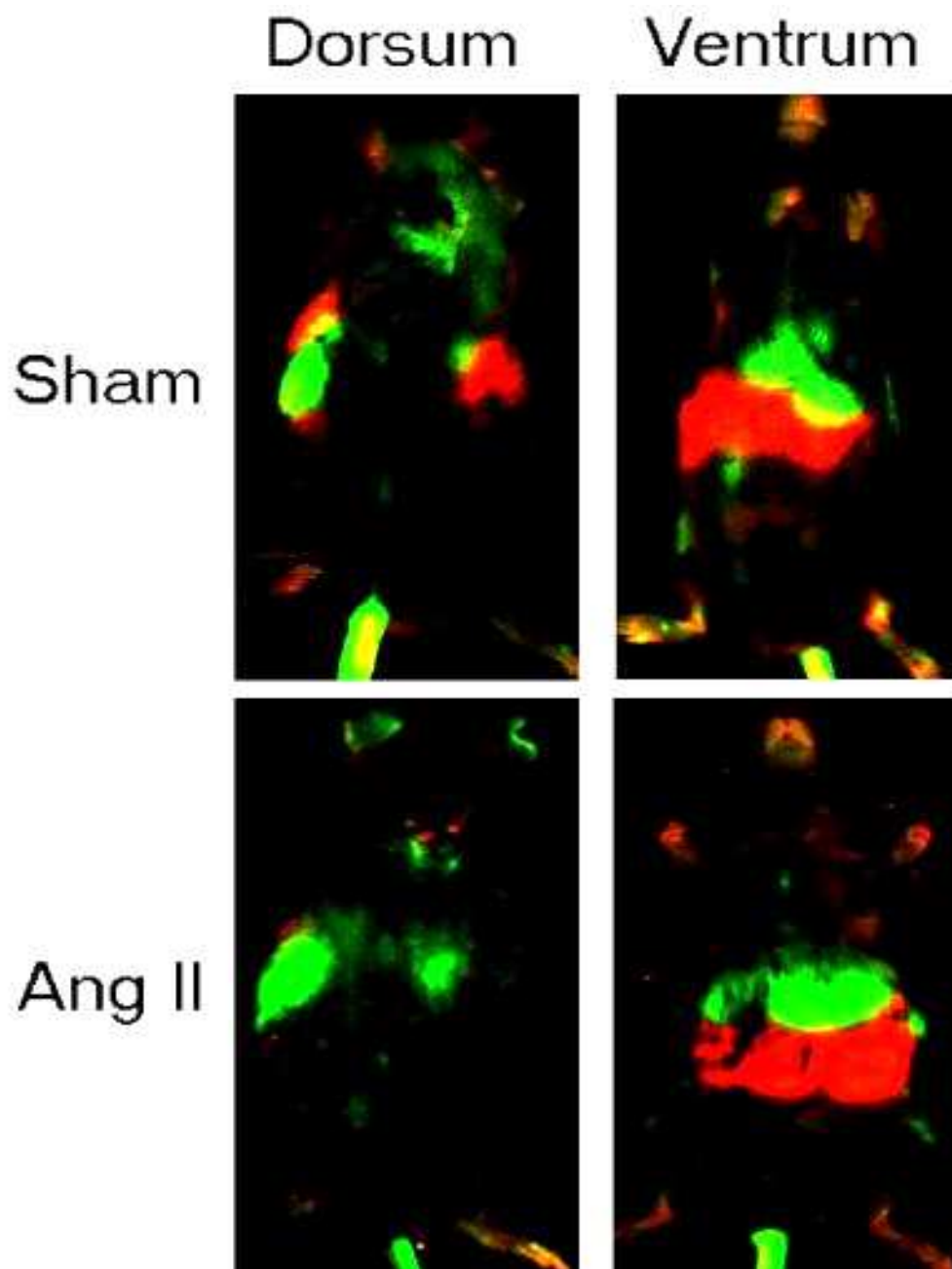


Figure 33. LI-COR imaging of $CCR2^{-/-}$ mice injected with DiR800-labeled WT monocytes. Sham-infused (top) and Ang II-infused mice (bottom) were imaged from the back (dorsum) and front (ventrum). Green color shows location of monocytes. Red color is tissue autofluorescence at 700 nm.

In addition, it can be seen at the mid-scapular incision where the osmotic pumps were inserted subcutaneously to deliver Ang II or saline and at the ears along the edges where punches were placed for identification. The red color seen in Figure 33 is tissue autofluorescence at 700 nm. The main organs with red autofluorescence are those of the gastrointestinal tract, specifically the stomach and colon (Figure 34).

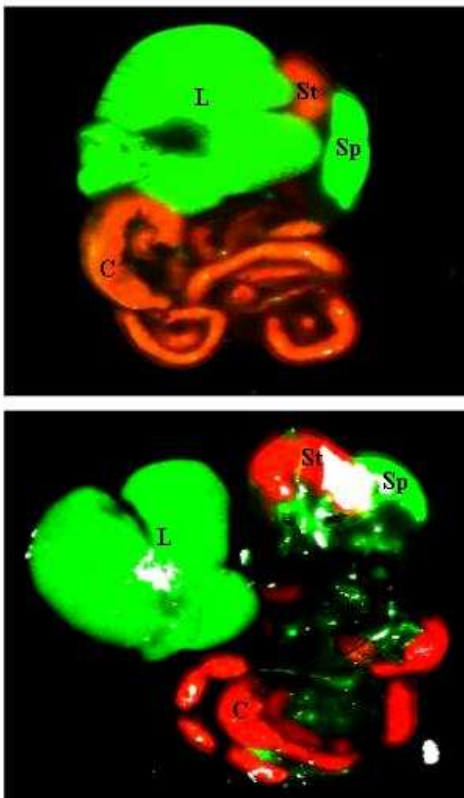


Figure 34. *Ex vivo* imaging of abdominal contents on LI-COR Odyssey. Organs of the GI tract were removed intact and imaged at 700 nm (Red) and 800 nm (Green) simultaneously. The liver (L), stomach (St), spleen (Sp), and colon (C) are identified. Green color shows the location of DiR800 labeled monocytes and can be seen in the liver and spleen. Red color shows autofluorescence of the stomach and colon.

As stated above, the main purpose of labeling $CCR2^{+/+}$ monocytes was to visualize their homing to the aorta. Since imaging of the entire animal on the LI-COR Odyssey did not produce enough resolution to detect the heart and aorta, these organs were removed for *ex vivo* imaging (Figure 35). Imaging of the hearts and aortas showed two hot spots for $CCR2^{+/+}$ monocyte recruitment in Ang II-treated mice. The first is at

the aortic root and ascending aorta (seen in 5/7 mice) and the second is at the suprarenal aorta, immediately above the branching of the renal arteries (seen in 6/7 mice). 4/7 mice had homing of CCR2^{+/+} monocytes into both regions. These are also the same areas where aortic dissections have been observed in this mouse model. Interestingly, it was observed that CCR2^{+/+} monocytes were detected predominantly in the infrarenal aorta, below the renal arteries.

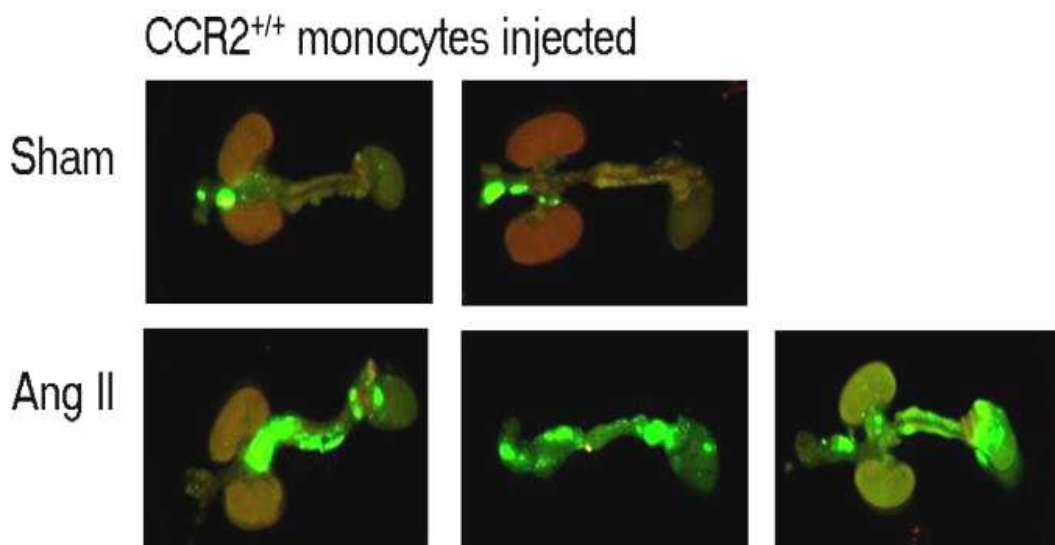


Figure 35. Imaging of DiR800-labeled CCR2^{+/+} monocytes in the aorta of CCR2^{-/-} mice. DiR800 labeled monocytes are seen in green. In aortas from sham-treated mice, homing was seen to the infrarenal region of the aorta (top), while in Ang II treated aortas, homing was seen predominantly in two hot spots. One hot spot was seen in the suprarenal aorta, immediately above the branching of the renal arteries (bottom left and middle) and the second hot spot was seen in the aortic root/ascending aorta region (bottom left and middle)

As a control for this adoptive transfer experiment, monocytes from CCR2^{-/-} mice were isolated and injected into CCR2^{-/-} recipient mice. This served as a good comparison to show the specificity of CCR2^{+/+} monocyte homing to the aorta and as control for the adoptive transfer process to ensure that the findings observed are not due to an artifact of

injection or introduction of 1.5×10^6 cells into circulation. $CCR2^{-/-}$ monocytes did not home to the same hot spots seen with $CCR2^{+/+}$ monocytes in treated mice; however, they were seen in the infrarenal aorta of both sham- and Ang II-treated mice (Figure 36).

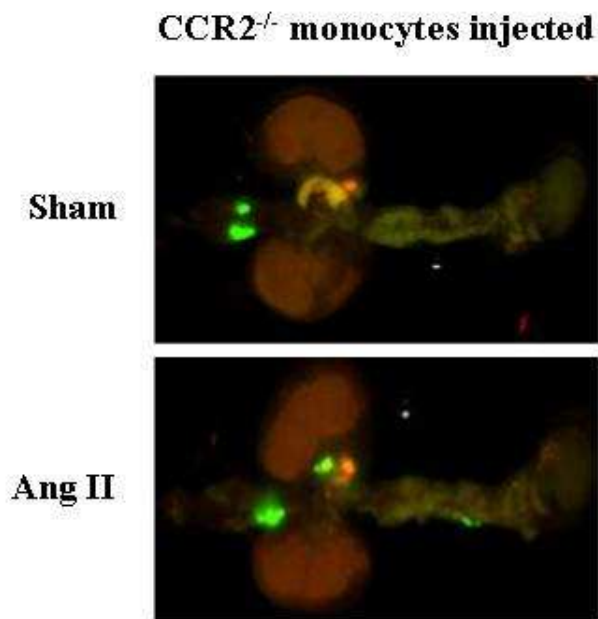


Figure 36. Imaging of DiR800-labeled $CCR2^{-/-}$ monocytes in the aorta of $CCR2^{-/-}$ mice. $CCR2^{-/-}$ monocytes were harvested from $CCR2^{-/-}$ mice and injected into $CCR2^{-/-}$ recipients with and without Ang II treatment (bottom and top, respectively). Green color shows location of monocytes.

The aortas were explanted into incubation medium for measurement of IL-6 and MCP-1 secreted from the aortas. The concentration of IL-6 in incubation media containing aortas from non-treated mice receiving $CCR2^{-/-}$ monocytes was $7,096 \pm 2,310$ pg/mL ($n=5$), and it was $7,066 \pm 2,176$ pg/mL ($n=5$) in media containing aortas from non-treated mice receiving $CCR2^{+/+}$ monocytes (Figure 37). Although the averages were slightly higher than that reported above for sham-treated $CCR2^{-/-}$ mice in Figure 28, the differences were not statistically significant ($P=0.40$ for both compared to sham-treated $CCR2^{-/-}$ alone). Similarly, the concentration of MCP-1 in incubation media containing

aortas from non-treated mice receiving CCR2^{-/-} monocytes was 339 ± 72 pg/mL, and it was 314 ± 96 pg/mL in media containing aortas from non-treated mice receiving CCR2^{+/+} monocytes. These values are not statistically significant from that reported for sham-treated CCR2^{-/-} mice in Figure 28 ($P=0.40$ for both compared to sham-treated CCR2^{-/-} alone). Moreover, with Ang II infusion in mice receiving CCR2^{-/-} monocytes, the concentration of aortic IL-6 and MCP-1 were 14,643 ± 1,558 pg/mL and 640 ± 58 pg/mL ($n=6$), respectively. These levels were significant increases of 2.1-fold for IL-6 and 1.9-fold for MCP-1 compared to non-treated mice receiving native monocytes ($P=0.01$ for IL-6 and $P=0.006$ for MCP-1). As expected, they were not statistically significant compared to the levels reported in Figures 28 and 29 for Ang II-treated CCR2^{-/-} mice ($P=0.26$ IL-6 and $P=0.14$ for MCP-1) and were not close to the concentrations obtained from the aortas of WT mice. Interestingly, adoptive transfer of CCR2^{+/+} monocytes into CCR2^{-/-} mice infused with Ang II restored the WT secretory phenotype. The concentration of IL-6 was 26,232 ± 6,098 pg/mL ($n=6$) and that was significantly greater (by 1.8-fold) than the concentration of aortic IL-6 from Ang II-infused mice receiving CCR2^{-/-} monocytes ($P<0.05$). Likewise, the concentration of MCP-1 was 2,861 ± 857 pg/mL and that was significantly greater (by 4.5-fold) than the concentration of MCP-1 from Ang II-infused mice receiving CCR2^{-/-} monocytes ($P<0.03$). These values were similar to those obtained for Ang II-treated WT mice as reported in Figures 13 and 14 and were not statistically different in comparison ($P=0.33$ for IL-6 and $P=0.16$ for MCP-1); however, the fold increase in MCP-1 was much greater between treated and non-treated CCR2^{-/-} mice receiving CCR2^{+/+} monocytes (9.1-fold) than the 6.5-fold increase seen in WT mice reported above. Although these measurements show that IL-6 and MCP-1 are being induced in response to Ang II in the presence of WT monocytes, it is unclear where these cytokines are being produced in the aorta.

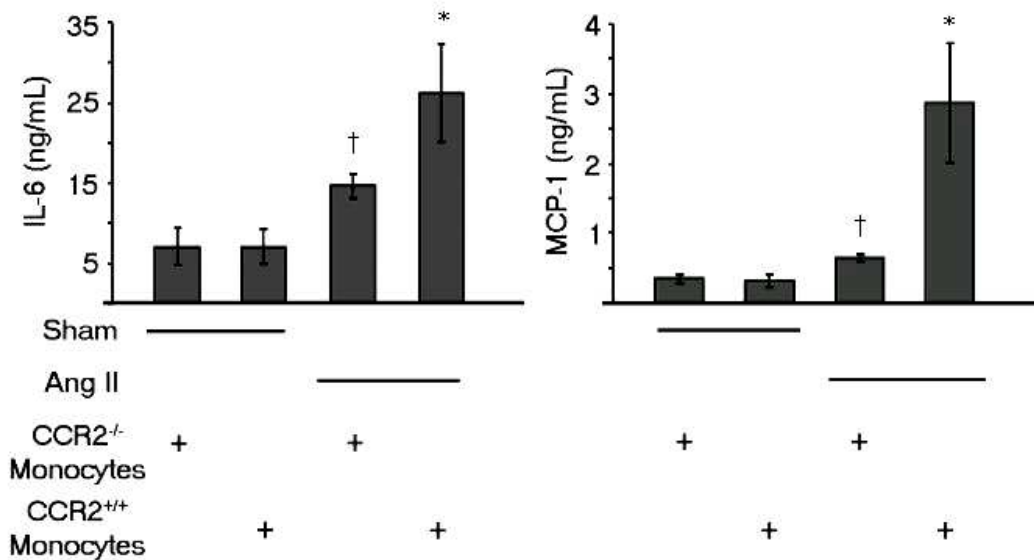


Figure 37. Secreted aortic IL-6 and MCP-1 levels from adoptive transfer experiments. CCR2^{-/-} or CCR2^{+/+} monocytes were injected into CCR2^{-/-} recipients with or without Ang II infusion. Aortas were harvested on day 4 post-injection and incubated in culture medium. †, $P < 0.05$ between sham-treated and treated mice receiving CCR2^{-/-} monocytes. *, $P < 0.05$ between sham-treated and treated mice receiving CCR2^{+/+} monocytes and between treated mice receiving CCR2^{+/+} monocytes and treated mice receiving CCR2^{-/-} monocytes.

Immunofluorescence analysis of cross sections of the aortas from CCR2^{-/-} mice receiving CCR2^{+/+} monocytes revealed that the IL-6 and MCP-1 was predominantly localized to the adventitia or adventitia-media border, respectively (Figure 38). IL-6 was detected in the intima also. Moreover, MCP-1 was seen in some regions of the media and faintly in the adventitia. The adoptively transferred WT macrophages were identified in cross sections without additional staining because of the PKH26 dye labeling prior to injection. Since aortic tissue does not have red autofluorescence, any red signal detected without additional staining had to be from the PKH26 labeled monocytes/macrophages.

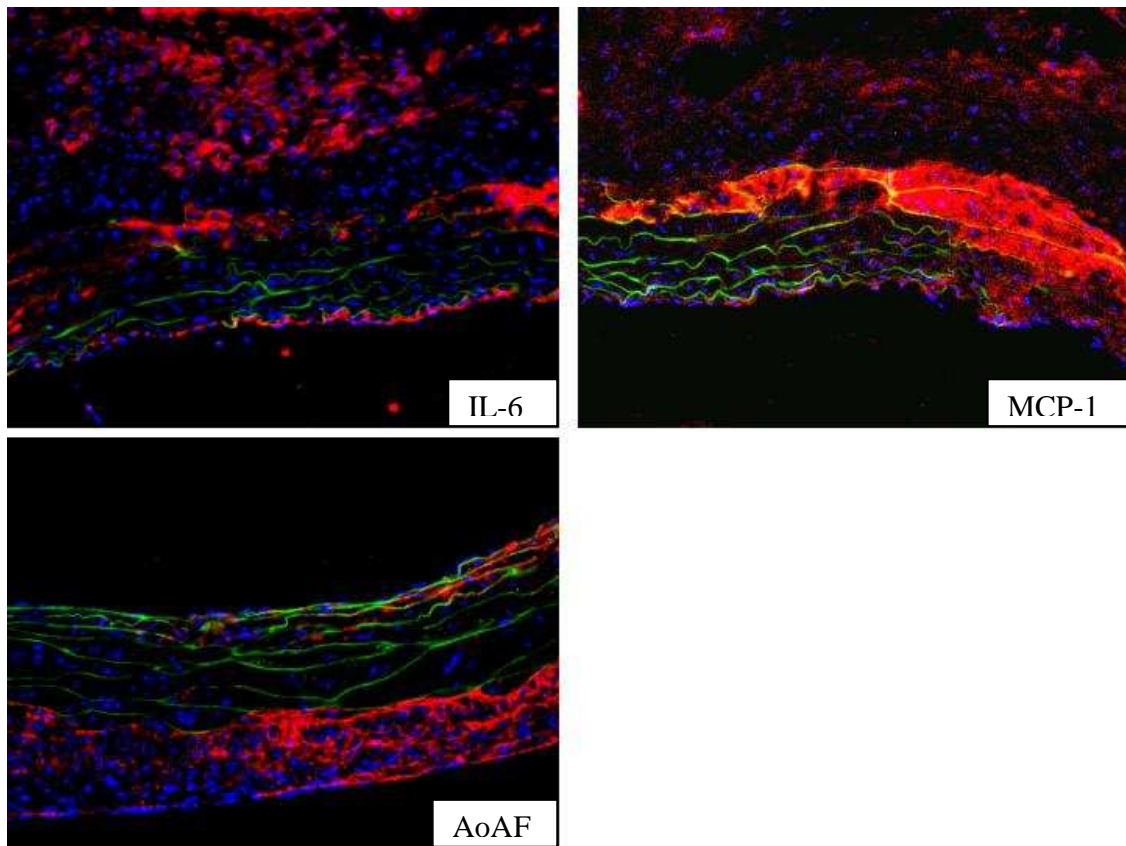


Figure 38. Staining for IL-6, MCP-1, and AoAF in the ascending aorta of Ang II-treated CCR2^{-/-} mice injected with WT monocytes. IL-6 (red) was detected primarily in the tunica adventitia (top left) while MCP-1 (red) was detected in the adventitia-media border and media (top right). AoAFs (red) were localized to the adventitia (bottom).

The macrophages seem to be invading into media and intima from the adventitia on the left and right of a tear through the media, Figure 39. A possible source producing the majority of IL-6 could be the adventitial fibroblasts since staining for AoAF overlaps the same region where IL-6 was detected. In addition, the MCP-1 could be coming from the CCR2^{+/+} macrophages recruited to the aorta since staining for MCP-1 overlapped the same region where macrophages were detected. These observations could not be

confirmed because the green autofluorescence mostly from the elastic lamellae prevented the use of green and red for co-localization studies.

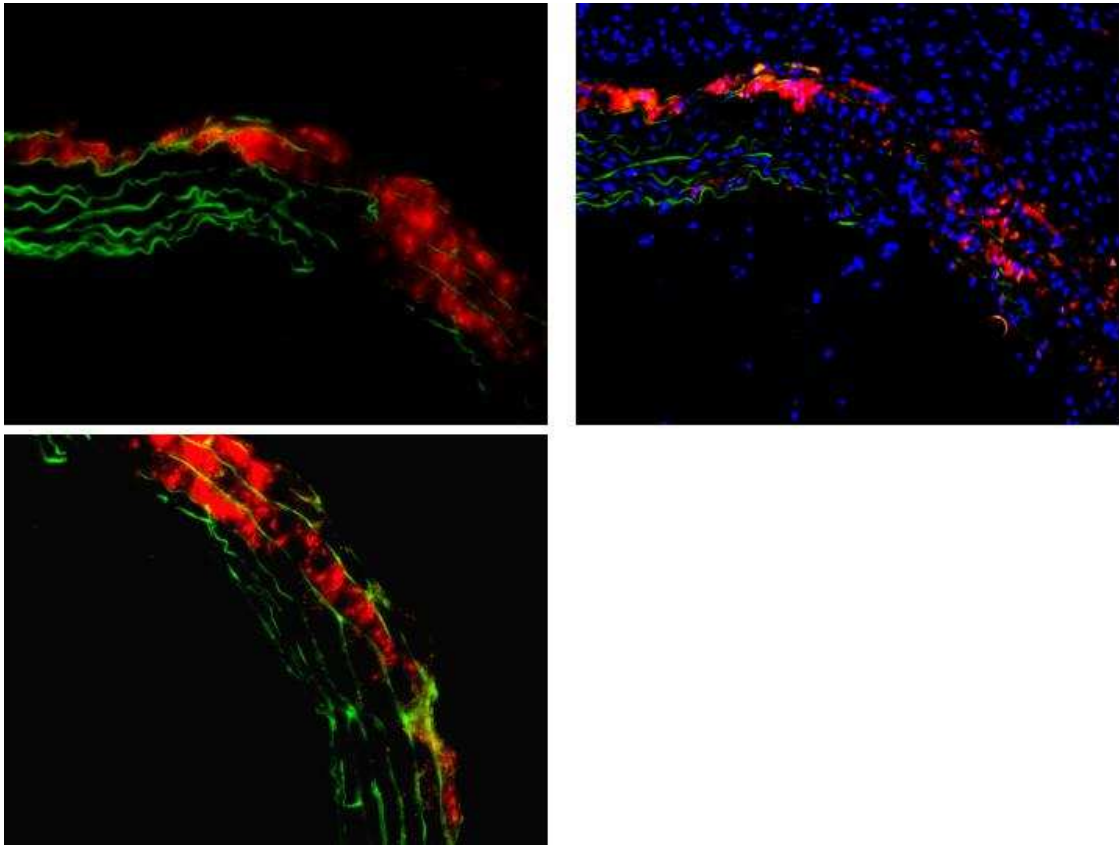


Figure 39. WT macrophages in the ascending aorta of Ang II-treated $CCR2^{-/-}$ mice. WT PKH26-labeled macrophages (red) were identified in the adventitia, media, and intima (top left) and confirmed to be cells with nuclei by DAPI staining (top right). Image of the adjacent area of the same section from the right (bottom)

Adoptive transfer of WT monocytes increased the incidence of aortic dissection. A total 4/7 of $CCR2^{-/-}$ mice receiving $CCR2^{+/+}$ monocytes and Ang II infusion developed aortic dissection while no dissections (0/5) were observed in treated mice receiving $CCR2^{-/-}$ monocytes, Figure 40. In addition, although no dissections were seen by day 6 of treatment in $CCR2^{-/-}$ mice, it was later found that the incidence of aortic dissection in

CCR2^{-/-} mice infused with Ang II for 10 d was actually 15 % (2/13). Adoptive transfer of CCR2^{+/+} monocytes into this background increased this incidence to 57 % on day 10. This incidence rate is also higher than the incidence of 35 % seen in WT mice.

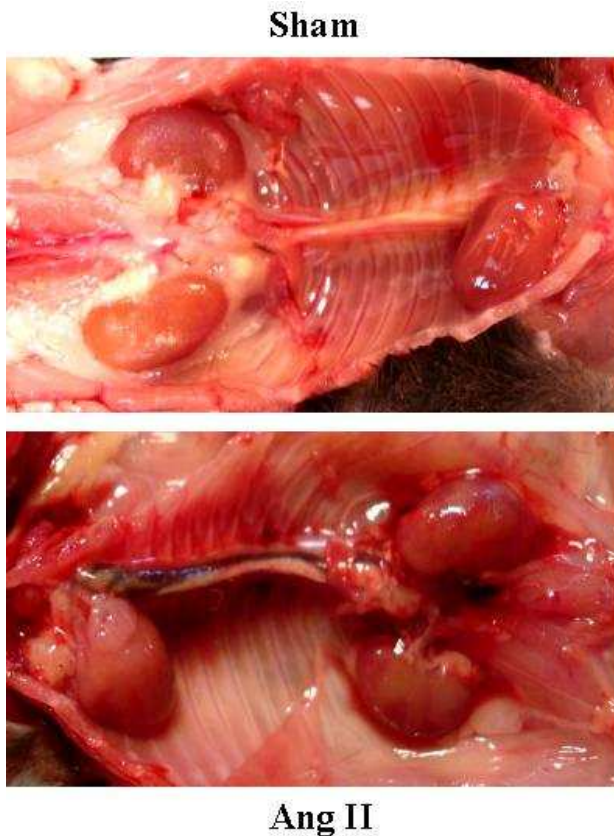


Figure 40. Aorta of CCR2^{-/-} mice receiving WT monocytes. Non-treated mice did not develop aortic dissection (top) while 57 % of the mice treated with Ang II developed aortic dissection as seen by the hematoma in aortic tissue.

In summary, CCR2^{-/-} mice did not develop the same level of responses with Ang II treatment, but adoptive transfer of CCR2^{+/+} monocytes into this background restored WT phenotype of secretion and aneurysm and dissection. The induction of aortic IL-6 and MCP-1 was significantly reduced and was associated with very low recruitment of aortic macrophages compared to WT mice. Moreover, these mice did not develop aortic dissection by 6 d of Ang II infusion like WT animals. CCR2^{+/+} monocytes adoptively

transferred into these knockout mice were seen to specifically home to areas where aortic dissections have been observed in the WT aortas in response to Ang II and to the infrarenal aorta in sham-treated mice. After 4 d of injection, WT monocytes caused a potentiation of aortic IL-6 and MCP-1 to levels seen in WT mice infused with Ang II over 6 to 10 d and aortic dissection at an incidence of 57 %, which is even greater than that seen in WT mice. Adoptive transfer of CCR2^{-/-} monocytes did not produce the same effects, but gave results equivalent to sham-treated and treated CCR2^{-/-} mice alone. The injected WT macrophages were seen to invade into the layers of the aorta from the tunica adventitia toward tears in the intima and media in cross section of aortic tissue. Based on knowledge that macrophages are capable of producing proteolytic enzymes to cause tissue destruction, this suggests that CCR2^{+/+} monocytes/macrophages might play a significant role in creating an environment conducive for aortic dissection.

Chapter 5: Role of IL-6 on MCP-1 Induction and Macrophage Differentiation

IL-6 plays multifaceted roles in vascular inflammation and cardiovascular diseases (18;108). It is also of particular interest to know the roles of IL-6 on cell types that play a prominent part in cardiovascular diseases, particularly macrophages.

IL-6 stimulation is well known to promote macrophage differentiation, growth arrest, and eventual apoptosis *in vitro* (242-248). Experiments using myeloid leukemia cells, M1 and HL-60, and the Y6 cell line show that 3 d of exposure to IL-6 induces development of mature macrophages (249-252). These cells increase in size, develop a large cytoplasm containing vacuoles, and have irregularly shaped nuclei (253-256). They also become attached to culture dishes *in vitro* instead of staying in suspension (257). Functionally, these cells have increased esterase and phagocytic activities (258). Surface expression of C3 complement, Fc, and macrophage-colony stimulating factor (M-CSF) receptors are up-regulated directly by IL-6 (259-261). CD36, an oxidized lipid uptake receptor, has been shown to be induced by IL-6 in mouse peritoneal macrophages (262). In contrast, a related receptor, the macrophage scavenger receptor 1a (MSR1a), has been shown to be down-regulated in THP-1 monocytes in response to IL-6 (263). Furthermore, IL-6 induces gene expression typical of macrophages. Early response genes: c-Jun, jun B, jun D, interferon-regulatory factor 1 (IRF1), *Jak3*, and Egr-1 are immediately up-regulated (264-267). However, expression of c-myc mRNA goes down within hours of IL-6 stimulation, facilitating growth arrest and differentiation (268-271). Bcl-2 and cyclin D1 are down-regulated subsequently, increasing susceptibility to apoptosis (272;273). Late response genes: *lysozyme* and *ferritin light-chain* are induced during terminal differentiation (274;275). Moreover, upon stimulation with IL-6, U937

monocytic cells up-regulate MCP-1 mRNA and protein, a chemokine more strongly expressed in macrophages than monocytes (276).

Thus, most roles for IL-6 on monocyte to macrophage differentiation have been discovered primarily *in vitro* using transformed cell lines, primary isolations from peripheral blood, or easily accessible macrophages like peritoneal macrophages, but not the actual monocytes or macrophages in cardiovascular tissues where the diseases occur. Those findings are extrapolated to tissue macrophages *in vivo*, but the *in vitro* results do not always correlate well with what is actually happening *in vivo*. Therefore, it is important to be able to study the effect of IL-6 on cardiovascular tissue macrophages *in vivo*. The digestion technique described in Chapter 3 allows for the study of aortic macrophages in vascular inflammation of the aorta and aortic dissection. In this chapter, we compare WT and IL-6^{-/-} mice in response to Ang II. Any differences observed in IL-6^{-/-} mice will be due to the lack of IL-6 since all other parameters will remain equal. Thus, these experiments allow for the direct study of the role of IL-6 on aortic macrophages.

BLUNTED AORTIC MCP-1 SECRETION IN IL-6^{-/-} VS. WILD-TYPE MICE IN RESPONSE TO ANG II

Since it is known that IL-6 can directly stimulate MCP-1 production in peripheral blood mononuclear cells, vascular smooth muscle cells, and endothelial cells (171;172;277), we hypothesized that the aortas from IL-6^{-/-} mice infused with Ang II produced less MCP-1 than WT mice. IL-6^{-/-} mice were infused with Ang II or saline for 6 d and their aortas were harvested for incubation in culture medium as described above. Measurement of MCP-1 showed a concentration of 222 ± 61 pg/mL (*n*=7) in media from sham-treated aortas and 749 ± 100 pg/mL (*n*=7) in media from Ang II-treated aortas (Figure 41). Although the increase was statistically significant with Ang II infusion

($P < 0.001$), the concentration was not as great as that observed from WT mice. The level of aortic MCP-1 from treated IL-6^{-/-} mice was significantly less than the $1,918 \pm 174$ pg/mL observed in treated WT mice ($P < 0.0001$) while the concentration for sham-treated samples were similar. Therefore we concluded that IL-6 controls aortic MCP-1 production *in vivo*.

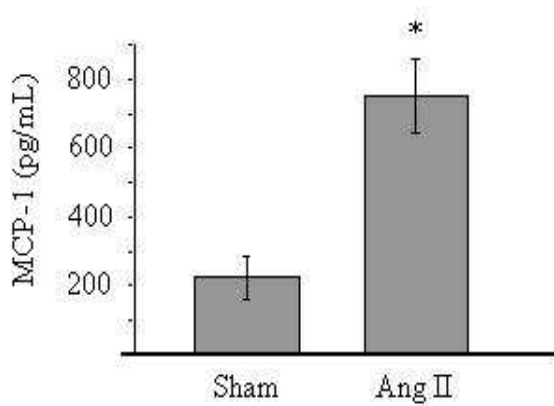


Figure 41. Secreted aortic MCP-1 levels in culture medium containing aortas from sham- or Ang II-infused IL-6^{-/-} mice after 6 d. *, $P < 0.05$ vs. sham-treatment. Data are expressed as mean \pm SEM

IL-6^{-/-} MICE HAVE REDUCED NUMBERS OF AORTIC MACROPHAGES WITH DIFFERENT PHENOTYPES COMPARED TO WILD-TYPE MICE

The amount of macrophages in the aorta was quantified using the newly described aortic digestion technique. CD14⁺CD11b⁺F4/80⁺ aortic macrophages in sham-treated mice were identified using flow cytometry (Figure 42). Figure 43 shows a representative flow cytometry graph of aortic macrophages from an Ang II-treated mouse. It is interesting to note that the CD14⁺CD11b⁺ aortic macrophages in IL-6^{-/-} mice were distinctly positive for F4/80 in response to Ang II treatment.

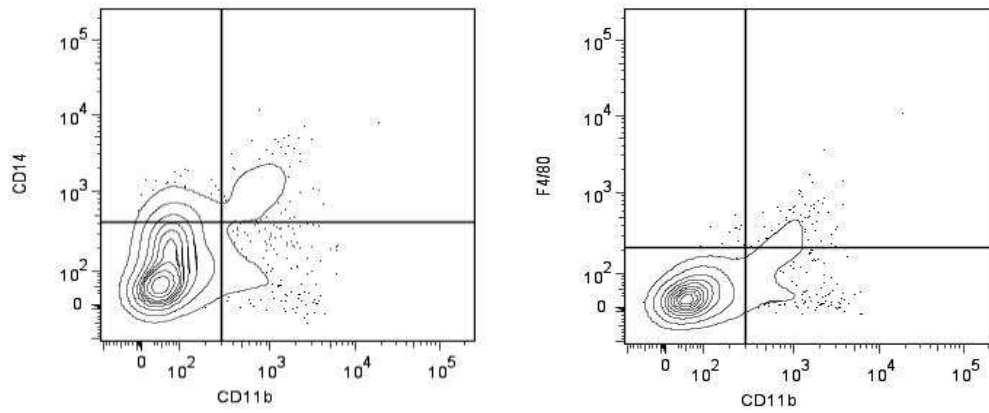


Figure 42. Aortic macrophages from sham-treated IL-6^{-/-} mice. CD14⁺CD11b⁺ macrophages were identified (left) and confirmed to be F4/80⁺ (right)

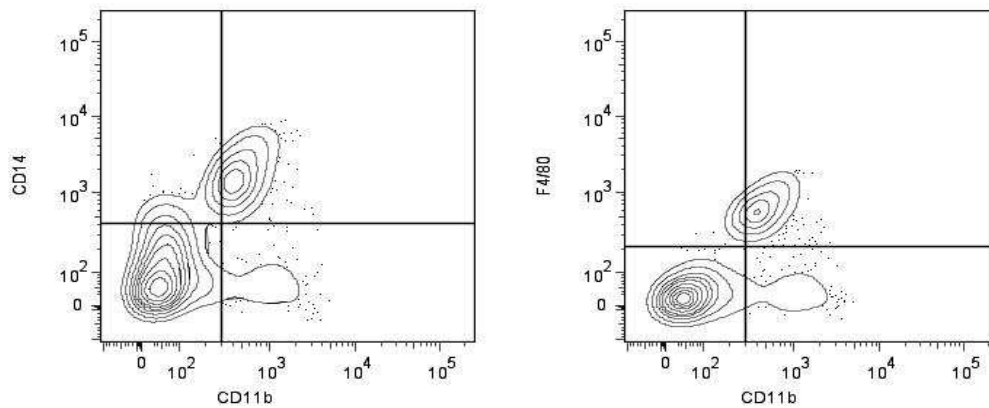


Figure 43. Aortic macrophages from Ang II-treated IL-6^{-/-} mice. CD14⁺CD11b⁺ macrophages were identified (left) and confirmed to be F4/80⁺ (right)

There were $4,812 \pm 998$ CD14⁺CD11b⁺ aortic macrophages ($n=8$) in Ang II-treated mice while the aortas from sham-treated mice had $1,317 \pm 217$ macrophages ($n=9$) (Appendix B, Table 1). Although there was a 3.7-fold increase in the number of macrophages, it was still well less than the 5.3-fold increase seen in treated WT mice without dissection and less than the 69-fold increase seen in WT mice with dissection. Moreover, the percentage of cells that were macrophages in the aorta was less compared

to WT animals, but greater than CCR2^{-/-} mice in both the sham-treated and treated groups (0.33 ± 0.05 % in sham-treated IL-6^{-/-} aorta vs. 0.46 ± 0.08 % in sham-treated WT vs. 0.24 ± 0.03 % in sham-treated CCR2^{-/-} and 1.20 ± 0.25 % vs. 2.44 ± 0.55 % vs. 0.66 ± 0.03 % in treated aortas, respectively). Interestingly, the numbers of resident aortic macrophages in IL-6^{-/-} mice were not significantly fewer than resident aortic macrophages in WT mice (*P*=0.09) or CCR2^{-/-} mice (*P*=0.07); they were almost halfway between the values from CCR2^{-/-} and WT mice. On the other hand, the numbers of recruited aortic macrophages in IL-6^{-/-} mice in response to Ang II were significantly fewer than recruited macrophages in WT mice (*P*<0.031), but significantly greater than in CCR2^{-/-} mice (*P*<0.033). In addition, no dissections were observed in IL-6^{-/-} infused with Ang II after 6 d.

Based on the flow cytometry data, it was observed that the surface expressions of CD14 and CD11b on aortic macrophages from treated IL-6^{-/-} mice were less than their expression on macrophages from treated WT animals. A comparison was performed between the expression of CD14, CD11b, and F4/80 on aortic macrophages from Ang II-infused IL-6^{-/-} mice, WT mice without dissections, and WT mice with aortic dissection (Figure 44). As shown, the expression of CD11b was the greatest on aortic macrophages from aortic dissections and the least on aortic macrophages from treated IL-6^{-/-} mice (Figure 44B). Macrophages from aortas without dissection had an intermediate expression of CD11b. The differences in expression of surface CD14 were not as distinct, but there were similar trends like for CD11b. A large range of expression for CD14 was observed on macrophages from WT aortas without dissection; macrophages from dissections had expression of CD14 towards the higher end while macrophages from treated IL-6^{-/-} mice had expression of CD14 towards the lower end of that range (Figure 44A).

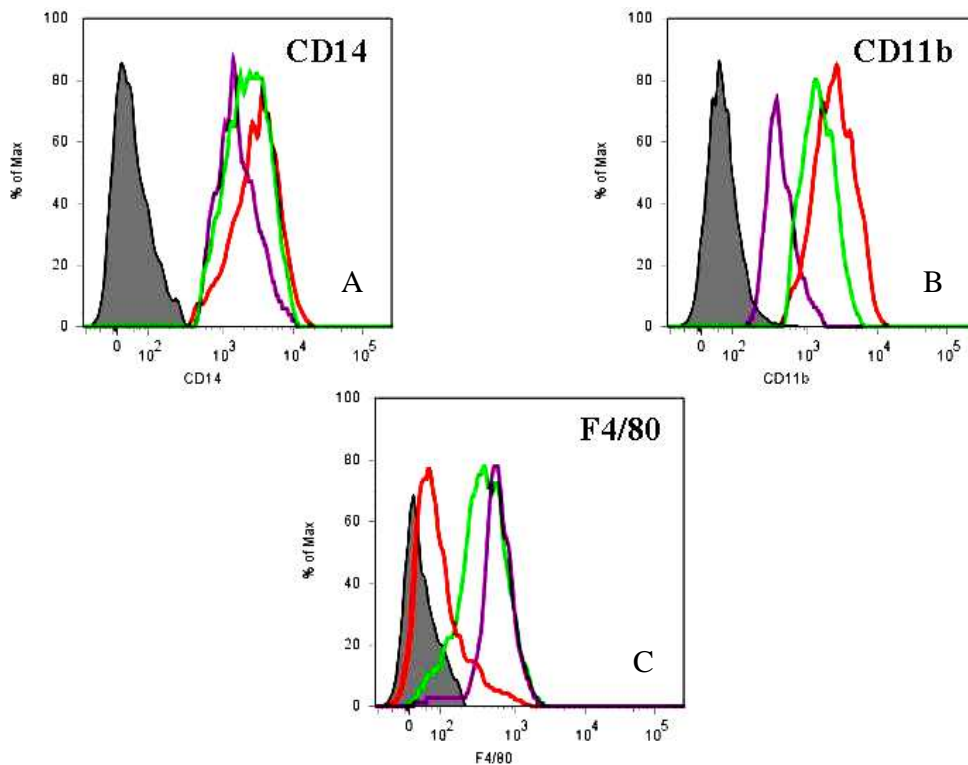


Figure 44. Comparison of surface CD14, CD11b, and F4/80 expression on aortic macrophages between treated IL-6^{-/-} and WT mice. The expression curves for Ang II-infused IL-6^{-/-} mice, treated WT mice, and treated WT mice with aortic dissection are represented in purple, green, and red, respectively.

F4/80 expression on treated WT mice was clearly positive as compared to the low or negative expression of this marker on macrophages from aortic dissections (Figure 44C). Interestingly, the expression of F4/80 on aortic macrophages from treated IL-6^{-/-} mice trended towards the higher end of the range seen in treated WT mice (Figure 44C).

IL-6 SIGNALING IS ACTIVE IN AORTIC MACROPHAGES FROM TREATED WILD-TYPE MICE, BUT NOT IN IL-6^{-/-} MICE

gp130-Jak/STAT3 signaling is required for IL-6-induced monocyte to macrophage differentiation *in vitro* (278). Mutation of the tyrosine residue at position

126 in the YXXQ motif of gp130 prevents STAT3 activation and the subsequent growth arrest and differentiation of M1 cells into macrophages (279). Furthermore, STAT3 activation downstream of the receptor has been shown to be required because dominant-negative forms of STAT3 block differentiation (280;281). Specifically, Minami et al. showed that inhibiting STAT3 prevented induction of the following macrophage markers: Fc receptors, *ferritin light chain*, and *lysozyme*; moreover, c-myc was not down-regulated and the cells continued to proliferate, unlike differentiated macrophages *in vitro* (282). Likewise, over-expression of *Jak3*, which is also induced rapidly by IL-6, accelerates macrophage differentiation (283). Moreover, as shown above, IL-6 causes aortic macrophages to be CD14^{hi}CD11b^{hi} macrophages that are different than normal, resident macrophages. In addition, it is also known that IL-6 induces particular functions in macrophages, like the production of cytokines and uptake of oxidized LDL. Thus, IL-6 activates the gp130-Jak/STAT signaling pathway leading to differentiation of monocytes into macrophages of a particular active type, which can significantly contribute to their role to the pathogenesis of cardiovascular diseases.

Therefore, it was of great interest to determine whether CD14⁺CD11b⁺ aortic macrophages had active IL-6 signaling. Since phosphorylated STAT3 (p-STAT3) was shown previously to be induced by IL-6 in LDLR^{-/-} mice infused with Ang II (123), it was used as the specific marker for IL-6 signaling. Aortic digestion followed by flow cytometry was performed to detect CD14, CD11b, and phospho-STAT3 at tyrosine 705. In sham-treated WT mice, resident CD14⁺CD11b⁺ were identified as described above, but they were not determined to be p-STAT3 positive (Figure 45). However, with Ang II infusion the recruited CD14⁺CD11b⁺ macrophages were positive for p-STAT3 (Figure 46).

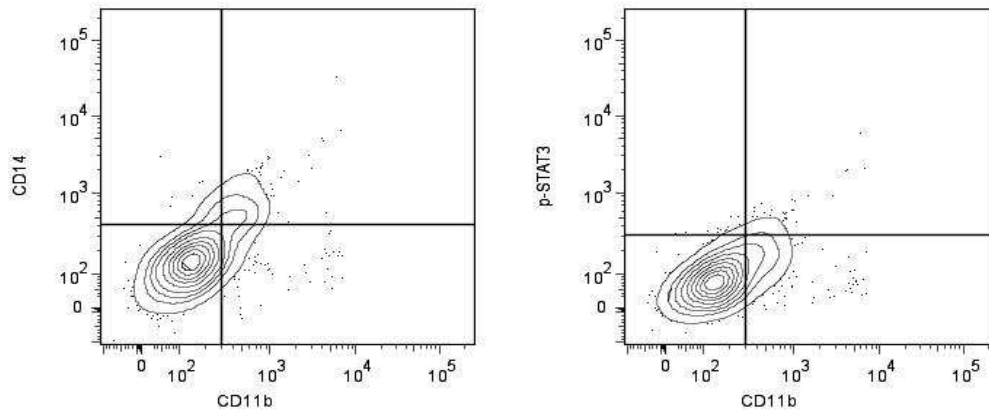


Figure 45. IL-6 signaling is not active in resident aortic macrophages of sham-treated WT mice. Aortic macrophages were identified as CD14⁺CD11b⁺ (left) and found to be negative for p-STAT3 at Tyr⁷⁰⁵

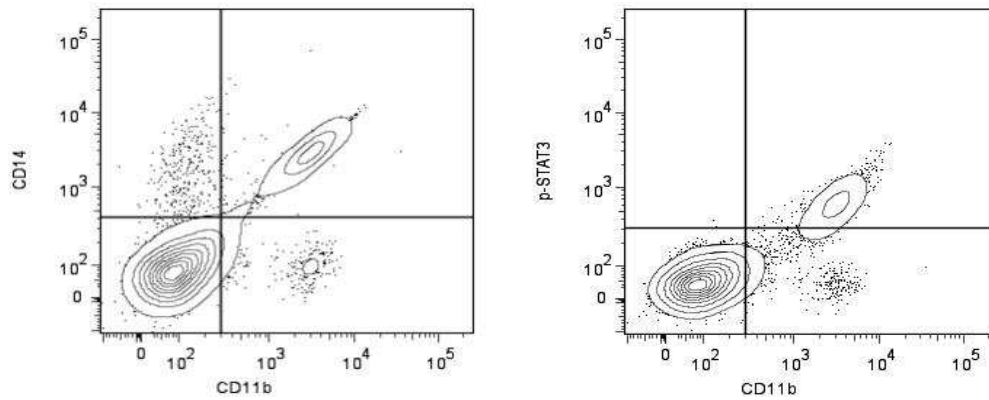


Figure 46. IL-6 signaling is active in recruited aortic macrophages of Ang II-infused WT mice. Aortic macrophages were identified as CD14⁺CD11b⁺ (left) and found to be positive for p-STAT3 at Tyr⁷⁰⁵

To confirm that this event was specific for activation of IL-6 signaling, aortic macrophages from IL-6^{-/-} mice were probed for p-STAT3. Neither aortic macrophages in

sham-infused nor Ang II-infused IL-6^{-/-} were positive for p-STAT3 (Figure 47 and Figure 48).

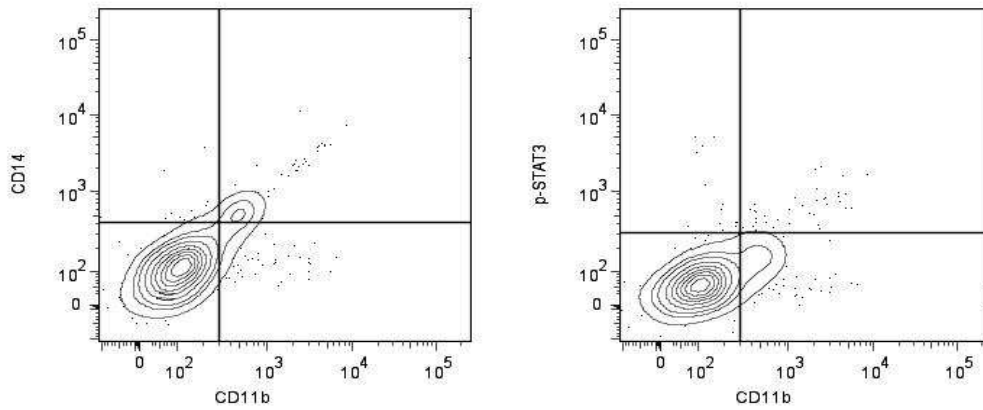


Figure 47. IL-6 signaling is not active in resident aortic macrophages of sham-treated IL-6^{-/-} mice. Aortic macrophages were identified as CD14⁺CD11b⁺ (left) and found to be negative for p-STAT3 at Tyr⁷⁰⁵

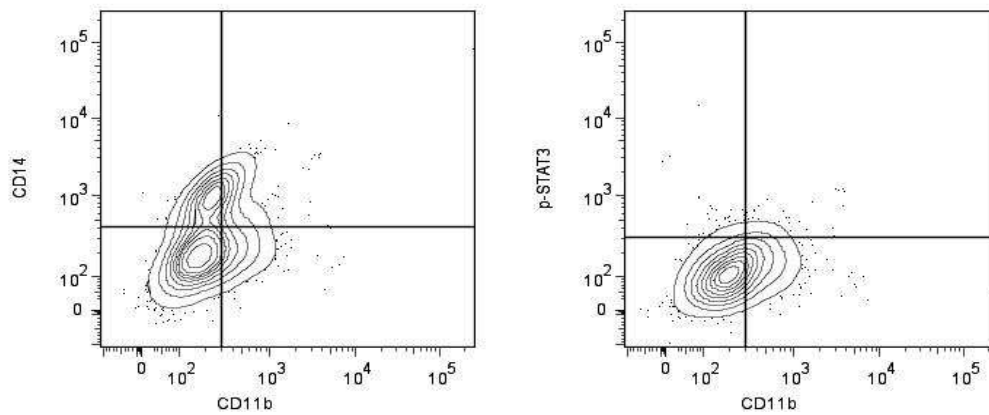


Figure 48. IL-6 signaling is not active in recruited aortic macrophages of Ang II-infused IL-6^{-/-} mice. Aortic macrophages were identified as CD14⁺CD11b⁺ (left) and found to be negative for p-STAT3 at Tyr⁷⁰⁵

In summary, Ang II treatment in IL-6^{-/-} mice produced less aortic MCP-1 secretion and less macrophage recruitment to the aorta than WT mice. The aortic macrophages that were present had lower expression of CD14 and CD11b, but similar

expression of F4/80 compared to WT macrophages. In comparison to CCR2^{-/-} mice, aortas from IL-6^{-/-} mice secreted less MCP-1 in both the sham-treated and treated conditions, but the differences were not statistically significant. Moreover, although the numbers of resident aortic macrophages were almost equivalent, Ang II treatment led to significantly more macrophages in the aorta. In addition, WT mice had recruited macrophages with active IL-6 signaling, but aortic macrophages in IL-6^{-/-} mice did not as expected.

Chapter 6: Aortic Adventitial Fibroblasts and Their Interaction with Monocytes

Several of the studies reported in Chapters 2 to 4 showed that the majority of aortic remodeling events occurred in the adventitia *in vivo* with Ang II treatment. As seen in Chapter 2, IL-6 was predominantly expressed in the adventitia in Ang II-treated WT mice and also in human aortic dissections. Moreover, MCP-1 expression was also detected in this layer. In addition, this was where macrophages were mostly recruited in the aorta along with adventitial thickening due to adventitial fibroblast proliferation in response to Ang II. Thus, it was of great interest to try to understand possible mechanisms that may contribute to these observations in the adventitia.

Since the major cell type in the tunica adventitia of the aorta is the aortic adventitial fibroblast, it was hypothesized that this cell type could contribute significantly to the adventitial inflammation and aortic dissection seen in response to Ang II. Much is known about endothelial cells and smooth muscle cells because they have long been considered to be the major, direct contributors to the formation atherosclerosis, yet little is known about the adventitial fibroblast. In this chapter, aortic adventitial fibroblasts are characterized with respect to the cytokines they produce and their response to Ang II. Their ability to upregulate major cytokines and proliferate are studied specifically. In addition, since macrophages were observed in the adventitia in close proximity to adventitial fibroblasts, interactions between these two cell types were examined. The interactions were studied by coculturing adventitial fibroblasts with monocytes to determine effects on adventitial fibroblast proliferation and the induction of cytokines that could contribute to the potentiation observed *in vivo* in response to CCR2⁺ macrophage recruitment.

AORTIC ADVENTITIAL FIBROBLASTS PRODUCE A VARIETY OF CYTOKINES INCLUDING IL-6 AND MCP-1

Human aortic adventitial fibroblasts were obtained from Lonza and maintained in stromal cell growth medium. To detect and quantify the variety of cytokines/chemokines produced by AoAFs, 50×10^3 AoAFs were grown for 36 h⁵ in 3 mL of complete growth medium. 25 uL aliquots of the conditioned media were assayed in duplicate with a BioSource human 25-plex panel bead-based Luminex assay (Invitrogen). As a comparison, a parallel experiment using 200×10^3 THP-1 monocytes was performed under the same conditions. Data were expressed as mean \pm S.D. from 6 individual samples for each cell type. As seen in appendix C (Table 2), IL-6 and MCP-1 were the two most abundant cytokines secreted by AoAFs. Other cytokines/chemokines detected at low levels were IL-receptor antagonist (IL-1Ra), IL-4, IL-5, IL-8, IL-10, IL-15, TNF- α , IFN- γ , GM-CSF, MIP-1 α , MIP-1 β , MIG, Eotaxin, and IP-10. Of those, IL-1Ra, IL-6, IL-10, IL-15, and MCP-1 were secreted more from AoAF than THP-1 monocytes. Moreover, GM-CSF and Eotaxin were only detected in AoAF cultures. On the other hand, THP-1 cells produced more IL-8, MIP-1 β , and IP-10. Furthermore, IL-1 β , IL-2, IL-12p40/p70, and RANTES were detectable only in THP-1 cultures.

Since IL-6 and MCP-1 were the two cytokines of main interest, their mRNA expression levels were further characterized in AoAFs. *In situ* hybridization (ISH) performed on these cells showed staining for IL-6 mRNA and MCP-1 mRNA at basal level (Figure 49). The difference in intensity may reflect the ELISA data showing that IL-6 was being produced and secreted by 1.7-fold more than MCP-1, 967.8 ± 149.4 pg/mL vs 583.7 ± 78.9 pg/mL, respectively.

⁵ h is the abbreviation for hour (s)

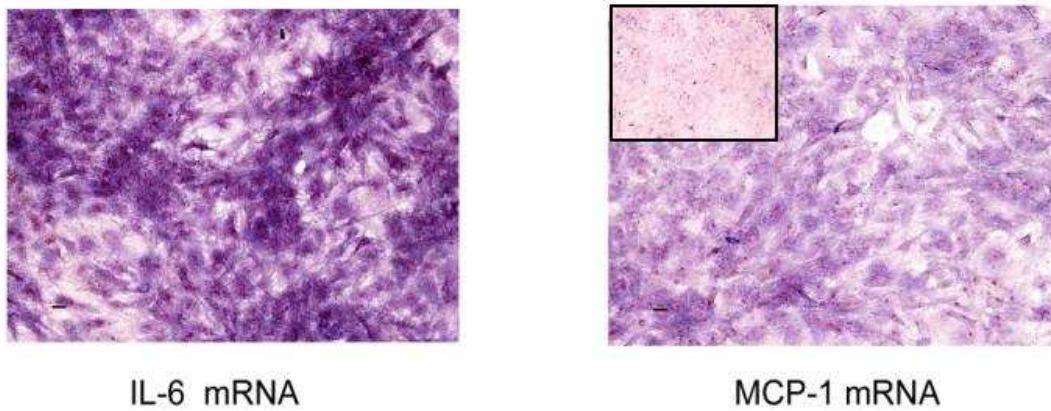


Figure 49. ISH for IL-6 and MCP-1 mRNA in AoAFs. Anti-sense DIG-labeled cRNA probes were used to hybridized to human IL-6 mRNA (left) and MCP-1 mRNA (right) as seen by purple staining. Representative hybridization with sense DIG-labeled probes showed low background staining (insert on right).

It is interesting to note that primary AoAFs produced high levels of both IL-6 and MCP-1 *in vitro*, with cytokine and mRNA being expressed greater for IL-6 than MCP-1. The latter observation is similar to the data presented in Chapter 2 showing that aortas from sham-treated and Ang II-infused mice secrete higher levels of IL-6 than MCP-1. In addition, immunofluorescence staining performed on aortic sections from Ang II infused animals shows that IL-6 and MCP-1 were predominantly detected in the adventitia where the adventitial fibroblasts are located. Taken together, these data suggest that the adventitial fibroblasts are a significant source of IL-6 and MCP-1 in the aorta.

ANG II STIMULATION INCREASES IL-6 AND MCP-1 MRNA AND PROLIFERATION OF ADVENTITIAL FIBROBLASTS

Since IL-6 and MCP-1 are the two cytokines of interest, it was determined whether Ang II stimulation could induce their expression. RNA was extracted from AoAFs induced with Ang II over 0 to 48 h and quantitated using real-time PCR. Ang II induced a rapid increase in IL-6 and MCP-1, but the change in expression levels of these two genes was different. IL-6 mRNA was induced by more than 4-fold starting at 1 h. It

reached a maximum of 10-fold at 3 h, and remained elevated at around 4-6-fold up to 48 h (Figure 50). On the other hand, MCP-1 mRNA levels showed a biphasic response (Figure 51). MCP-1 was induced by only 1.8-fold at 1h and at maximum (2-fold) at 3 h. The level returned back to baseline by 6 h and then increased to 1.7-fold at 12 h. At 24 and 48 h, the level was at baseline again.

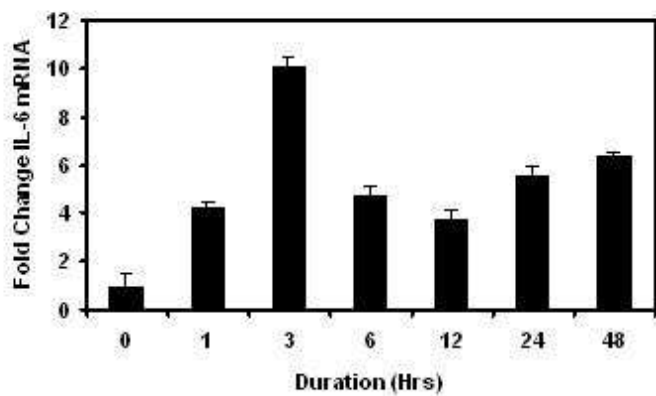


Figure 50. Ang II induced IL-6 mRNA in AoAFs from 1 to 48 h of stimulation. Data are expressed as mean \pm S.D.

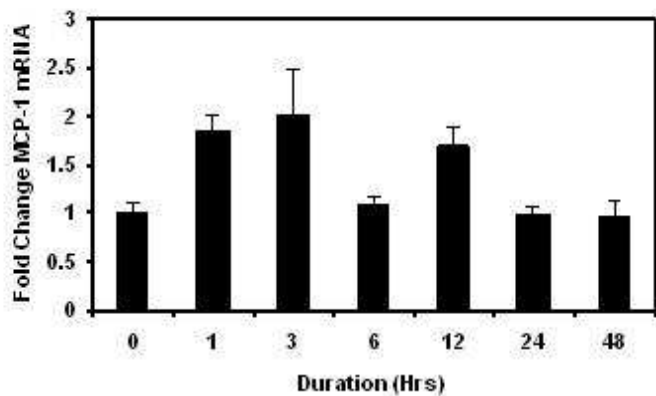


Figure 51. Ang II induced MCP-1 mRNA in AoAFs from 1 to 48 h of stimulation. Data are expressed as mean \pm S.D.

The ability of human AoAFs to proliferate in response to Ang II was measured. This was of interest because the adventitial thickening observed in inflammatory abdominal aneurysm and in mice infused with Ang II was due in part to increasing numbers of adventitial fibroblasts. Based on previous work showing that Ang II could induce proliferation of primary rat aortic adventitial fibroblasts (205;206), it was hypothesized that Ang II would induce primary human adventitial fibroblasts to proliferate also. Cell proliferation was assessed indirectly by ^3H -Thymidine incorporation to measure DNA synthesis during cell cycle progression. It was observed that 1 μM of Ang II, a dose previously shown to induce maximal proliferation of rat AoAFs, induced a small but significant increase in ^3H -Thymidine incorporation after 12 h of stimulation (Figure 52). A greater induction was not seen in the range from 0.1 nM to 10 μM (not shown).

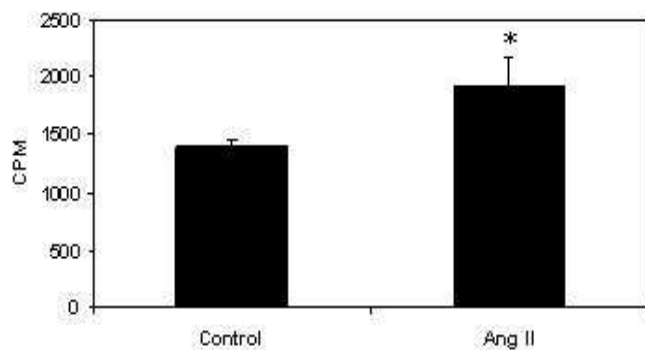


Figure 52. Ang II induced ^3H -Thymidine incorporation in AoAFs. *, $P < 0.031$ between control and Ang II. Data are expressed as mean \pm S.D.

The ability of Ang II to induce cell proliferation was also assessed directly by cell counting using the Z2 Coulter Counter (Beckman-Coulter) after 4 d of treatment (Figure 53). As shown, Ang II caused a 14% increase in cell number.

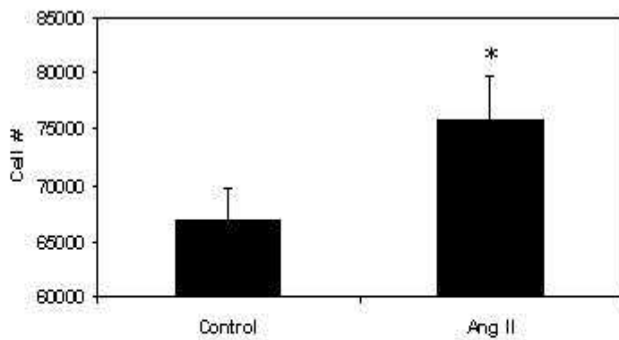


Figure 53. Ang II induced AoAF proliferation after 4 d of treatment as measured by cell counting. *, $P < 0.033$ between control and Ang II. Data are expressed as mean \pm S.D.

MCP-1 FROM AOAFs CAN RECRUIT MONOCYTES AND MONOCYTES CAN INDUCE PROLIFERATION OF AOAF

Since MCP-1 can be produced in natural variants that are not active (284), the MCP-1 from AoAFs was checked to determine whether it could recruit monocytes. Medium from AoAF culture (conditioned medium) was collected and used as a chemoattractant in Boyden Chamber assays. The concentration of MCP-1 in this medium was quantified to be 1,577.54 pg/mL. Complete growth medium (unconditioned medium) was the control. THP-1 monocytes were placed in the top chamber and allowed to migrate through permeable membrane inserts, containing 8 μ m pores, separating the top from the bottom chambers. After incubation for 2 h at 37°C, the THP-1 cells that have migrated through the membrane were collected and counted using the Z2 Coulter Counter. Figure 54 shows representative pictures of the bottom chamber after 2 h using unconditioned and conditioned media as the chemoattractants. Quantitation revealed that AoAF-conditioned medium induced a 3.04 ± 0.05 -fold increase in cell migration ($225,960 \pm 10,550$ cells vs. $74,307 \pm 2102$) (Figure 55).

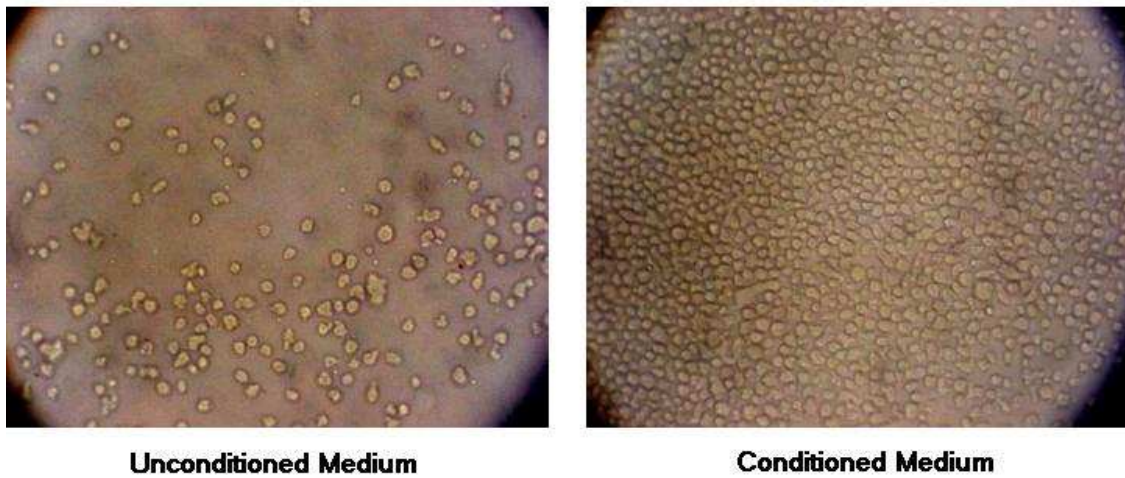


Figure 54. AoAFs can attract monocytes. THP-1 monocytes migrated to AoAF-conditioned medium (right) more than unconditioned medium (left).

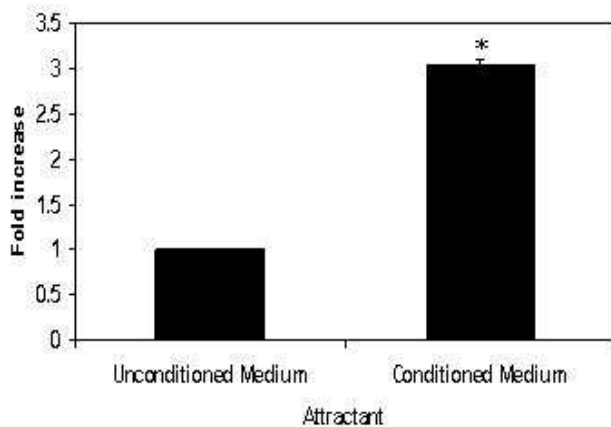


Figure 55. Quantification of migrated monocytes to AoAF-conditioned medium compared to unconditioned medium. A 3-fold increase was observed with conditioned medium vs. control. Data were expressed as mean \pm S.D. *, $P < 0.0006$.

To ensure that the MCP-1 in conditioned medium was responsible for attracting monocytes, the MCP-1 was neutralized with varying concentrations of a neutralizing antibody. Inhibition of MCP-1 showed that the monocyte migration was dependent on MCP-1 produced by AoAFs. Addition of 5 μ g of neutralizing antibody into 1 mL of conditioned media significantly inhibited monocyte migration compared to migration to

conditioned medium alone ($P<0.01$) (Figure 56). This represented a 31.2 % reduction. Increasing the amount of antibodies decreased migration in a step-wise fashion. A 15 $\mu\text{g}/\text{mL}$ concentration of antibodies further significantly inhibited migration compared to 5 $\mu\text{g}/\text{mL}$ ($P<0.02$). The total reduction was 57.7 % at that concentration.

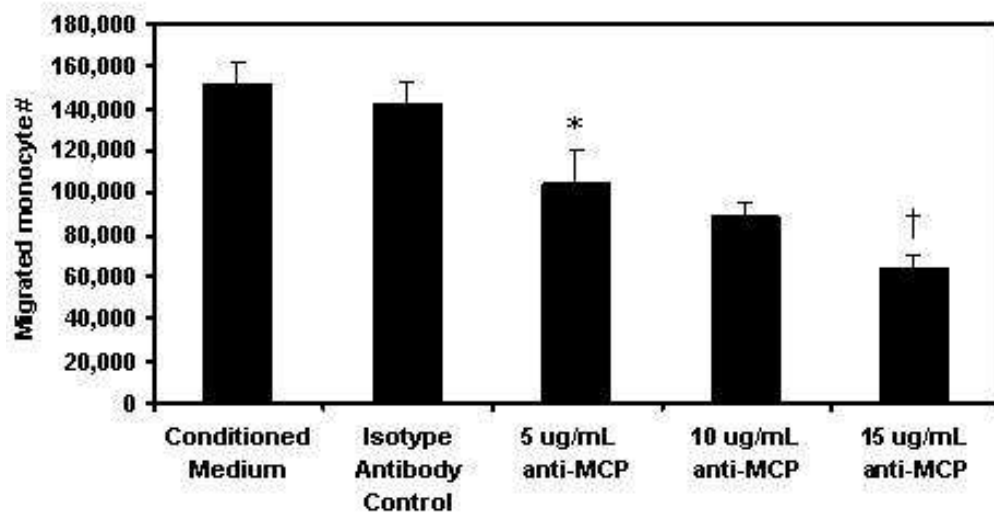


Figure 56. MCP-1 from AoAFs attracts monocytes. THP-1 monocytes migrated to AoAF-conditioned medium, but addition of neutralizing MCP-1 antibodies at increasing concentrations inhibited migration. Maximum effect observed at 15 $\mu\text{g}/\text{mL}$. *, $P<0.01$ comparing 5 $\mu\text{g}/\text{mL}$ to conditioned medium. †, $P<0.02$ comparing 15 $\mu\text{g}/\text{mL}$ to 5 $\mu\text{g}/\text{mL}$. Data are expressed as mean \pm S.D.

Monocytes are known to secrete multiple growth factors and cytokines such as IL-1, TNF, p43, and substances similar to PDGF that are thought to induce fibroblast proliferation (285;286). Therefore, it was determined whether the migrated monocytes could induce proliferation of aortic adventitial fibroblasts. Because the resulting mixture consists of two cell populations, direct counting with the Z2 Coulter Counter could not be used to measure the number of fibroblasts and exclude the monocytes. To overcome this obstacle, the adventitial fibroblasts were labeled with PKH26 and flow cytometry was

used to distinguish the two cell types based on the PE fluorescence of PKH26. Labeled fibroblasts were easily distinguishable from unlabeled AoAFs (Figure 57). After 4 d of coculture, THP-1 monocytes were not positive for PKH26 (Figure 58), confirming that the labeling did not transfer from one cell to the other, validating that the PE signal detected in this assay was specific for the AoAFs.

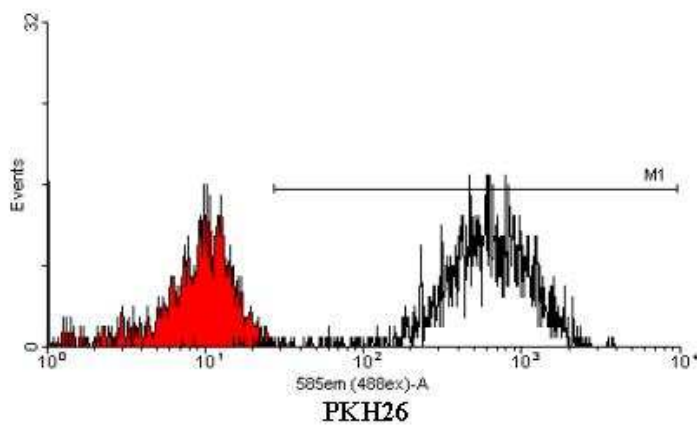


Figure 57. PKH26 labeled AoAFs. Unlabeled (red curve) fibroblasts were dim for PE autofluorescence whereas labeled AoAFs were strongly positive (open curve). The region labeled M1 is the gate dividing unlabeled from labeled fibroblasts. This region was kept constant and cells in M1 were counted as fibroblasts in coculture.

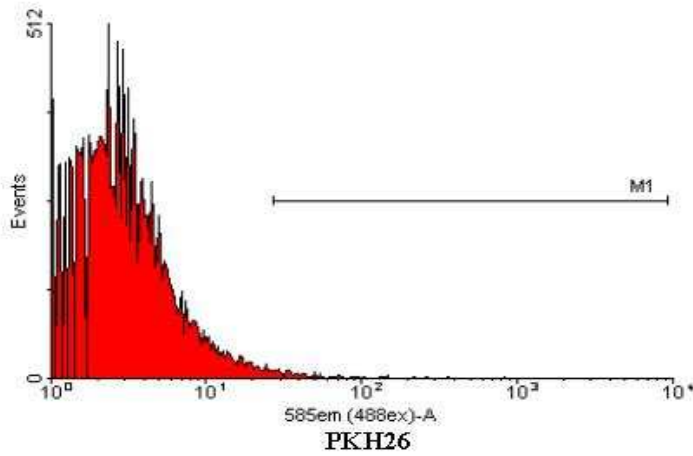


Figure 58. No transfer of PKH26 dye to THP-1 monocytes. THP-1 monocytes obtained from coculture. THP-1 cells did not fall significantly into the M1 positive region.

In coculture, the AoAFs were clearly identified in the M1 region and counted by flow cytometry (Figure 59). Compared to AoAFs cultured without monocytes for the same duration, there was a statistically significant but small increase in AoAF cell number in coculture samples ($p < 0.025$) (Figure 60).

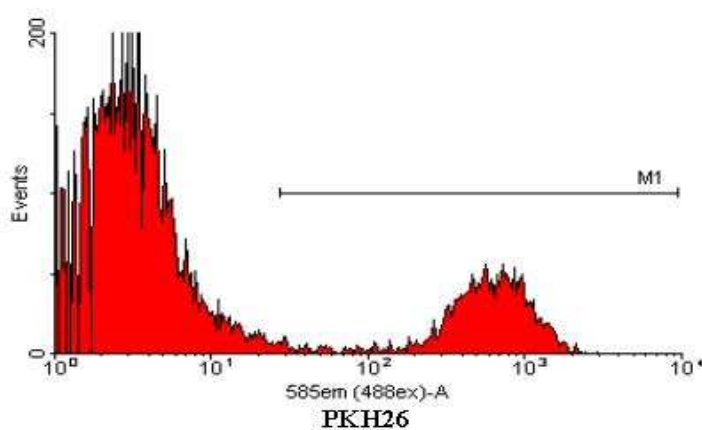


Figure 59. AoAFs counted by flow cytometry. Cells in the M1 region were considered AoAFs. Monocytes compose the population to the left of M1.

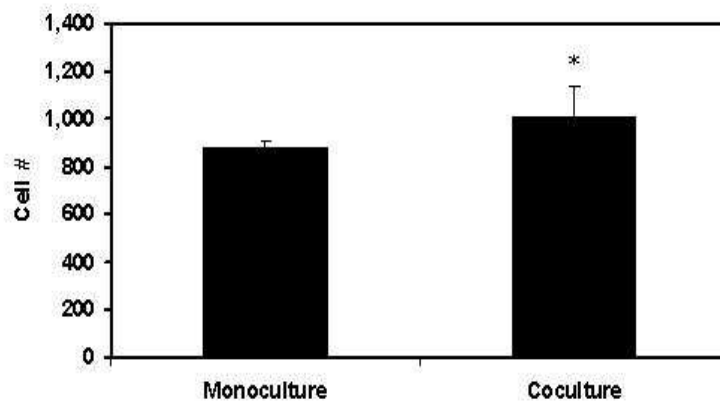


Figure 60. Quantification of AoAFs in monoculture vs. coculture. In coculture, there was a statistically significant increase in cell number; *, $P < 0.025$. Data are expressed as mean \pm S.D.

COCULTURE OF MONOCYTES AND ADVENTITIAL FIBROBLASTS INDUCES IL-6 AND MCP-1 AS WELL AS MONOCYTE TO MACROPHAGE DIFFERENTIATION

Since adoptive transfer of $CCR2^{+/+}$ monocytes into $CCR2^{-/-}$ potentiated the production and secretion of aortic IL-6 and MCP-1 and macrophages are present primarily in the tunica adventitia in close proximity to aortic adventitial fibroblast, it was determined whether coculture of monocytes and fibroblasts could induce these cytokines and macrophage differentiation. In these experiments, 125×10^3 AoAFs were cocultured with 500×10^3 THP-1 monocytes for 5 d in 1.5 mL of RPMI medium containing 5 % FBS; as controls, each cell type was also grown in monoculture under the same conditions. There was no measurable level of IL-6 (< 3.2 pg/mL) in the medium bathing 500×10^3 THP-1 monocytes while medium from AoAF monocultures had a concentration of $10,669 \pm 513$ pg/mL. In coculture, the level of IL-6 was $24,130 \pm 1,881$ pg/mL, a 2.3-fold statistically significant increase in IL-6 compared to the sum of the concentrations from the monocultures of THP-1 and AoAF cells ($P < 0.0021$) (Figure 61). The “sum of monocultures” was used to represent the summation of the contribution of IL-6 from each cell type; it is also the concentration expected if there were an additive effect in coculture.

This summation is mathematically appropriate because the volume of media was kept constant along with the cell numbers for each cell type in monoculture. Since $24,130 \pm 1,881$ pg/mL is more than the expected additive value of $10,669 \pm 513$ pg/mL, there was a synergistic interaction potentiating IL-6 production/secretion in coculture. To determine whether cell-cell contact was required for this induction of IL-6, the coculture experiments were also done in the presence of permeable Transwell inserts containing 0.3 μ m diameter pores to physically separate monocytes (placed on top of the insert) from AoAFs (grown on the bottom of wells), but still allow for fluid exchange. As seen in Figure 61, the potentiation of IL-6 in coculture was cell-contact independent and the level produced was not statistically different from coculture alone ($P=0.44$). That suggests that the potentiation of IL-6 in coculture is due most likely to paracrine signaling. The identity of the agent(s) stimulating the induction of IL-6 is not known.

Coculture of THP-1 monocytes and AoAF also induced monocyte to macrophage differentiation. Monocytes are round and rather small cells while macrophages are much bigger and contain vacuoles in their cytoplasm along with an irregular shape. As seen in Figure 62, the THP-1 monocytes differentiated into macrophage-looking cells in coculture with numerous cytoplasmic vacuoles and irregular shapes.

The cells were further characterized based on staining for CD14 and CD11b, the two surface markers of interest, by flow cytometry. Since CD14 is highly expressed on monocytes cultured *in vivo* on plastic plates, the conversion to macrophages will not be clearly observed based on CD14 expression. To overcome this, the THP-1 monocytes were cultured with 10 ng/mL of both IL-4 and GM-CSF, a cytokine environment that promotes monocyte conversion into immature dendritic cells (iDCs). In this environment, monocytes will differentiate into CD14⁻CD11b⁻ iDCs by default.

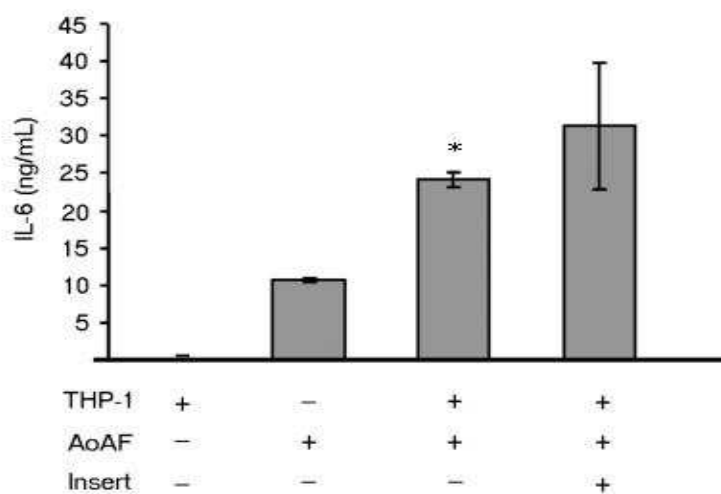


Figure 61. Concentration of IL-6 in monocultures and coculture of THP-1 monocytes and human AoAFs. Transwell inserts were used to separate the two cell populations in coculture to determine whether cell-cell contact was required for potentiation of IL-6. There was a significant synergistic induction of IL-6 in coculture compared to sum of monocultures; *, $P < 0.0021$. This induction was contact independent. Data are expressed as mean \pm SEM of 3 experiments.

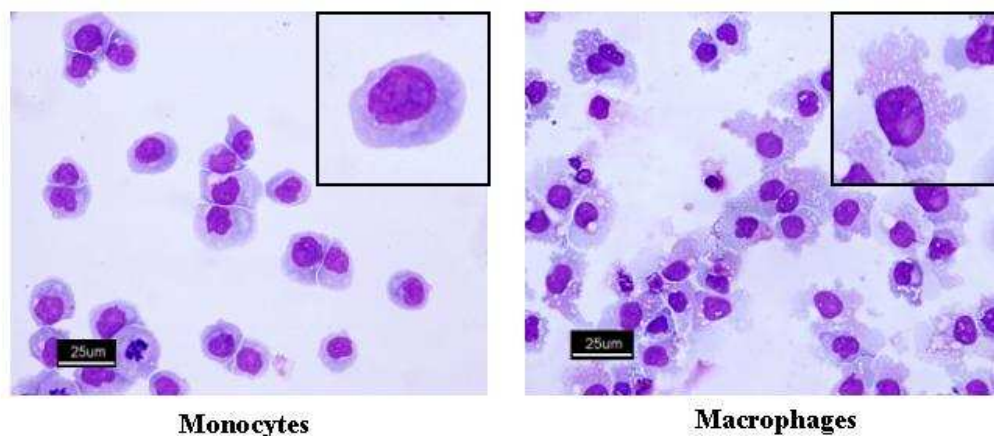


Figure 62. THP-1 monocytes (left) differentiated into macrophages (right) in coculture with AoAFs as observed by Giemsa staining. 20x. Inserts show a representative cell of each type.

If differentiation into macrophages occurs in coculture, CD14⁺CD11b⁺ cells will be obtained instead. As shown in Figure 63, the surface expression of CD14 was clearly upregulated on the macrophages as compared to the iDCs.

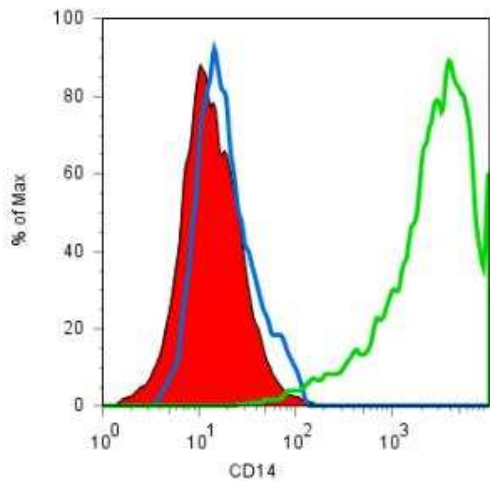


Figure 63. Comparison of surface CD14 expression on THP-1 cells (blue curve) in monoculture and derived macrophages (green curve) from coculture in the presence of IL-4 and GM-CSF. Curve representing the isotype control is seen in red.

The surface expression of CD11b also was dramatically upregulated on the derived macrophages as compared to the iDCs (Figure 64). In these experiments, CD11c was used to help identify iDCs, which are CD11c⁺CD11b⁻. 94.7 % of THP-1 cells were CD11c⁺CD11b⁻ iDCs in monoculture and only 5.14 % were CD11c⁺CD11b⁺ macrophages. After 5 d of coculture, 92.32 % of the cells were CD11c⁺CD11b⁺ macrophages and only 7.59 % were CD11c⁺CD11b⁻ iDCs. Thus, the monocytes differentiated into CD14⁺CD11c⁺CD11b⁺ macrophages in coculture and not CD14⁻CD11c⁺CD11b⁻ iDCs.

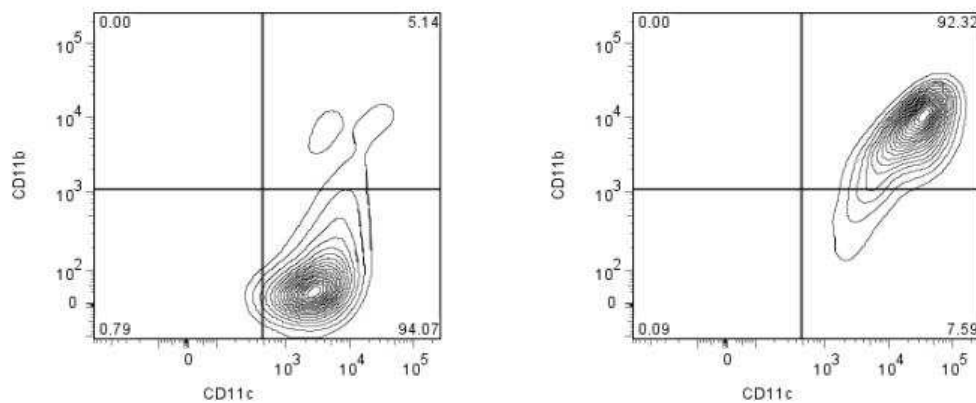


Figure 64. THP-1 cells differentiate into CD11c⁺CD11b⁺ macrophages in coculture. In an environment of IL-4/GM-CSF, monocytes became CD11c⁺CD11b⁻ cells by default (left). In coculture, the cells became CD11c⁺CD11b⁺ macrophages instead (right)

To ensure that these findings were not specific to the THP-1 transformed monocyte cell line, the experiments above were repeated with primary monocytes isolated from cord blood or adult peripheral blood using the Monocyte Isolation Kit II, a negative selection kit from Miltenyi. In this kit, antibodies directed against CD3, CD7, CD16, CD19, CD56, CD123, and CD235a were used to remove non-monocytes from blood, leaving the monocytes untouched. Similar to the results shown above, culturing primary human monocytes with human aortic adventitial fibroblasts in the presence of IL-4/GM-CSF induced IL-6 and MCP-1, Figure 65. With monocytes from cord blood, there was a 3.5-fold increase in IL-6 as compared to the sum of IL-6 concentrations from monocultures of monocytes and fibroblasts ($141,984 \pm 27,569$ vs. $34,472 \pm 4,240$, $P < 0.015$). Moreover, MCP-1 increased by 14.1-fold ($160,794 \pm 12,707$ vs. $11,928 \pm 330$, $P < 0.0007$). Likewise, with monocytes from adult peripheral blood, there were a 6.3-fold increase in IL-6 ($205,006 \pm 44,375$ vs. $32,457 \pm 179$, $P < 0.031$) and a 13.2-fold increase in MCP-1 ($235,840 \pm 7,262$ vs. $17,819 \pm 434$, $P < 0.00054$). Monocyte to macrophage

differentiation was also observed with these cells. Figure 66 shows a representative picture of the default differentiation of primary monocytes to iDCs and a picture of a macrophage in coculture. The iDCs have the characteristic pseudopodia extending from a round cell body while the macrophages are bigger cells containing multiple vacuoles in their cytoplasm along with an irregular cell border.

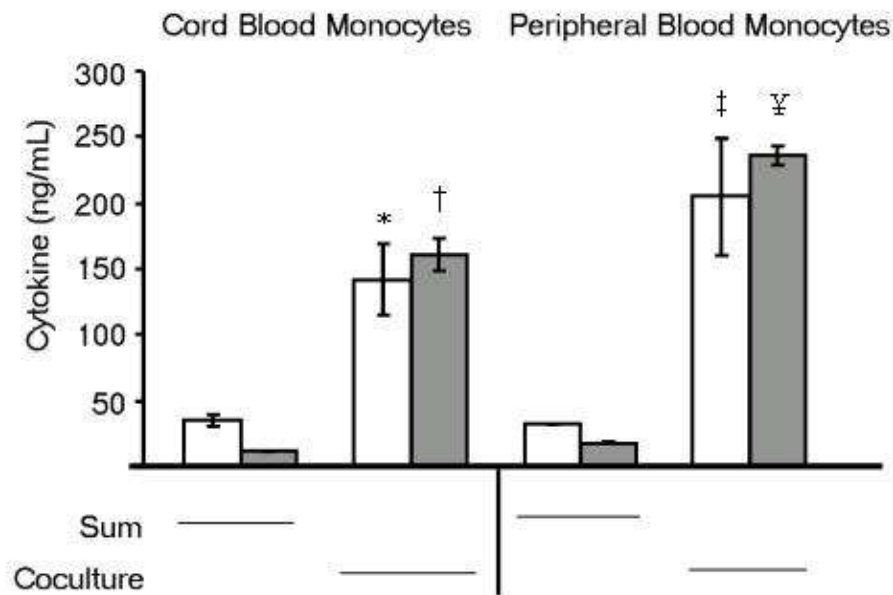


Figure 65. Induction of IL-6 and MCP-1 levels in coculture with primary monocytes. Cord blood monocytes or adult peripheral blood monocytes were isolated untouched and cultured with AoAFs for 5 d. There was a significant 3.5-fold increase in IL-6 (open bars) in coculture with cord blood monocytes (*, $P < 0.015$) and a 14.1-fold increase in MCP-1 (closed bars) as compared to the sum of cytokines levels from monocultures (†, $P < 0.0007$). With peripheral blood monocytes, there was a significant 6.3-fold increase in IL-6 (‡, $P < 0.031$) and a 13.2-fold increase in MCP-1 as compared to the sum of cytokine levels from monocultures (¥, $P < 0.00054$). Data are expressed as mean \pm SEM from at least 3 experiments.

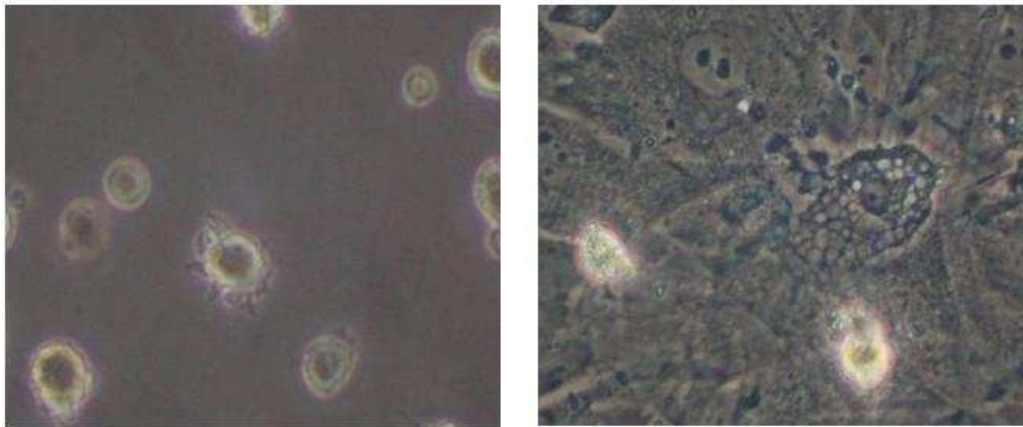


Figure 66. Representative picture of iDC (left) and macrophage (right) from coculture using primary monocytes. Pseudopodia extending from the iDC cell body can be observed while multiple vacuoles in the cytoplasm are clearly seen in the bigger macrophage. 10x

MACROPHAGE DIFFERENTIATION AND MCP-1 AND MMP-9 PRODUCTION IS DEPENDENT ON IL-6

Because IL-6 was shown in Chapter 5 to strongly control the expression of CD11b and CD14, albeit to a lesser extent, on aortic macrophages with Ang II treatment and aortic dissection, it was hypothesized that IL-6 was also controlling the expression of surface CD14 and CD11b as well as the potentiation of MCP-1 in coculture. Adult peripheral blood monocytes were cultured in the presence of IL-4/GM-CSF in monoculture or coculture with AoAFs and the changes in surface expression of CD14, CD11b, and CD1a were assessed by flow cytometry. 10 μ g of anti-IL-6 and anti-sIL-6R antibodies were added every 3rd d starting on day 0. CD1a was used in place of CD11c as a specific marker for iDC; it is not expressed on monocytes or macrophages. Dendritic cells were previously described to be CD1a⁺CD14⁻ while macrophages were CD1a⁻CD14⁺ (287-289). In addition, positive staining for HLA-DR was used to exclude fibroblasts from analysis of monocytes/macrophages in coculture (Figure 67). Only cells

within the HLA-DR gate were analyzed for CD1a, CD14, and CD11b expression. As described above, 125×10^3 aortic adventitial fibroblasts and 500×10^3 monocytes were cocultured, a 1:4 ratio, respectively. Thus, 80 % of all cells were monocytes and 20 % were fibroblasts in coculture.

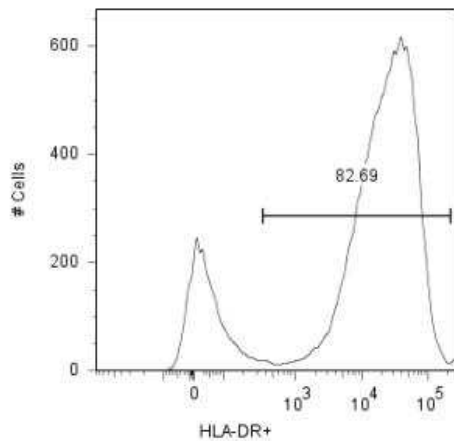


Figure 67. HLA-DR gating of primary monocytes/macrophages in coculture. This was done to exclude fibroblasts from analysis. As expected, approximately 80 % of all cells in coculture were HLA-DR⁺

After 5 d of culture, monocultures of monocytes became mostly CD1a⁺CD14⁻ iDCs (72.86 %) and only 0.94 % of the cells were CD1a⁻CD14⁺, Figure 68. In coculture, 97.04 % were CD1a⁻CD14⁺ macrophages; 0.07 % of the cells were CD1a⁺CD14⁻ iDCs. With addition of 10 μ g of anti-IL-6 and anti-sIL-6R, there was a shift toward reduction in expression of CD14.

In a second experiment, iDCs were observed to be CD14⁻CD11b⁺ while macrophages were CD14⁺CD11b⁺. Inhibition of IL-6 signaling reduced CD11b surface expression in coculture (Figure 69). Comparisons between expression of CD14 and CD11b in monoculture, coculture, and coculture with IL-6 inhibition are shown in Figure 70.

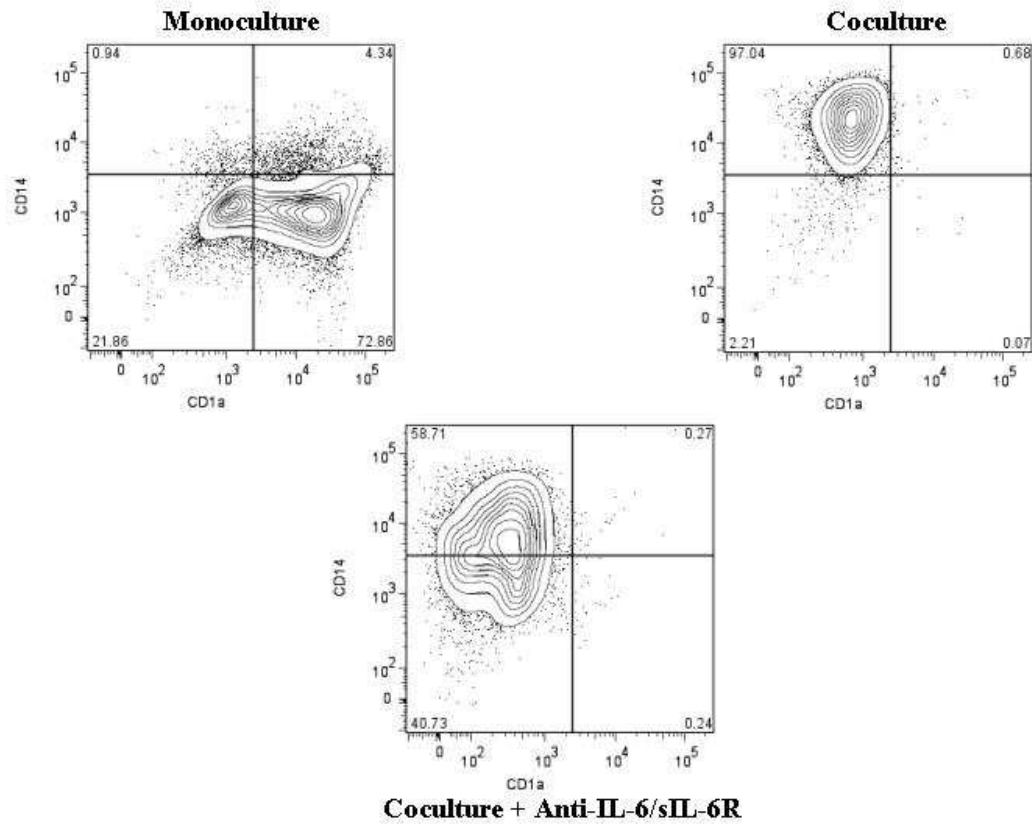


Figure 68. IL-6 regulates the expression of surface CD14. In the presence of IL-4/GM-CSF, monocytes differentiated into CD1a⁺CD14⁻ iDCs, but in coculture CD1a⁻CD14⁺ macrophages were observed. Inhibition of IL-6 and sIL-6 reduced the expression of CD14 in coculture.

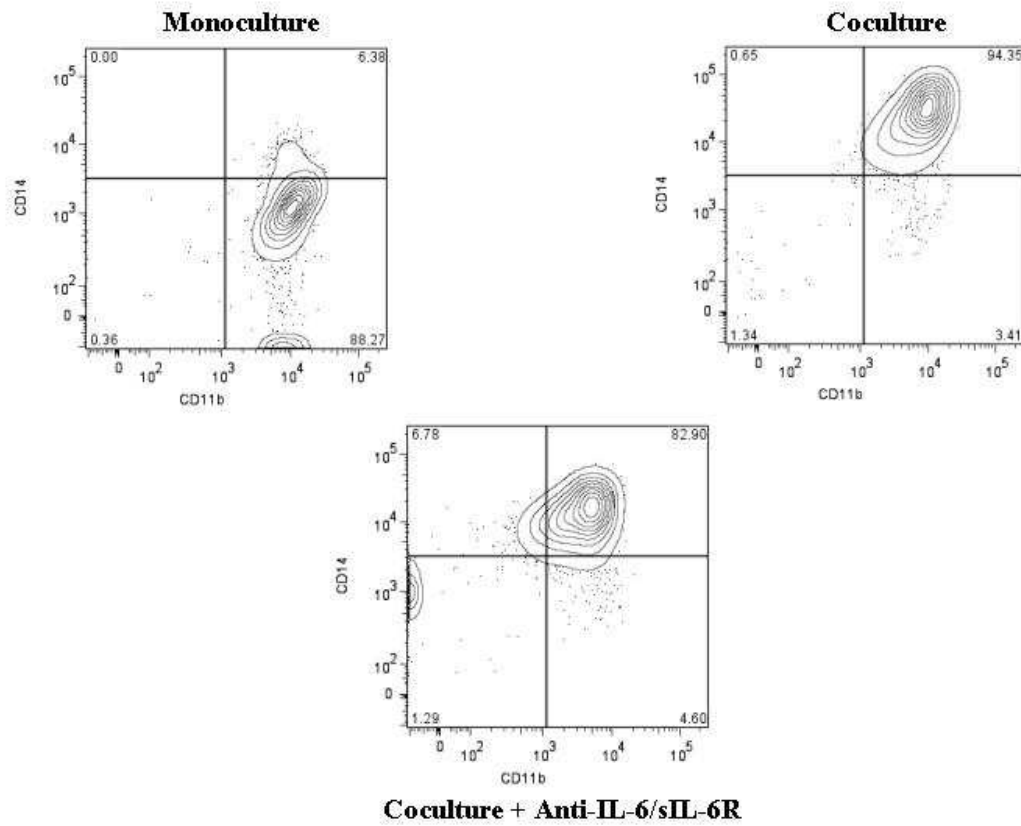


Figure 69. IL-6 regulates the expression of surface CD11b. In the presence of IL-4/GM-CSF, monocytes differentiated into CD14⁺CD11b⁺ iDCs, but in coculture CD14⁺CD11b⁺ macrophages were observed. Inhibition of IL-6 and sIL-6 reduced the expression of CD11b in coculture.

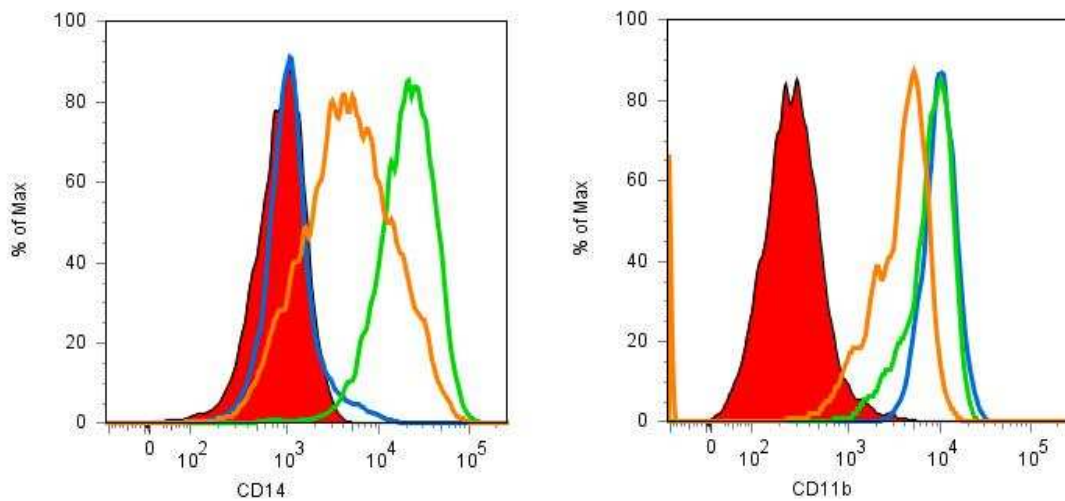


Figure 70. Comparison of surface CD14 and CD11b expression with inhibition of IL-6 signaling. iDCs (blue curve) were negative for CD14 while macrophages in coculture (green curve) were positive. IL-6 inhibition (orange curve) reduced the expression level of CD14 in coculture. For CD11b, iDCs and macrophages were positive for CD11b, and IL-6 inhibition reduced its expression in coculture. The red curves depict the respective isotype controls.

Unlike THP-1 monocytes cultured in the presence of IL-4/GM-CSF, iDCs derived from primary monocytes were CD11b positive. This could be due to the presence of a greater concentration of IL-6 in monocultures of primary monocytes than in monoculture of THP-1 monocytes in the presence of IL-4/GM-CSF (33 pg/mL vs. 10 pg/mL). The IL-6 inhibition experiment was repeated with THP-1 monocytes to determine the effect of IL-6 on CD11b expression on those cells. As seen in Figure 71, coculture induced CD11b expression and neutralization of IL-6 and sIL-6R inhibited CD11b expression.

The concentration of MCP-1 in culture medium was quantified after inhibition of IL-6 in coculture. As seen in Figure 72, the concentration of IL-6 in coculture was $205,006 \pm 44,375$ pg/mL and addition of neutralizing antibodies lowered the concentration to $26,957 \pm 759$ pg/mL, a level close to the sum of concentrations from

monocultures ($32,457 \pm 179$ pg/mL). Measurement of MCP-1 showed that there was a small, but statistically significant reduction in MCP-1 concentration with neutralization of IL-6 ($P < 0.05$).

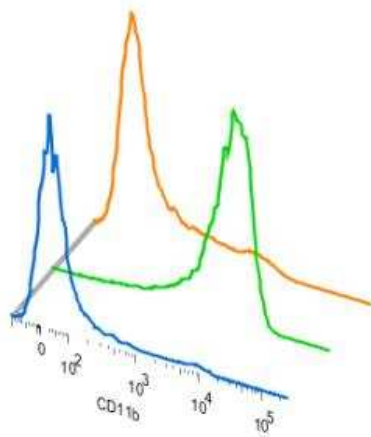


Figure 71. IL-6 regulates surface CD11b expression on THP-1 monocytes. THP-1 cells grown in monoculture with IL-4/GM-CSF were negative for CD11b (blue curve). In coculture, CD11b was upregulated (green curve). Inhibition of IL-6 signaling inhibited the expression of CD11b (orange).

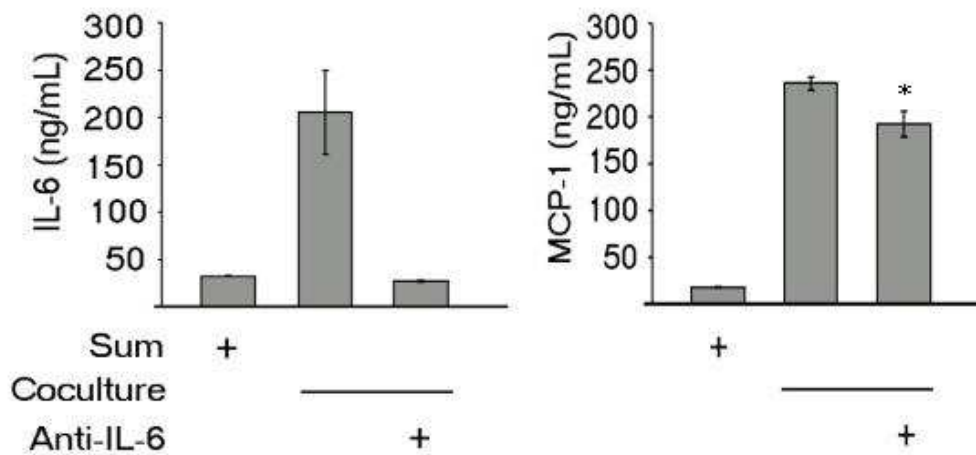


Figure 72. Inhibition of IL-6 reduces MCP-1 levels in coculture. 10 μ g of anti-IL-6/sILR antibodies were added to coculture and the level of soluble IL-6 was decreased to a level similar to the sum of IL-6 from monocultures (left). This reduction caused a statistically significant reduction in MCP-1 levels in coculture (right). *, $P < 0.05$ comparing coculture to coculture with IL-6 neutralization.

The changes in expression of MMP-9 also were of interest since MMP-9 has been shown to play a key role in aneurysm formation (43). MMPs are enzymes that cleave extracellular matrix proteins such as elastin, gelatin, and collagen and have been shown to be increased in human aneurysm tissue (41). MMP-9 from macrophages along with MMP-2 from mesenchymal cells have been shown to be required for aneurysm development in an experimental aneurysm murine model (43). In addition, MMP-9 transcripts and protein level are significantly reduced in ApoE^{-/-}IL-6^{-/-} mice and IL-6^{-/-} mice compared to ApoE^{-/-} mice (194). Thus, we hypothesized that IL-6 also regulated the expression of MMP-9 in coculture. Using the same samples above, MMP-9 was also measured by flow cytometry to detect intracellular proteins. In the presence of IL-4/GM-CSF, iDCs were observed to express MMP-9 and in coculture, there was an increase in

MMP-9 in the macrophages (Figure 73). With inhibition of IL-6 signaling, the expression level of MMP-9 in coculture was reduced to the level of iDCs.

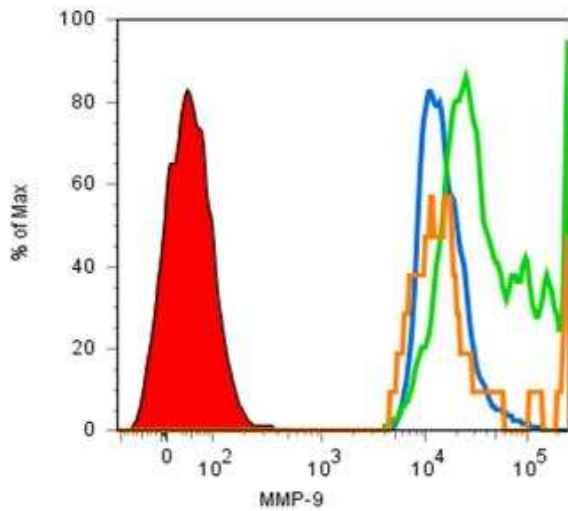


Figure 73. IL-6 controls the expression of MMP-9. Using flow cytometry, the expression level of MMP-9 was detected in iDCs (blue curve) differentiated from primary adult peripheral monocytes. In coculture, the level of MMP-9 was increased in macrophages (green curve), but addition of anti-IL-6/sIL-6R antibodies reduced the level of MMP-9 (orange curve). The red curve depicts the isotype control.

To clearly show that IL-6 regulates the expression of MCP-1 in monocytes/macrophages, THP-1 monocytes were directly stimulated with 8 ng/mL of recombinant IL-6. Real-time PCR was used to measure the induction of MCP-1 transcripts, and ELISA was used to quantitate the concentration of MCP-1 in culture medium after stimulation from 0 to 96 h. IL-6 stimulation induced MCP-1 mRNA to 3-fold after 24 h. The level of transcripts increased to a maximum at 48 h and then gradually decreased from 72 to 96 h, but remained between a 3-5-fold increase. On the contrary, the level of MCP-1 protein was observed to gradually increase throughout the

entire duration of stimulation. There was a maximum 3-fold increase at 96 h compared to control, time 0 h.

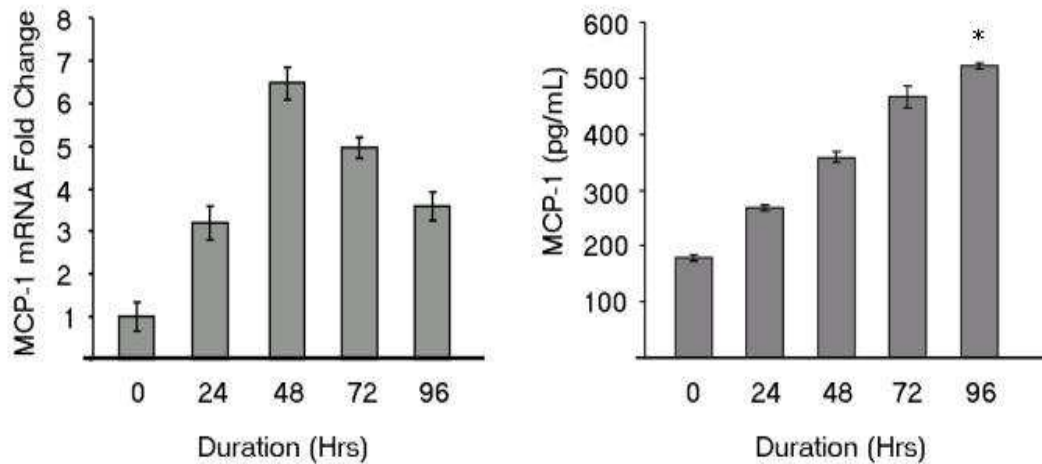


Figure 74. IL-6 stimulation of THP-1 monocytes induces MCP-1 mRNA and MCP-1 protein. Monocytes were stimulated with 8 ng/mL of recombinant IL-6 from 0 to 96 h. Fold induction of mRNA for MCP-1 was detected by real-time PCR (left). There was a 6.5-fold induction of transcripts compared to control, time 0. ELISA measurement of MCP-1 concentration showed that MCP-1 increased stepwise over time, reaching a maximum increase of 3-fold (right). *, $P < 0.000001$ comparing 96 h to control.

In summary, the aortic adventitial fibroblasts were observed to be able to produce and secrete a variety of cytokines and chemokines, but IL-6 and MCP-1 were the most abundant. The expression levels of both genes were shown to be rapidly and highly inducible by Ang II. Ang II also had a weakly mitogenic effect on adventitial fibroblasts. The MCP-1 produced by these cells was shown to be able to recruit monocytes and the monocytes, once recruited, were able to weakly stimulate proliferation of these cells. In coculture of fibroblasts and monocytes, the monocytes were shown to differentiate into macrophages, even in the presence of an environment that favors differentiation into dendritic cells. Further characterization showed that the macrophages derived from THP-1 monocytes in coculture increased surface expression of CD14 and CD11b. Similarly,

primary monocytes became CD1a⁺CD14⁻ iDC with classical morphology in monoculture and CD1a⁻CD14⁺ macrophages with numerous cytoplasmic vacuoles in coculture; however, the expression of CD11b was not different between iDCs and macrophages. In addition to macrophage differentiation, large increases in IL-6 and MCP-1 occurred in coculture. The potentiation of IL-6 was shown to be contact independent, suggesting a soluble mediator, while the induction of MCP-1 was partially dependent on IL-6. Direct IL-6 stimulation was shown to induce MCP-1 transcripts and protein in monocytes/macrophages, presenting a plausible mechanism for the induction of MCP-1 in this *in vitro* system and *in vivo*. Furthermore, inhibition of IL-6 signaling was shown to reduce CD14 and CD11b expression along with MMP-9 expression in coculture. These data confirm the observations presented in Chapter 5 with IL-6^{-/-} mice and previously published data on MMP-9 expression in ApoE and IL-6 double knockout mice.

Chapter 7: Conclusion and Future Directions

CONCLUSION

In this study, we present an animal model of acute aortic dissection without hyperlipidemia and a powerful technique to specifically study aortic macrophages. Using these new tools and *in vitro* studies, we elucidated some important roles for aortic macrophages, adventitial fibroblasts, IL-6, and MCP-1 in vascular inflammation. We provide clear evidence that IL-6 regulates monocyte to macrophage differentiation and activation in the aorta along with the induction of MCP-1. Also, we demonstrate for the first time that monocyte recruitment to the aorta potentiates MCP-1 and IL-6, which we show to be predominantly produced in the adventitia of our animal model and in sporadic human thoracic aortic dissection. These data provide a very plausible mechanism for this induction *in vitro*. In summary, these findings show that IL-6 can induce aortic MCP-1 and MCP-1 responsive macrophages are necessary for full aortic IL-6 potentiation, which suggest an important IL-6-MCP-1 amplification loop that accelerates vascular inflammation. Collectively, the data paints a picture showing how vascular inflammation is accelerated leading to aneurysm formation and can be applied to atherosclerosis and other cardiovascular diseases.

There are several interesting observations in our study. Most notably, the levels of aortic MCP-1 and IL-6 increased together with Ang II treatment. Analysis of our data revealed that these two cytokines are monocyte/macrophage dependent. Macrophages regulate their expression, but with different mechanisms. The increase in MCP-1 was directly proportional to the increase in number of aortic macrophages in IL-6^{-/-} mice (3.4-fold increase in MCP-1 and 3.7-fold increase in macrophages), CCR2^{-/-} mice (2.4-fold and a 2.8-fold increase, respectively), and WT mice (6.5-fold and 5.3-fold, respectively).

This direct relationship was further confirmed by adoptive transfer experiments where CCR2⁺ monocytes caused a 9.1-fold increase in MCP-1. Moreover, MCP-1 induction was found to be also partially dependent on IL-6 since IL-6^{-/-} mice developed a blunted response with treatment. A possible mechanism was shown *in vitro* when inhibition of IL-6 reduced the increase in MCP-1 in coculture, and stimulation of monocytes with IL-6 induced MCP-1 mRNA and protein. The induction of IL-6 in WT mice by Ang II is also partially monocyte/macrophage dependent, but in a slightly different way. Adoptive transfer experiments actually prove that a particular cell type, the CCR2⁺ monocyte, is required for full 3.6-fold potentiation of IL-6 in the aorta. Without CCR2⁺ monocytes, the increase was only 2-fold as seen in Ang II-treated CCR2^{-/-} mice or in Ang II-treated CCR2^{-/-} mice receiving CCR2^{-/-} monocytes. These findings further define and clarify the contribution of CCR2⁺ monocytes and macrophages to vascular inflammation.

The data we present here also implicate the sources for aortic MCP-1 and IL-6. As mentioned above, the induction of MCP-1 is directly proportional to the increase in aortic macrophages and suggests that the macrophages are the major source of MCP-1. This is substantiated by the fact that monocytes/macrophages produce MCP-1 *in vitro*. Staining for MCP-1 also showed localization to the outer media/adventitia border where macrophages, aortic adventitial fibroblasts, and smooth muscle cells can be found. We also report here that the AoAFs have the ability to produce MCP-1 *in vitro*. Moreover, under the influence of IL-4/GM-CSF, 125x10³ primary human AoAFs produced 25ng of MCP-1 while 500x10³ peripheral blood monocyte produced 1ng over 5 d of culture. For IL-6, the major source is likely the AoAFs since IL-6 was seen localized to the stromal cells in the adventitia in our mouse model. *In vitro*, 125x10³ AoAFs produced 979 times as much IL-6 as 500x10³ peripheral blood monocytes over 5 d of culture (49ng vs 50pg).

Future studies can prove these implications *in vivo* using the aortic digestion technique presented here.

Although aortic tissue digestions are commonly done for isolation of cells to culture, we adapted this technique to study aortic macrophages and how their phenotype changes with disease progression. Using our technique, we showed that aortic macrophages were CD14⁺CD11b⁺F4/80⁺ in sham-treated WT mice while macrophages from dissecting aortas expressed higher CD14 and CD11b, but were surprisingly F4/80⁻, which indicated activation. In contrast, IL-6^{-/-} mice treated with Ang II for 6 d did not develop aneurysms and have aortic macrophages that were CD14^{lo}CD11b^{lo}F4/80⁺. Thus, we think that IL-6 is differentiating monocytes to become CD14^{hi}CD11b^{hi} activated aortic macrophages that contribute to the induction of IL-6, express MCP-1, and cause aortic dissection. Using the aortic digestion techniques we describe here, this particular macrophage can be characterized further on its surface, intracellular contents, and signaling profiles. That knowledge may lead the way for selective therapeutic targeting of these pathogenic macrophages.

CD11b is an integrin known to be involved in monocyte/macrophage adhesion, migration, and phagocytosis (235;290;291). It forms a complex with CD18 to become an $\alpha_m\beta_2$ integrin receptor known as Mac-1. Ligands for this receptor include fibrinogen, factor X, and intercellular adhesion molecule-1 (ICAM-1) (235;290), which as been shown to be upregulated by IL-6 trans-signaling *in vivo* (170;173). Blockade of CD11b has been shown to reduce vessel wall macrophage infiltration (290;292). It is also known that CD11b can form a complex with urokinase-type plasminogen activator receptor (uPAR), which increases in expression on macrophages (293-299). This functional unit has been shown to allow for firm adhesion while the ligand for uPAR, urokinase-type plasminogen activator (uPA), decreases adhesion (296;300). uPA has been

reported to increase by thirteen-fold in the aneurismal tissue of Ang II-infused apoE^{-/-} mice and to cleave plasminogen to produce plasmin, which can activate MMPs (115;116). With the data presented here, the environment facilitating aneurysm development with Ang II infusion is better understood. Not only can the Ang II-induced IL-6 increase ICAM-1, but it also augments CD11b expression on macrophages to promote firm adhesion to ICAM-1 and other extracellular matrixes or cells. At the same time, uPA facilitates dissociation, allowing for migration, and MMP activation. This creates an environment where macrophages can attach, migrate, and degrade tissue from the adventitia inward (Illustration 2).

We and others have reported that macrophages are found predominantly in the tunica adventitia in humans and animal models of cardiovascular diseases (39;113;116;123;124;150;301;302). In this report, we also observed them in the media associated with tears in the elastic lamellae of both the thoracic and abdominal aortas. Our data suggest that the macrophages in the media were likely coming from the adventitia based on the pattern of appearance of these macrophages in the aorta. Their recruitment may be mediated by the MCP-1 expressed in the outer media and media/adventitia border as we have shown. This medial invasion from the adventitia has also been observed and supported by others (4;5;22;116). The phenomenon is supported by a study that showed that macrophages artificially recruited to the adventitia migrate towards the intima over time (303). In this study we provide insight into how induction of IL-6 in the adventitia can up-regulate CD11b expression to facilitate the movement of macrophages from the adventitia into the media, facilitating dissection.

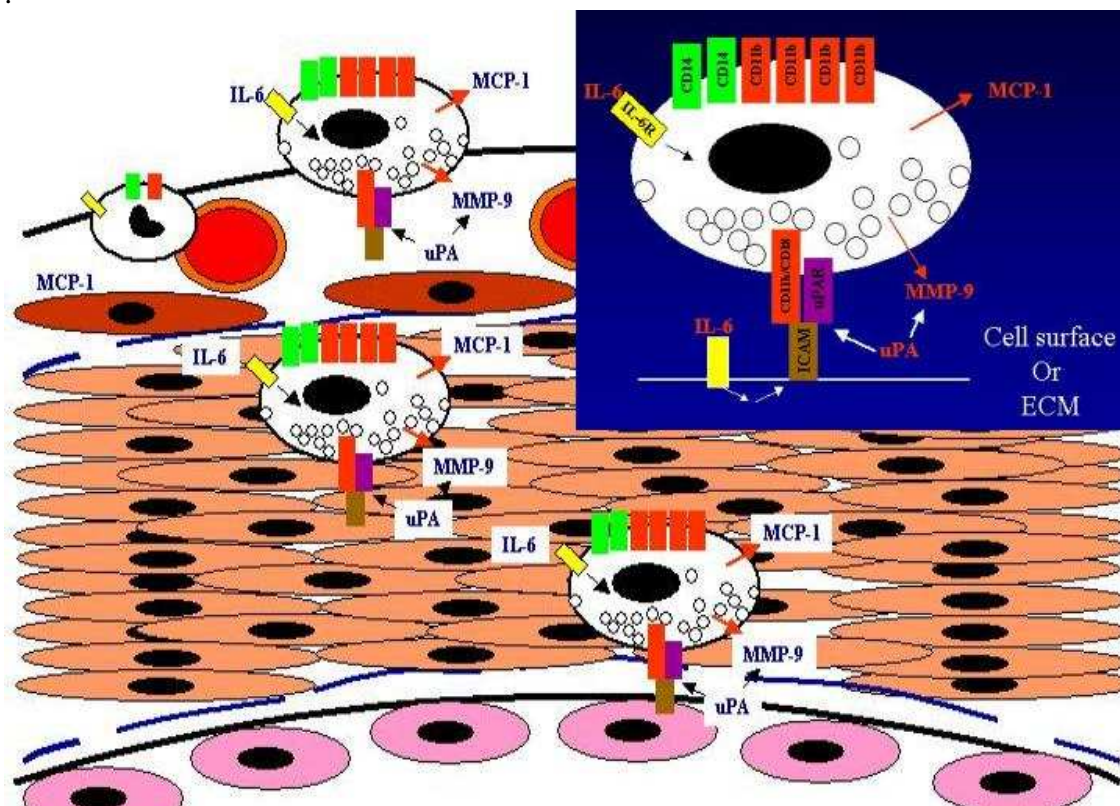


Illustration 2. IL-6-differentiated macrophages expressing high surface CD11b and CD14, MCP-1, and MMP-9 invade into the vessel wall from the adventitia. uPAR/uPA aids IL-6-differentiated macrophages to attach and migrate (insert).

Another important finding of our study was that adoptive transfer of a finite number of WT monocytes, 1.5×10^6 , into a background that lacks it can restore levels of aortic IL-6 and MCP-1 to that seen in treated WT mice. This number of monocytes has been reported to be in the physiological range of normal mice and not in excess like typical adoptive transfer experiments (39;43;241). Moreover, the adoptive transfer also induced dissecting aneurysms at a greater incidence than that seen in WT mice (57 % vs. 35 %). In addition, this experiment also revealed that monocytes preferentially homed to the aortic root/ascending aorta and the suprarenal aorta, which are the two locations

where dissections were observed in our model. We have noticed extensive neovascularization in these areas, which can help explain monocyte recruitment there, but it is unclear why these specific regions are more prone to neovascularization. These two “hot spots” are also the locations of increased IL-6 expression in the aorta (115;124). Furthermore, we report for the first time the disruption of medial elastic lamellae along with macrophage presence and dissecting aneurysm formation in the aortic root/ascending aorta region of Ang II-treated mice. These features have been reported previously in the abdominal aorta, but not in the thoracic aorta (113;124;304). This is an important observation because human thoracic aneurysms are commonly found in this area. These data clearly demonstrate the important role of CCR2⁺ monocytes in vascular inflammation and dissecting aneurysm disease.

Surprisingly, the coculture experiments using primary AoAFs and monocytes reproduced our main findings *in vivo* rather well. IL-6 and MCP-1 levels were simultaneously potentiated in coculture, and the fold induction of MCP-1 was higher than IL-6 just like in the aorta of Ang II-treated mice. Coculture caused monocyte to macrophage differentiation, and IL-6 was shown to specifically regulate CD14 and CD11b expression *in vitro* also. Moreover, neutralization of IL-6 in coculture resulted in decreased MCP-1 levels, mimicking the finding in IL-6^{-/-} mice. These results, together with the observation *in vivo* that IL-6, MCP-1, macrophages, and fibroblasts are predominantly localized to the tunica adventitia, support adventitial fibroblasts and monocytes/macrophages as major contributors to adventitial inflammation.

The aortic digestion technique and analysis by flow cytometry described here is a very powerful method. Currently, most research on aortic diseases like atherosclerosis, aneurysm, and aortic dissection rely on immunohistochemistry or immunofluorescence done on aortic tissue. Although these techniques are good at identifying the mere

presence of a certain event of interest like cells and their localization in different areas of tissue, the main disadvantage is that the events are rather difficult to quantitate with these techniques. Attempts have been made to make them quantitative like by counting events per area or volume, but they rely significantly on the observer's interpretation of a positive (or "black") or negative (or "white") event. Many times the scoring is hard because the results looks "gray" and so the observer has to make a decision that may not be the same as another observer. In addition, if the interpretation was not done blinded, there can be significant observer bias introduced. Most times, that may be the case because the person doing the immunostaining will also be the person evaluating the results. Moreover, since sections of tissue have to be cut rather thin, usually between 5-10 μm , thousands of slices have to be evaluated in order to acquire a complete understanding of the event of interest in the entire tissue like the aorta. In addition, flow cytometry can measure the intensity of expression of multiple surface proteins, intracellular proteins, or markers of active internal cell signaling pathways, and quantify the number of these proteins using a defined reference like a standard curve. With the aortic digestion technique, the entire aorta was teased apart to yield a single-cell suspension of all cells, and flow cytometry was used to systematically quantitate the number of events based on defined criteria that was set a priori. This eliminated having to manually interpret "gray" events and overcame observer bias. In this research aortic macrophages were identified and quantified for the first time. The expression of surface CD14, CD11b, and F4/80 were observed to change with treatment, disease status, and in different genotype backgrounds. In addition, the technique also allowed for scoring of phosphorylated STAT3 as a measurement of intracellular signaling downstream of IL-6 in these cells. The potential of characterizing the aortic macrophages further with flow cytometry is almost unlimited.

We also conclude that the adventitial fibroblasts can contribute significantly to vascular inflammation. Not only can they produce and secrete cytokines like IL-6 and MCP-1 in copious amounts, they are highly responsive to Ang II. Ang II potently increases IL-6 and MCP-1 cytokine expression and causes AoAF cell proliferation. Moreover the MCP-1 coming from these cells are functional and can recruit monocytes. Furthermore, we believe that they are the crucial part of a monocyte-fibroblast interaction that further potentiates cytokine production and adventitial thickening seen *in vivo* with Ang II infusion. To directly prove these contributions of AoAFs, these cells will have to be selectively depleted *in vivo*.

It must be noted that a lifetime deficiency of CCR2 or IL-6 does not totally protect mice from aortic dissection in response to our dosage of Ang II with longer infusion. When we infused CCR2 and IL-6 knockout mice for 10 d, we found that 2/13 (15.4 %) of CCR2^{-/-} mice and 1/8 (12.5%) of IL-6^{-/-} mice developed aortic dissection, which is still half the incidence observed in WT mice by 6 d. These observations suggest that Ang II-induced aneurysm and aortic dissection formation is partly CCR2 and IL-6 independent and underscore our understanding that it is dependent on a complex, multitude of processes whose interaction ultimately results in a loss of aortic wall integrity. Nevertheless, our results more importantly suggest that MCP-1 and IL-6 signaling accelerate the development and increase the incidence of aneurysm and aortic dissections.

In summary, we elucidated roles for IL-6, MCP-1, adventitial fibroblasts and macrophages that together provides a novel mechanism for the acceleration of vascular inflammation (Illustration 3). We propose that IL-6 is stimulated by Ang II in aortic cells like the VSMCS and AoAFs and is further induced when monocytes are recruited to the adventitia where it comes into close proximity to adventitial fibroblasts. Increased IL-6

then promotes monocyte differentiation into a highly mobile, activated macrophage that can invade into the media with the aid of MMP-9 and potentiates MCP-1 production. Increased MCP-1 recruits more monocytes into the adventitia, facilitated by increased vasa vasorum, and the process repeats. These steps provide valuable insight into effectively disrupting the vascular inflammation common to many cardiovascular diseases.

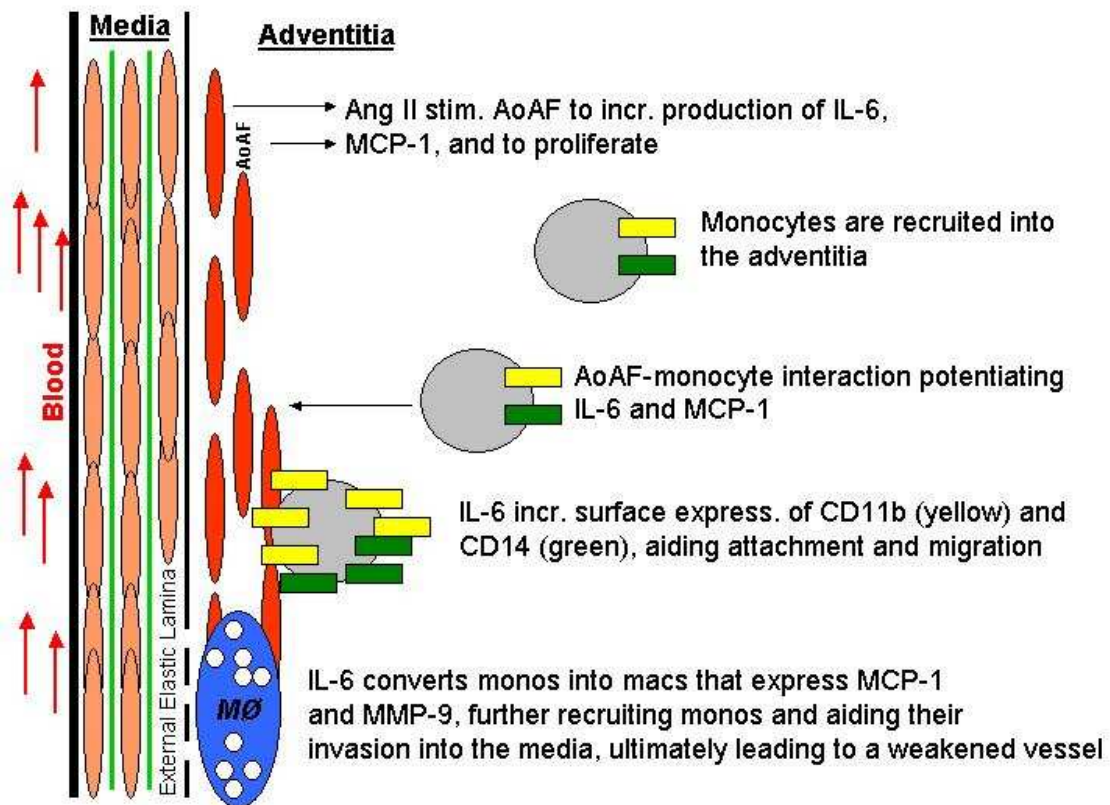


Illustration 3. Proposed sequence of events leading to acceleration of vascular inflammation and aortic aneurysm and dissection in response to Ang II. Ang II stimulates IL-6 and MCP-1 production from native cells of the aorta like AoAFs. The MCP-1 recruits monocytes into the adventitia where a monocyte-AoAF interaction potentiates IL-6 and MCP-1. The increased IL-6 increases monocyte surface expression of CD11b and CD14, allowing them to attach and migrate. IL-6 further differentiates the monocytes into macrophages that express MCP-1 and MMP-9. The increased production of MCP-1 recruits more monocytes, and this proposed sequence of events repeat, creating an IL-6-MCP-1 amplification loop that accelerates and sustains vascular inflammation eventually leading to aneurysm and dissection.

FUTURE DIRECTIONS

The data and new methods described here give rise to further questions and some interesting ideas that are worth pursuing. In addition, the techniques used can be modified to obtain better results or data of interest. The following are some topics to consider.

The research presented here shows that the phenotypes of aortic macrophages change with disease status and that they can be characterized and quantitated based on surface and intracellular proteins using the aortic digestion/flow cytometry techniques described. The aortic macrophages can be further characterized using reasonable hypotheses to ultimately create profiles distinguishing normal versus pathological macrophages. These profiles may be useful for identifying stages of disease and ultimately to calculate risk of rupture or dissection of aneurysms.

The monocyte precursor to the $CD14^{hi}CD11b^{hi}F4/80^{-}$ macrophages might be different from normal monocytes. If so, their identification in peripheral blood and can be used as a novel serum biomarker to detect disease. In the research presented here only a quick analysis was performed on the peripheral blood monocytes from sham-treated and Ang II-infused mice. A thorough analysis of the majority of these monocytes or blood flowing through the ascending aorta or suprarenal aorta at a fixed time-point is worth performing to determine if the precursor to the pathological macrophages can be detected in blood and are different. This also should be done for other leukocytes of interest in aneurysm formation, especially T cells, and in the context of other cardiovascular diseases such as atherosclerosis. The identification of precursors or the actual pathological cell types in peripheral blood can be a powerful tool to detect aneurysm disease and to monitor its progression.

The aortic digestion technique can be improved to accelerate the digestion process. The method described here takes between 1-4 h depending on the cell of interest; for complete digestion to detect macrophages, 3-4 h is recommended. This is in addition to the time required for harvesting the aorta from animals. Also, the subsequent flow cytometry staining takes approximately 2 h. Thus, experiments can take the entire day to perform and many cells may die during the process. To overcome that, the concoction of enzymes can be modified or increased in concentration as long as the antigens of interest are not adversely affected. In other studies that have digested murine aortas for identification of cells like T cells, hyaluronidase was used to facilitate the digestion of extracellular matrix. The addition of that enzyme may help speed the digestion and reduce time from tissue to cell isolation.

The aortic digestion/flow cytometry method described here can be used to study any cell type in the aorta. As seen in the data presented above and in previous publications, there are multiple changes that occur in the aorta with disease. Many other leukocytes such T cells, B cells, plasma cells, mast cells, neutrophils and DC cells in addition to monocytes are recruited to the aorta in atherosclerosis and aneurysms (39;301). In addition, native aortic cells can also be studied. As mentioned in Chapter 1, smooth muscle cell dysfunction leads to TAAD. With the digestion method, these cells can be individually studied on multiple parameters simultaneously including detection of markers for cell death and expression of surface and intracellular proteins and their modification status. Moreover, the ability to quantitate cell number may resolve the question of whether smooth muscle cells increase or decrease in density with TAs. Murine aortic smooth muscle cells have been identified and quantitated in a recent pilot study in this laboratory. Any aortic cell can be identified based on a specific marker or series of markers and quantitated. Besides quantitating the number of cells and intensity

of expression of proteins, subsets of interest can be sorted to obtain a purified population and then experimented upon *in vitro*. That gives the advantage of obtaining results for a uniform population and not a mixture of cells that may dilute the results.

As briefly mentioned in the conclusion above, the vasa vasorum seemed to undergo neovascularization or increase in volume at the areas where dissections occur. Neovascularization and increase in volume of the vasa vasorum have been observed in aneurysm and atherosclerosis and are thought to facilitate the recruitment of leukocytes to the area of pathology. Moreover, the development of aneurysm and atherosclerosis are believed to be dependent on neovascularization of the vasa vasorum since changes in the vasa vasorum are observed prior to pathology. However, why certain areas of the aorta develop these changes in the vasa vasorum is not known. We have preliminary evidence *in vitro* that the adventitial fibroblast-monocyte interaction can induce vascular endothelial growth factor, the main cytokine that induces neovascularization. That suggests another mechanism in which monocytes and AoAFs can contribute to aneurysm or atherosclerosis; the recruitment of monocytes into the adventitia may accelerate the neovascularization of vasa vasorum there. The source(s) of the VEGF, either the monocytes or adventitial fibroblasts or both, remains to be determined.

Depletion of AoAFs will provide direct evidence for the role that cell type in vascular inflammation, particularly aneurysms and atherosclerosis. Although specifically knocking out this cell type is not currently available, there is a possible way to remove them. Research on angioplasty-induced endoluminal injury has shown that adventitial fibroblasts can be labeled with LacZ by application of a viral vector expressing the LacZ gene into the adventitia. In place of LacZ, a gene inducing apoptosis can be inserted to cause the AoAFs to die. This will result in AoAF depletion, but there are several drawbacks with this technique to keep in mind. First, the depletion may only be

temporary as progenitor cells proliferate to replace the dead fibroblasts. Moreover, the method will not be totally specific for AoAFs since other cell types resident in the adventitia will be affected including macrophages, nerve cells, and cells composing the vasa vasorum. In addition, the viral infection may also affect smooth muscle cells in the outer media. To selectively remove AoAFs, further studies on their origins and characteristics are needed to reveal unique cell marker(s) that can be targeted. Once that is known, manipulation of gene(s) encoding the marker(s) will allow for specific targeting of this cell type to inhibit or remove it *in vivo*. Ang II infusion in that background will clearly demonstrate the role of AoAFs to Ang II-induced aortic diseases.

In addition, a potentially new method of targeted drug delivery for atherosclerosis and aneurysm can be developed based on the observation from the adoptive transfer experiments that monocytes home specifically to the two “hot spots” coinciding with where aneurysms and dissections are found. This cell-based therapy utilizes the innate ability of phagocytosis in monocytes and macrophages to uptake large amounts of foreign compounds and to carry it to areas of interest. Briefly, monocytes from patients can be purified unmodified from peripheral blood, allowed to take up a drug or treatment, and reinjected back into easy access veins of the same patients. From there, the monocytes are expected to migrate toward areas of inflammation as well as the liver and spleen for clearance. Once at the area of interest, the monocytes/macrophages will die naturally as seen in atherosclerosis to release its contents, or they can be induced to die if treated with a cell death-inducing agent prior to injection. Since blood circulates throughout the entire body in about 1-1.5 min, theoretically the cells only have to be alive for a few minutes in order to home to the aorta. Data from the adoptive transfer experiments suggest that the inflamed aorta acts as a sink for monocytes since labeled monocytes can still be detected in circulation 4 d post injection in sham-treated but not diseased mice despite equal

recruitment to the liver and spleen based on intensity of labeling detected in those organs. The main benefit of this therapy would be targeted delivery of drugs to areas where it is wanted and not randomly. This is especially of interest in the treatment of cancer to reduce side effects that are seen from systemic delivery of chemotherapy. The recruitment to the liver may divert some monocytes from the area of interest for clearance, but this occurs with standard drug delivery also. That is not expected to be a major problem since the inflamed aorta acts as a sink for monocytes. An advantage of this therapy is that unlimited numbers of monocytes can be isolated from humans. Based on our adult monocyte isolation protocol, 10 mL of blood from a healthy adult will yield approximately 3 million monocytes; therefore, 500 mL, a typical volume for blood donation, will yield 150 million monocytes. Since hematopoiesis is a continuous process, an unlimited number of monocytes can be obtained over time and repeat therapy is possible to deliver effective doses to the specific area of interest. Another advantage of this therapy is that the cells used will be native and will not induce an adverse immune response.

In addition, further studies on other roles of IL-6 in aneurysm formation and dissection should be performed. This research highlights some potential aspects to pursue. Stimulation of monocytes with IL-6 was shown to induce MMP-9 expression, but whether this results from IL-6 directly upregulating MMP-9 transcription and translation or indirectly by differentiating monocytes to macrophages is not clear. Animal studies have shown that IL-6^{-/-} mice have reduced MMP-9 mRNA in their aorta (194). Therefore, it seems like IL-6 controls MMP-9 expression. In addition, it is of interest to study the regulation of VEGF by IL-6 in cells native to the aorta and leukocytes. Moreover, molecular studies can reveal great insight into how IL-6 signals to regulate VEGF and MMP-9 at their promoters and whether there is cross signaling from

NF- κ B. These two areas of research will provide insight into how IL-6 facilitates the recruitment of monocytes and regulates an important enzyme that weakens aortic tissue as well as the molecular signaling involved. Together with the findings presented here, a more complete picture of the role of IL-6 in aneurysm and dissection will be obtained and new molecular targets may be revealed for the design of novel therapeutics that will be applicable to many cardiovascular diseases.

Appendicies

APPENDIX A: METHODS

Animal care and usage. All mice were housed in the UTMB Animal Resource Center in accordance with its Institutional Animal Care and Use Committee guidelines. C57BL/6J WT and IL-6^{-/-} mice were obtained as retired breeders from The Jackson Laboratory and housed until animals were from 7-12 mo of age. CCR2^{-/-} breeding pairs were obtained from The Jackson Laboratory and bred in house. Age-matched CCR2^{-/-} and IL-6^{-/-} mice were used in all experiments. Both CCR2^{-/-} and IL-6^{-/-} mice are in the C57BL/6J background. For Ang II infusion, anesthetized mice received subcutaneous Alzet osmotic minipumps (Durect Corp.) delivering either saline (sham-treatment) or Ang II (synthesized by the UTMB peptide synthesis core) at 2,500 ng kg⁻¹ min⁻¹ for 6 or 10 d.

Explantation of aorta and cytokine analysis. Mice were perfused with PBS via the left ventricle to remove blood from tissue. Hearts and aortas were excised as a unit and placed in sterile PBS. Peri-adventitial fat was removed. As soon as the aortas were clean, they were placed in 0.5 mL of DMEM medium (Cellgro) containing 1x ITS (Sigma) and 0.1 % BSA (Sigma) and incubated in a tissue culture hood at 37° C for 4 h. After incubation, the medium was removed and stored frozen at -80° C. All detection of IL-6 and MCP-1 in culture medium was analyzed using a multi-plex, bead-based ELISA kit (Lincoplex/Millipore mouse or human adipocyte/cytokine panel) according to manufacture's instructions. Samples were run in 25 µL duplicates.

Immunohistochemistry and immunofluorescence. Slides containing frozen mouse aortic cross-sections (6 µm) were immediately fixed with 4 % PFA for 30 mins upon removal from -80° C. Blocking was performed using 0.1 % Triton-X, 5 % normal serum

of the species producing the highly cross-absorbed Alexa 568 conjugated secondary antibody (Invitrogen) for 15 min⁶ at 37° C. Blocking was removed by tapping slides and primary antibodies were added at the following concentrations: 1:100 anti-CD11b (M1/70-eBioscience), 1:100 anti-fibroblasts (ER-TR7- BACHEM), 1:50 anti-MCP-1 (ECE.2-Abcam), 1:200 anti-IL-6 (eBioscience), and 1: 200 anti-macrophages (MOMA-2-Abcam). Incubations in primary antibody were performed for 2 h at 37° C or overnight at 4° C. Washes were performed with PBS containing 0.05 % Tween 20 and 1 % BSA 3 times for 5 min each on a tilting platform. Alexa 568-conjugated secondary antibodies were added at a dilution of 1:200 and incubated for 45 min at 37° C. After incubation, slides were washed as above 3 times. The slides were stained with DAPI for 5 min and then rinsed before mounting. PFA-fixed, paraffin-embedded human aortic tissue sections were microwaved for antigen retrieval and stained according to the instructions of the VECTASTAIN ABC-AP kit (Vector Laboratories) using a 1:100 dilution of anti-IL-6 antibody (clone 6708-R&D systems). Vector Red (Vector Laboratories) was used as the substrate. The precipitate is red and also gives a red fluorescence. Micrographs were taken with an E800-UIC Upright Epifluorescence microscope and images collected by ACT-1 software. Anonymous human samples of sporadic ascending aortic aneurysm and type A dissection, stable ascending aneurysm, and normal control samples were kindly provided by Dong-Chuan Guo from the laboratory of Dr. Dianna Milewicz at UTHSC-Houston.

Aortic digestion. Aortas were removed from mice, cut into 3-4 mm pieces, and placed into 1 mL of aortic digestion solution. This solution contains 1.25 mg/mL collagenase (Sigma), 50 µg/mL porcine pancreatic elastase (Sigma), and 5 mM CaCl in 0.9 mL base solution of Accumax (Innovative Cell Technologies). The tissue was

⁶ min is the abbreviation for minute (s)

allowed to digest at room temperature with agitation for 3-4 h. This digestion process did not affect surface protein expression as determined using THP-1 monocytes and macrophages. After digestion, the cells were washed once in FACS buffer (0.5 % BSA, 0.02 % NaN_3 in PBS) with centrifugation at 300g for 5 min. Blocking and the protocol for flow cytometry are described below. For samples with significant RBC contamination, a RBC lysis step was performed after the initial wash. For detection of p-STAT3, aortas were digested in the presence of phosphatase inhibitors (5 mM depolymerized sodium orthovanadate and 50 mM NaF). After digestion, the cells were quickly washed and then fixed in 0.5 % PFA for 10 min. Cell permeabilization was performed with 100 % cold methanol for at least 10 min on ice. All washes and incubations were done in the presence of phosphatase inhibitors.

Flow cytometry. Murine Fc receptors were blocked using antibodies against mouse CD16/32 antigens (eBioscience) for 10 mins on ice. The cells were then washed and resuspended in 100 μL FACS buffer. Fluorochrome-conjugated antibodies [FITC CD11b (M1/70), PE CD14 (Sa2-8), APC F4/80 (BM8) all from eBioscience, CCR2 (M-50) from Santa Cruz Biotechnology, Alexa Fluor 647 p-STAT3 Y705 (4/P-Stat3) from BD Bioscience] were added and samples were incubated for 30-45 min at room temperature, protected from light with occasional resuspension. The corresponding isotype control antibodies were added to “isotype samples” at the same concentrations as the antibodies of interest. After incubation, all samples were washed 3x in FACS buffer with centrifugation at 300g for 5 min. Cells were fixed in 0.5 % PFA and analyzed by FASCanto the following day. Compensation was performed using positive samples containing aortic macrophages stained for one color. For indirect staining using an unconjugated primary antibody, a 1:2000 dilution of the conjugated secondary antibody was used. Human cells were blocked with human serum and staining was performed as

above with the following antibodies: FITC CD1a (HI149), PE CD14 (61D3), PE CD11c (3.9), PE-Cy7 CD11b (ICRF44), APC HLA-DR (LN3) all from eBioscience and MMP-9 from Sigma. Debris and dead cells, as defined by low forward scatter, were excluded from analysis. Data were analyzed with Flowjo or Cyflogic.

Murine monocyte isolation. Blood was obtained from C57BL/6J mice by cardiac puncture. Approximately 0.7-1.0 mL of blood was obtained per mouse and collected in EDTA coated vials. RBC lysis solution (Invitrogen) was added to the blood in a ratio of 3:1 for 5 min at room temperature. The cells were centrifuged at 1,000g for 3 min to remove RBC lysis solution. The pellet of leukocytes was resuspended and washed in cell isolation buffer (2 % heat-inactivated FBS, 2mM EDTA in PBS) with centrifugation at 400g for 10 min. Cell counting of leukocytes was done by the trypan blue exclusion method with a hemocytometer. Next, the protocol for negative isolation of monocytes was performed according to the SpinSep Monocyte Isolation Custom Kit instructions (Stem Cell Technologies). Briefly, an antibody cocktail was added to the leukocytes at a concentration of 10 $\mu\text{L}/5 \times 10^7$ nucleated cells per mL and incubated at 4° C for 15 min. The cells were washed and 250 μL of SpinSep Dense Particles were added per 5×10^7 cells. This cell/particle suspension was incubated on ice for 20 min with occasional mixing. After incubation, the mixture was diluted with 6 mL of isolation buffer and gently layered on top of 4 mL of SpinSep Density Medium at room temperature. Centrifugation was performed for 10 min at 1,200g at room temperature with brakes off. The enriched cells from the interface were carefully removed into a new tube and washed. PBS was added to resuspend the monocytes before injection. A typical isolation took 4 h. We were able to isolate 1.5×10^6 monocytes from eight mice. Monocytes were 7 % of all leukocytes. The purity was >95 % as assessed by staining for CD14.

Labeling of mouse monocytes. Mouse monocytes were labeled with DiR800 (Invitrogen) and PKH26 (Sigma) simultaneously according to the product protocol for PKH26. Briefly, cells were resuspended in 1 mL solution A of PKH26. 4 μ M solution of PKH26 dye in 1 mL was made in Solution B and a 1:500 dilution of 10 mg/mL DiR800 was added. Solution A was combined with Solution B and the cells were incubated for 3 min at room temperature. The final concentration of PKH26 was 2 μ M and DiR800 was 0.01 mg/mL. After incubation, the cells were washed with PBS 3 times. Complete removal of DiR800 dye was checked by LICOR imaging.

Adoptive transfer of mouse monocytes and in vivo imaging. 1.5×10^6 monocytes in 150 μ L of PBS were injected via tail vein using a 26 gauge needle (BD). The tails were warmed under lighting to dilate veins and cleaned with alcohol swabs. A tourniquet was made at the base of the tail to enhance dilatation. Cells were injected when no resistance was felt upon pressing on the needle's plunger. When any resistance was felt, the needle was immediately withdrawn. This procedure enabled for injection of the entire 150 μ L cell suspension. 4 d after injection of labeled monocytes, the mice were anesthetized and shaved to remove hair on the ventrum and dorsum. Mice were placed on the LICOR Odyssey and scanned using the DNA Gel setting at an offset of 2-4 mm and an intensity of 4 in the 800 channel and 1 in the 700 channel. For detection of cells in the aorta, the aortas were excised and placed in 60 mm culture dishes. They were scanned with the DNA Gel setting at an offset of 2 mm and an intensity of 4 in the 800 channel and 1 in the 700 channel. These machine settings and scan area were kept consistent for each mouse. For detection of PKH26, the aortic root/ascending aorta was embedded and quickly frozen in OCT on dry ice. Detection of PKH26 in 6 μ M cross-sections was done with fluorescence microscopy.

Cells. Primary cultures of human aortic adventitial fibroblasts (AoAF) were purchased (Lonza) and grown in Stromal Cell Growth Medium (SCGM) containing 5 % FBS (Lonza). THP-1 monocytes were obtained from ATCC and grown in RPMI 1640 medium containing 10 % FBS. Cord blood monocytes were obtained from cord blood using cord blood donated to the laboratory of Dr. Randy Urban. Adult peripheral blood monocytes were obtained from blood of a volunteer.

Coculture. Coculture experiments were performed at a ratio of 4:1, monocytes to fibroblasts, respectively. 500×10^3 monocytes were added to a culture of 125×10^3 adventitial fibroblasts in 1.5 mL of RPMI medium containing 5 % FBS for 4-5 d. For analysis of cytokines in culture medium, the medium was removed and kept at -80°C . For flow cytometry, cells were dislodged with 1 mL of 2 mM EDTA. IL-4 and GM-CSF were added to the culture medium at a concentration of 10 ng/mL every 3 d starting day 0 of coculture. For neutralization of IL-6, 10 μg of anti-IL-6 and anti-sIL-6R antibodies were added daily from day 0. For Transwell experiments, monocytes were added to the top of polycarbonate inserts with 0.4 μm pores and the fibroblasts were grown on the bottom well (Corning Lifesciences).

Real-time PCR for human MCP-1 from THP-1. RNA was extracted from 1×10^6 THP-1 cells using TriReagent following manufacture's instructions. 0.5 μg of RNA was reverse-transcribed using Superscript III (Invitrogen) according to provided directions. Real-time PCR reactions were performed in triplicates using 1 μL of resulting cDNA per 20 μL reaction volume containing iQ SYBR Green supermix (Bio-Rad Laboratories, Inc.). GAPDH was used as the housekeeping gene. Primers for human MCP-1/CCL2 were CATTGTGGCCAAGGAGATCTG (forward) and CTTCGGAGTTTGGGTTTGCTT (reverse). PCR was performed on the MyiQ system

(Bio-Rad Laboratoireis, Inc.) according to preset protocol. MCP-1 mRNA was analyzed by the $\Delta\Delta\text{Ct}$ method.

Real-Time PCR for IL-6 and MCP-1 from AoAFs. Total cellular RNA was extracted from AoAFs using TRI-REAGENT (Sigma). 1 μg of RNA sample was fractionated by electrophoresis on a 1 % MOPS/formaldehyde agarose gel to ensure RNA integrity. Validated human IL-6 (FW- 5'-GGCACTGGCAGAAAACAACC-3' and RW- 5'-GCAAGTCTCCTCATTGAATCC-3') and MCP-1 (FW- 5'-CATTGTGGCCAAGGAGATCTG-3' and RW- 5'-CTTCGGAGTTTGGGTTTGCTT-3') gene specific primers were obtained from RT Primer Database (<http://medgen.ugent.be/rtprimerdb>). Reverse transcription was performed with 1 μg of total RNA using random nonomers as primers and the Superscript III reverse transcription system (Invitrogen) as recommended by the manufacturer. One μL of the reverse transcription reaction was used as template for the subsequent PCR reaction, which was carried out in triplicate. The reaction mixture consisted of Syber-green super-mix (BioRad), template cDNA, and target primer at a concentration of 200-400 nM. Thermal cycling was performed with a BioRad myIQ5 real-time PCR system (BioRad) under factory defaults (50° C, 2 min; 95° C, 10 min; and 40 cycles at 95° C for 15 sec., 60° C for 1 min). Threshold cycle number (Ct) was obtained for each sample. Relative transcript levels were quantified as a comparison of measured Ct values for each reaction. GAPDH mRNA levels were measured for each sample and utilized as the internal control. Fold change values were calculated using the $2^{-\Delta\Delta\text{Ct}}$ method.

Multiplex-ELISA. 50×10^3 AoAFs and 200×10^3 THP-1 monocytes were grown in their respective medium for 36 h. 25 μL samples of fibroblast-conditioned or monocyte-conditioned medium were assayed in duplicate using Biosource Multiplex kits (Biosource), and a standard curved assayed in parallel was used to determine cytokine

concentrations. Data was expressed as mean \pm standard deviation for 6 individual samples for each cell type.

In situ hybridization. SP6 and T7 RNA polymerases were used to produce sense and anti-sense digoxigenin (DIG)-labeled cRNAs from human IL-6 and MCP-1 cDNA fragments cloned in pCR II-TOPO (Invitrogen). AoAFs were fixed in 4 % paraformaldehyde for 30 min at room temperature, then prehybridized with hybridization buffer (4X SSC; 10 % dextran sulfate; 1X Denhardt's solution containing 0.02 % Ficoll 400, 0.02 % polyvinyl pyrrolidone, 0.02 % BSA; 2 mM EDTA; 50 % deionized formamide; 500 μ g/mL herring sperm DNA) for 1 h at 37° C. Hybridization in buffer containing 20 ng IL-6 cRNA or 20 ng MCP-1 cRNA probe was performed overnight at 37° C. Sections were blocked with Roche Blocking Buffer (Roche) for 30 min at room temperature, then incubated with anti-DIG antibody (in blocking buffer) for 2 h at room temperature. NBT/BCIP color substrate incubation was performed for detection of DIG-labeled probes hybridized to IL-6 mRNA or MCP-1 mRNA. The cells were counterstained for 5-10 min with nuclear fast red stain and mounted in Dako mounting media.

Cell migration assay. Migration to THP-1 monocytes to AoAF-conditioned medium was assessed by Boyden chamber assay using Transwell polycarbonate membrane inserts with 8 μ m pores (Corning Lifesciences). Briefly, 2×10^6 THP-1 cells in 100 μ L of serum-free Stromal Cell Medium (SCM) were placed on the top chamber and 600 μ L of AoAF-conditioned medium or Stromal Cell Growth Medium was placed on the bottom chamber. After a 2 h incubation at 37° C, the number of cells migrated to the bottom chamber was assessed using a Z2 Coulter Counter (Beckman-Coulter). For inhibition studies, neutralizing MCP-1 antibodies (BioLegend clone 2H5) or Hamster

IgG control (eBioscience) antibodies were incubated with AoAF-conditioned medium for 30 min prior to plating.

Cell proliferation assay. AoAFs were plated at 50×10^3 cells/well and grown in SCGM for 24 h. The medium was then replaced with SCM containing 0.25 % BSA, 0.2 % FBS. The cells were stimulated with 1 μ M Ang II for 4 d. AoAFs were detached in 0.5 mL ACCUMAX and diluted into 9.5 mL of an ISOTON II solution for counting with a Z2 Coulter Counter.

Thymidine incorporation assay. AoAFs were plated at 50×10^3 cells/well in twelve-well plates and grown in SCGM for 24 h. The medium was replaced with SCM containing 0.25 % BSA, 0.2 % FBS. Cells were stimulated with 1 μ M Ang-II for 16 h. During the final 4 h, ^3H -thymidine (2 μ Ci/mL) was added. Plates were briefly washed with 2 mL of cold PBS and then 2 mL of cold 10 % TCA were added and incubated at 4° C for 2 h. Cells were washed with 95 % ethanol and allowed to dry for 1 min. 500 μ L of 0.2 N NaOH was added to dissolve the cells for 2 h. 450 μ L of lysate was added to 5 mL of scintillation cocktail, mixed, and dark-adapted for at least 2 h before counting CPM in a Geiger counter (Beckman-Coulter USA).

Flow Cytometry for cells in culture. AoAFs were labeled with 2 μ M PKH26 (Sigma) prior to start of coculture experiments while THP-1 cells were unlabeled. Cells in coculture were detached with 10 mM EDTA/ACCUMAX, centrifuged, and resuspended in PBS containing 0.5 % BSA, and kept on ice until time of analysis using a FASCanto (BD Bioscience). For overnight storage, cells were resuspended in 0.5 % paraformaldehyde-PBS solution, vortexed immediately, then kept in the dark on a rotating holder at 4° C. The PE signal from PKH26 was detected by flow cytometry.

Data analysis. Data were reported as mean \pm standard deviation (SD) or mean \pm standard error (SE) as indicated from at least 3 separate experiments unless stated

otherwise in Results. Differences were analyzed by Student's t-test (one-tail, assuming unequal variances). Values of $P < 0.05$ were considered significant.

APPENDIX B: TABLE 1-AORTIC MACROPHAGES

Table 1. Quantitation of macrophages in aorta

Mice	Group		# Macrophage	% Macrophage	<i>n</i>
C57BL/6J	Sham		1,840 ± 314	0.46 ± 0.08	15
	Ang II	No Dissection	9,750 ± 2,218	2.44 ± 0.55	11
		Dissection	127,452 ± 9,575	31.87 ± 2.39	4
IL-6 ^{-/-}	Sham		1,317 ± 217	0.33 ± 0.05	9
	Ang II		4,812 ± 998	1.20 ± 0.25	8
CCR2 ^{-/-}	Sham		942 ± 102	0.24 ± 0.03	7
	Ang II		2,626 ± 106	0.66 ± 0.03	7

Table 1. Quantitation of macrophages in the aorta. Numbers of CD14⁺CD11b⁺ macrophages in sham-treated and Ang II-treated WT, IL-6^{-/-}, and CCR2^{-/-} mice were quantitated by flow cytometry after 6 d of Ang II infusion and expressed as a percentage of all cells counted. Data are mean ± SEM.

APPENDIX C: TABLE 2-CYTOKINES SECRETED FROM HUMAN AOAFS AND MONOCYTES

Table 2. Adventitial fibroblast and monocyte cytokine secretion

Cytokines/Chemokines	AoAF (pg/mL ± S.D.)	THP-1 (pg/mL ± S.D.)
IL-1β	OOOR<	71.8 ± 12.4
IL-1Ra	89.3 ± 24.3	33.3 ± 17.4
IL-2	OOOR<	10.8 ± 4.0
IL-4	6.3 ± 0.2	5.9 ± 0.3
IL-5	2.0 ± 0.2	1.4 ± 0.1
IL-6	967.8 ± 149.4	3.4 ± 0.9
IL-8	8.4 ± 1.5	21.2 ± 5.2
IL-10	27.5 ± 4.3	12.7 ± 0.7
IL-12p40/p70	OOOR<	1.4 ± 1.0
IL-15	15.3 ± 2.5	10.8 ± 3.4
TNF-α	3.2 ± 0.7	33.3 ± 17.4
IFN-γ	2.4 ± 0.3	1.9 ± 0.7
GM-CSF	18.3 ± 3.8	OOOR<
MIP-1α	17.7 ± 3.9	20.7 ± 5.0
MIP-1β	18.1 ± 4.9	276.4 ± 60.9
Eotaxin	1.2 ± 0.4	OOOR<
RANTES	OOOR<	163.9 ± 14.3
MCP-1	583.7 ± 78.9	19.7 ± 3.1
IP-10	1.9 ± 0.1	8.2 ± 1.2

OOOR< (Out Of Range Low)

Table 2. Cytokines secreted from aortic adventitial fibroblasts and monocytes. 50x10³ primary human aortic adventitial fibroblasts and 200x10³ THP-1 monocytes were cultured for 36 h and the conditioned media were assayed in duplicate with BioSource human cytokine 25-plex panel bead-based Luminex assay. Data are mean ± S.D.

References

1. Isselbacher, E.M. 2004. Diseases of the aorta. In *Cecil Textbook of Medicine*. L.Goldman, and Ausiello, D., editors. W.B. Saunders. Philadelphia, PA. 460-462.
2. Kumar, V., Fausto, N., and Abbas, A. 2004. *Robbins and Cotran Pathologic Basis of Disease*. W.B. Saunders. Philadelphia, PA.
3. Michel, J.B., Thauinat, O., Houard, X., Meilhac, O., Caligiuri, G., and Nicoletti, A. 2007. Topological determinants and consequences of adventitial responses to arterial wall injury. *Arterioscler. Thromb. Vasc. Biol.* **27**:1259-1268.
4. He, R., Guo, D.C., Estrera, A.L., Safi, H.J., Huynh, T.T., Yin, Z., Cao, S.N., Lin, J., Kurian, T., Buja, L.M. et al. 2006. Characterization of the inflammatory and apoptotic cells in the aortas of patients with ascending thoracic aortic aneurysms and dissections. *J Thorac. Cardiovasc. Surg.* **131**:671-678.
5. Guo, D.C., Papke, C.L., He, R., and Milewicz, D.M. 2006. Pathogenesis of thoracic and abdominal aortic aneurysms. *Ann. N. Y. Acad. Sci.* **1085**:339-352.
6. Kuivaniemi, H., Platsoucas, C.D., and Tilson, M.D., III 2008. Aortic aneurysms: an immune disease with a strong genetic component. *Circulation* **117**:242-252.
7. Tilson, M.D., III 2005. The polymorphonuclear leukocyte and the abdominal aortic aneurysm: a neglected cell type and a neglected disease. *Circulation* **112**:154-156.
8. Lederle, F.A., Johnson, G.R., Wilson, S.E., Chute, E.P., Littooy, F.N., Bandyk, D., Krupski, W.C., Barone, G.W., Acher, C.W., and Ballard, D.J. 1997. Prevalence and associations of abdominal aortic aneurysm detected through screening. Aneurysm Detection and Management (ADAM)

Veterans Affairs Cooperative Study Group. *Ann. Intern. Med.* **126**:441-449.

9. Sakata, N., Nabeshima, K., Iwasaki, H., Tashiro, T., Uesugi, N., Nakashima, O., Ito, H., Kawanami, T., Furuya, K., and Kojima, M. 2007. Possible involvement of myofibroblasts in the development of inflammatory aortic aneurysm. *Pathol. Res. Pract.* **203**:21-29.
10. Stella, A., Gargiulo, M., Pasquinelli, G., Preda, P., Faggioli, G.L., Cenacchi, G., and D'Addato, M. 1991. The cellular component in the parietal infiltrate of inflammatory abdominal aortic aneurysms (IAAA). *Eur. J Vasc. Surg.* **5**:65-70.
11. en.wikipedia.org/wiki/Aortic_dissection on 9/11 2008. Aortic dissection. 1-13.
12. Green, G.R., and Kron, I.L. 2003. Aortic Dissection. In *Cardiac surgery in the adult*. L.H.Cohn, and Edmunds, L.H.Jr., editors. McGraw-Hill. New York, NY. 1095-1122.
13. Dzau, V., and Creager, M. 2001. Diseases of the aorta. In *Harrison's Principals of Internal Medicine*. E.Braunwald, Fauci, A.S., Kasper, D.L., Hauser, S.L., Longo, D.L., and Jameson, J.L., editors. McGraw-Hill. New York, NY. 1431-1433.
14. Pannu, H., Avidan, N., Tran-Fadulu, V., and Milewicz, D.M. 2006. Genetic basis of thoracic aortic aneurysms and dissections: potential relevance to abdominal aortic aneurysms. *Ann. N. Y. Acad. Sci.* **1085**:242-255.
15. Milewicz, D.M., Guo, D.C., Tran-Fadulu, V., Lafont, A.L., Papke, C.L., Inamoto, S., and Pannu, H. 2008. Genetic Basis of Thoracic Aortic Aneurysms and Dissections: Focus on Smooth Muscle Cell Contractile Dysfunction. *Annu. Rev. Genomics Hum. Genet.* **9**:283-302.
16. Pannu, H., Tran-Fadulu, V., Papke, C.L., Scherer, S., Liu, Y., Presley, C., Guo, D., Estrera, A.L., Safi, H.J., Brasier, A.R. et al. 2007. MYH11 mutations result in a distinct vascular pathology driven by insulin-like growth factor 1 and angiotensin II. *Hum. Mol. Genet.* **16**:2453-2462.

17. Guo, D.C., Pannu, H., Tran-Fadulu, V., Papke, C.L., Yu, R.K., Avidan, N., Bourgeois, S., Estrera, A.L., Safi, H.J., Sparks, E. et al. 2007. Mutations in smooth muscle alpha-actin (ACTA2) lead to thoracic aortic aneurysms and dissections. *Nat. Genet.* **39**:1488-1493.
18. Brasier, A.R., Recinos, A., III, and Eleдрisi, M.S. 2002. Vascular inflammation and the renin-angiotensin system. *Arterioscler. Thromb. Vasc. Biol.* **22**:1257-1266.
19. Maurer, M., and von, S.E. 2004. Macrophage inflammatory protein-1. *Int. J Biochem. Cell Biol.* **36**:1882-1886.
20. Ross, R. 1999. Atherosclerosis--an inflammatory disease. *N. Engl. J Med.* **340**:115-126.
21. Tang, P.C., Yakimov, A.O., Teesdale, M.A., Coady, M.A., Dardik, A., Elefteriades, J.A., and Tellides, G. 2005. Transmural inflammation by interferon-gamma-producing T cells correlates with outward vascular remodeling and intimal expansion of ascending thoracic aortic aneurysms. *FASEB J* **19**:1528-1530.
22. Herron, G.S., Unemori, E., Wong, M., Rapp, J.H., Hibbs, M.H., and Stoney, R.J. 1991. Connective tissue proteinases and inhibitors in abdominal aortic aneurysms. Involvement of the vasa vasorum in the pathogenesis of aortic aneurysms. *Arterioscler. Thromb.* **11**:1667-1677.
23. Thompson, R.W., Geraghty, P.J., and Lee, J.K. 2002. Abdominal aortic aneurysms: basic mechanisms and clinical implications. *Curr. Probl. Surg.* **39**:110-230.
24. Shimizu, K., Mitchell, R.N., and Libby, P. 2006. Inflammation and cellular immune responses in abdominal aortic aneurysms. *Arterioscler. Thromb. Vasc. Biol.* **26**:987-994.
25. Eliason, J.L., Hannawa, K.K., Ailawadi, G., Sinha, I., Ford, J.W., Deogracias, M.P., Roelofs, K.J., Woodrum, D.T., Ennis, T.L., Henke, P.K. et al. 2005. Neutrophil depletion inhibits experimental abdominal aortic aneurysm formation. *Circulation* **112**:232-240.

26. Tsuruda, T., Kato, J., Hatakeyama, K., Kojima, K., Yano, M., Yano, Y., Nakamura, K., Nakamura-Uchiyama, F., Matsushima, Y., Imamura, T. et al. 2008. Adventitial Mast Cells Contribute to Pathogenesis in the Progression of Abdominal Aortic Aneurysm. *Circ. Res.* 102:1368-1377.
27. Pearce, W.H., and Koch, A.E. 1996. Cellular components and features of immune response in abdominal aortic aneurysms. *Ann. N. Y. Acad. Sci.* **800**:175-185.
28. Ocana, E., Bohorquez, J.C., Perez-Requena, J., Brieva, J.A., and Rodriguez, C. 2003. Characterisation of T and B lymphocytes infiltrating abdominal aortic aneurysms. *Atherosclerosis* **170**:39-48.
29. Curci, J.A., and Thompson, R.W. 2004. Adaptive cellular immunity in aortic aneurysms: cause, consequence, or context? *J Clin. Invest.* **114**:168-171.
30. Koch, A.E., Haines, G.K., Rizzo, R.J., Radosevich, J.A., Pope, R.M., Robinson, P.G., and Pearce, W.H. 1990. Human abdominal aortic aneurysms. Immunophenotypic analysis suggesting an immune-mediated response. *Am. J Pathol.* **137**:1199-1213.
31. Brophy, C.M., Reilly, J.M., Smith, G.J., and Tilson, M.D. 1991. The role of inflammation in nonspecific abdominal aortic aneurysm disease. *Ann. Vasc. Surg.* **5**:229-233.
32. Forester, N.D., Cruickshank, S.M., Scott, D.J., and Carding, S.R. 2005. Functional characterization of T cells in abdominal aortic aneurysms. *Immunology* **115**:262-270.
33. Xiong, W., Zhao, Y., Prall, A., Greiner, T.C., and Baxter, B.T. 2004. Key roles of CD4+ T cells and IFN-gamma in the development of abdominal aortic aneurysms in a murine model. *J Immunol.* **172**:2607-2612.
34. Lindeman, J.H., Abdul-Hussien, H., Schaapherder, A.F., Van Bockel, J.H., Von der Thusen, J.H., Roelen, D.L., and Kleemann, R. 2008. Enhanced expression and activation of pro-inflammatory transcription factors distinguish aneurysmal from atherosclerotic aorta: IL-6- and IL-8-dominated

inflammatory responses prevail in the human aneurysm. *Clin. Sci. (Lond)* **114**:687-697.

35. Gregory, A.K., Yin, N.X., Capella, J., Xia, S., Newman, K.M., and Tilson, M.D. 1996. Features of autoimmunity in the abdominal aortic aneurysm. *Arch. Surg.* **131**:85-88.
36. Platsoucas, C.D., Lu, S., Nwaneshiudu, I., Solomides, C., Agelan, A., Ntaoula, N., Purev, E., Li, L.P., Kratsios, P., Mylonas, E. et al. 2006. Abdominal aortic aneurysm is a specific antigen-driven T cell disease. *Ann. N. Y. Acad. Sci.* **1085**:224-235.
37. Chan, W.L., Pejnovic, N., Liew, T.V., and Hamilton, H. 2005. Predominance of Th2 response in human abdominal aortic aneurysm: mistaken identity for IL-4-producing NK and NKT cells? *Cell Immunol.* **233**:109-114.
38. Hannawa, K.K., Eliason, J.L., Woodrum, D.T., Pearce, C.G., Roelofs, K.J., Grigoryants, V., Eagleton, M.J., Henke, P.K., Wakefield, T.W., Myers, D.D. et al. 2005. L-selectin-mediated neutrophil recruitment in experimental rodent aneurysm formation. *Circulation* **112**:241-247.
39. Sun, J., Sukhova, G.K., Yang, M., Wolters, P.J., MacFarlane, L.A., Libby, P., Sun, C., Zhang, Y., Liu, J., Ennis, T.L. et al. 2007. Mast cells modulate the pathogenesis of elastase-induced abdominal aortic aneurysms in mice. *J Clin. Invest.* **117**:3359-3368.
40. Newman, K.M., Jean-Claude, J., Li, H., Scholes, J.V., Ogata, Y., Nagase, H., and Tilson, M.D. 1994. Cellular localization of matrix metalloproteinases in the abdominal aortic aneurysm wall. *J Vasc. Surg.* **20**:814-820.
41. Freestone, T., Turner, R.J., Coady, A., Higman, D.J., Greenhalgh, R.M., and Powell, J.T. 1995. Inflammation and matrix metalloproteinases in the enlarging abdominal aortic aneurysm. *Arterioscler. Thromb. Vasc. Biol.* **15**:1145-1151.
42. Thompson, R.W., Holmes, D.R., Mertens, R.A., Liao, S., Botney, M.D., Mecham, R.P., Welgus, H.G., and Parks, W.C. 1995. Production and localization of 92-kilodalton gelatinase in abdominal aortic aneurysms. An elastolytic

metalloproteinase expressed by aneurysm-infiltrating macrophages. *J Clin. Invest.* **96**:318-326.

43. Longo, G.M., Xiong, W., Greiner, T.C., Zhao, Y., Fiotti, N., and Baxter, B.T. 2002. Matrix metalloproteinases 2 and 9 work in concert to produce aortic aneurysms. *J Clin. Invest.* **110**:625-632.
44. Pyo, R., Lee, J.K., Shipley, J.M., Curci, J.A., Mao, D., Ziporin, S.J., Ennis, T.L., Shapiro, S.D., Senior, R.M., and Thompson, R.W. 2000. Targeted gene disruption of matrix metalloproteinase-9 (gelatinase B) suppresses development of experimental abdominal aortic aneurysms. *J Clin. Invest.* **105**:1641-1649.
45. Newman, K.M., Jean-Claude, J., Li, H., Ramey, W.G., and Tilson, M.D. 1994. Cytokines that activate proteolysis are increased in abdominal aortic aneurysms. *Circulation* **90**:II224-II227.
46. Walton, L.J., Franklin, I.J., Bayston, T., Brown, L.C., Greenhalgh, R.M., Taylor, G.W., and Powell, J.T. 1999. Inhibition of prostaglandin E2 synthesis in abdominal aortic aneurysms: implications for smooth muscle cell viability, inflammatory processes, and the expansion of abdominal aortic aneurysms. *Circulation* **100**:48-54.
47. Zhao, L., Moos, M.P., Grabner, R., Pedrono, F., Fan, J., Kaiser, B., John, N., Schmidt, S., Spanbroek, R., Lotzer, K. et al. 2004. The 5-lipoxygenase pathway promotes pathogenesis of hyperlipidemia-dependent aortic aneurysm. *Nat. Med.* **10**:966-973.
48. Miller, F.J., Jr., Sharp, W.J., Fang, X., Oberley, L.W., Oberley, T.D., and Weintraub, N.L. 2002. Oxidative stress in human abdominal aortic aneurysms: a potential mediator of aneurysmal remodeling. *Arterioscler. Thromb. Vasc. Biol.* **22**:560-565.
49. Holmes, D.R., Wester, W., Thompson, R.W., and Reilly, J.M. 1997. Prostaglandin E2 synthesis and cyclooxygenase expression in abdominal aortic aneurysms. *J Vasc. Surg.* **25**:810-815.

50. Szekanecz, Z., Shah, M.R., Pearce, W.H., and Koch, A.E. 1994. Human atherosclerotic abdominal aortic aneurysms produce interleukin (IL)-6 and interferon-gamma but not IL-2 and IL-4: the possible role for IL-6 and interferon-gamma in vascular inflammation. *Agents Actions* **42**:159-162.
51. Juvonen, J., Surcel, H.M., Satta, J., Teppo, A.M., Bloigu, A., Syrjala, H., Airaksinen, J., Leinonen, M., Saikku, P., and Juvonen, T. 1997. Elevated circulating levels of inflammatory cytokines in patients with abdominal aortic aneurysm. *Arterioscler. Thromb. Vasc. Biol.* **17**:2843-2847.
52. Duftner, C., Seiler, R., Klein-Weigel, P., Gobel, H., Goldberger, C., Ihling, C., Fraedrich, G., and Schirmer, M. 2005. High prevalence of circulating CD4+. *Arterioscler. Thromb. Vasc. Biol.* **25**:1347-1352.
53. Galle, C., Schandene, L., Stordeur, P., Peignoys, Y., Ferreira, J., Wautrecht, J.C., Dereume, J.P., and Goldman, M. 2005. Predominance of type 1 CD4+ T cells in human abdominal aortic aneurysm. *Clin. Exp. Immunol.* **142**:519-527.
54. Schonbeck, U., Sukhova, G.K., Gerdes, N., and Libby, P. 2002. T(H)2 predominant immune responses prevail in human abdominal aortic aneurysm. *Am. J Pathol.* **161**:499-506.
55. Davis, V.A., Persidskaia, R.N., Baca-Regen, L.M., Fiotti, N., Halloran, B.G., and Baxter, B.T. 2001. Cytokine pattern in aneurysmal and occlusive disease of the aorta. *J Surg Res.* **101**:152-156.
56. Shimizu, K., Shichiri, M., Libby, P., Lee, R.T., and Mitchell, R.N. 2004. Th2-predominant inflammation and blockade of IFN-gamma signaling induce aneurysms in allografted aortas. *J Clin. Invest.* **114**:300-308.
57. Koch, A.E., Kunkel, S.L., Pearce, W.H., Shah, M.R., Parikh, D., Evanoff, H.L., Haines, G.K., Burdick, M.D., and Strieter, R.M. 1993. Enhanced production of the chemotactic cytokines interleukin-8 and monocyte chemoattractant protein-1 in human abdominal aortic aneurysms. *Am. J Pathol.* **142**:1423-1431.

58. Dawson, J., Cockerill, G.W., Choke, E., Belli, A.M., Loftus, I., and Thompson, M.M. 2007. Aortic aneurysms secrete interleukin-6 into the circulation. *J Vasc. Surg.* **45**:350-356.
59. Dawson, J., Cockerill, G., Choke, E., Loftus, I., and Thompson, M.M. 2006. Aortic aneurysms as a source of circulating interleukin-6. *Ann. N. Y. Acad. Sci* **1085**:320-323.
60. Habashi, J.P., Judge, D.P., Holm, T.M., Cohn, R.D., Loeys, B.L., Cooper, T.K., Myers, L., Klein, E.C., Liu, G., Calvi, C. et al. 2006. Losartan, an AT1 antagonist, prevents aortic aneurysm in a mouse model of Marfan syndrome. *Science* **312**:117-121.
61. Ahimastos, A.A., Aggarwal, A., D'Orsa, K.M., Formosa, M.F., White, A.J., Savarirayan, R., Dart, A.M., and Kingwell, B.A. 2007. Effect of perindopril on large artery stiffness and aortic root diameter in patients with Marfan syndrome: a randomized controlled trial. *JAMA* **298**:1539-1547.
62. Yetman, A.T., Bornemeier, R.A., and McCrindle, B.W. 2005. Usefulness of enalapril versus propranolol or atenolol for prevention of aortic dilation in patients with the Marfan syndrome. *Am. J Cardiol.* **95**:1125-1127.
63. Brooke, B.S., Habashi, J.P., Judge, D.P., Patel, N., Loeys, B., and Dietz, H.C., III 2008. Angiotensin II blockade and aortic-root dilation in Marfan's syndrome. *N. Engl. J Med.* **358**:2787-2795.
64. Jones, G.T., Thompson, A.R., van Bockxmeer, F.M., Hafez, H., Cooper, J.A., Golledge, J., Humphries, S.E., Norman, P.E., and van Rij, A.M. 2008. Angiotensin II type 1 receptor 1166C polymorphism is associated with abdominal aortic aneurysm in three independent cohorts. *Arterioscler. Thromb. Vasc. Biol.* **28**:764-770.
65. Furubayashi, K., Takai, S., Jin, D., Muramatsu, M., Ibaraki, T., Nishimoto, M., Fukumoto, H., Katsumata, T., and Miyazaki, M. 2007. The significance of chymase in the progression of abdominal aortic aneurysms in dogs. *Hypertens. Res.* **30**:349-357.

66. Ihara, M., Urata, H., Kinoshita, A., Suzumiya, J., Sasaguri, M., Kikuchi, M., Ideishi, M., and Arakawa, K. 1999. Increased chymase-dependent angiotensin II formation in human atherosclerotic aorta. *Hypertension* **33**:1399-1405.
67. Nishimoto, M., Takai, S., Fukumoto, H., Tsunemi, K., Yuda, A., Sawada, Y., Yamada, M., Jin, D., Sakaguchi, M., Nishimoto, Y. et al. 2002. Increased local angiotensin II formation in aneurysmal aorta. *Life Sci.* **71**:2195-2205.
68. Ejiri, J., Inoue, N., Tsukube, T., Munezane, T., Hino, Y., Kobayashi, S., Hirata, K., Kawashima, S., Imajoh-Ohmi, S., Hayashi, Y. et al. 2003. Oxidative stress in the pathogenesis of thoracic aortic aneurysm: protective role of statin and angiotensin II type 1 receptor blocker. *Cardiovasc. Res.* **59**:988-996.
69. Lavoie, J.L., and Sigmund, C.D. 2003. Minireview: overview of the renin-angiotensin system--an endocrine and paracrine system. *Endocrinology* **144**:2179-2183.
70. Chung, O., Kuhl, H., Stoll, M., and Unger, T. 1998. Physiological and pharmacological implications of AT1 versus AT2 receptors. *Kidney Int. Suppl* **67**:S95-S99.
71. Smith, G.R., and Missailidis, S. 2004. Cancer, inflammation and the AT1 and AT2 receptors. *J Inflamm. (Lond)* **1**:3.
72. Schmidt-Ott, K.M., Kagiya, S., and Phillips, M.I. 2000. The multiple actions of angiotensin II in atherosclerosis. *Regul. Pept.* **93**:65-77.
73. Campbell, D.J., and Habener, J.F. 1986. Angiotensinogen gene is expressed and differentially regulated in multiple tissues of the rat. *J Clin. Invest.* **78**:31-39.
74. Bader, M., and Ganten, D. 2008. Update on tissue renin-angiotensin systems. *J Mol. Med.* **86**:615-621.

75. Bader, M., Peters, J., Baltatu, O., Muller, D.N., Luft, F.C., and Ganten, D. 2001. Tissue renin-angiotensin systems: new insights from experimental animal models in hypertension research. *J Mol. Med.* **79**:76-102.
76. Engeli, S., Negrel, R., and Sharma, A.M. 2000. Physiology and pathophysiology of the adipose tissue renin-angiotensin system. *Hypertension* **35**:1270-1277.
77. Campbell, D.J., and Habener, J.F. 1987. Cellular localization of angiotensinogen gene expression in brown adipose tissue and mesentery: quantification of messenger ribonucleic acid abundance using hybridization in situ. *Endocrinology* **121**:1616-1626.
78. Phillips, M.I., Speakman, E.A., and Kimura, B. 1993. Levels of angiotensin and molecular biology of the tissue renin angiotensin systems. *Regul. Pept.* **43**:1-20.
79. Leake, D.S., and Peters, T.J. 1981. Proteolytic degradation of low density lipoproteins by arterial smooth muscle cells: the role of individual cathepsins. *Biochim. Biophys. Acta.* **664**:108-116.
80. Wiener, E., and Curelaru, Z. 1975. The intracellular distribution of cathepsins and other acid hydrolases in mouse peritoneal macrophages. *J Reticuloendothel. Soc.* **17**:319-332.
81. Diet, F., Pratt, R.E., Berry, G.J., Momose, N., Gibbons, G.H., and Dzau, V.J. 1996. Increased accumulation of tissue ACE in human atherosclerotic coronary artery disease. *Circulation* **94**:2756-2767.
82. Fukuhara, M., Geary, R.L., Diz, D.I., Gallagher, P.E., Wilson, J.A., Glazier, S.S., Dean, R.H., and Ferrario, C.M. 2000. Angiotensin-converting enzyme expression in human carotid artery atherosclerosis. *Hypertension* **35**:353-359.
83. Potter, D.D., Sobey, C.G., Tompkins, P.K., Rossen, J.D., and Heistad, D.D. 1998. Evidence that macrophages in atherosclerotic lesions contain angiotensin II. *Circulation* **98**:800-807.

84. Okamura, A., Rakugi, H., Ohishi, M., Yanagitani, Y., Takiuchi, S., Moriguchi, K., Fennessy, P.A., Higaki, J., and Ogihara, T. 1999. Upregulation of renin-angiotensin system during differentiation of monocytes to macrophages. *J Hypertens.* **17**:537-545.
85. Kinoshita, A., Urata, H., Bumpus, F.M., and Husain, A. 1991. Multiple determinants for the high substrate specificity of an angiotensin II-forming chymase from the human heart. *J Biol. Chem.* **266**:19192-19197.
86. Snyder, R.A., Kaempfer, C.E., and Wintroub, B.U. 1985. Chemistry of a human monocyte-derived cell line (U937): identification of the angiotensin I-converting activity as leukocyte cathepsin G. *Blood* **65**:176-182.
87. Dzau, V.J. 2001. Theodore Cooper Lecture: Tissue angiotensin and pathobiology of vascular disease: a unifying hypothesis. *Hypertension* **37**:1047-1052.
88. Ruiz-Ortega, M., Lorenzo, O., Ruperez, M., Esteban, V., Suzuki, Y., Mezzano, S., Plaza, J.J., and Egido, J. 2001. Role of the renin-angiotensin system in vascular diseases: expanding the field. *Hypertension* **38**:1382-1387.
89. Griendling, K.K., Minieri, C.A., Ollerenshaw, J.D., and Alexander, R.W. 1994. Angiotensin II stimulates NADH and NADPH oxidase activity in cultured vascular smooth muscle cells. *Circ. Res.* **74**:1141-1148.
90. Rajagopalan, S., Kurz, S., Munzel, T., Tarpey, M., Freeman, B.A., Griendling, K.K., and Harrison, D.G. 1996. Angiotensin II-mediated hypertension in the rat increases vascular superoxide production via membrane NADH/NADPH oxidase activation. Contribution to alterations of vasomotor tone. *J Clin. Invest.* **97**:1916-1923.
91. Zhang, H., Schmeisser, A., Garlichs, C.D., Plotze, K., Damme, U., Mugge, A., and Daniel, W.G. 1999. Angiotensin II-induced superoxide anion generation in human vascular endothelial cells: role of membrane-bound NADH-/NADPH-oxidases. *Cardiovasc. Res.* **44**:215-222.
92. Yanagitani, Y., Rakugi, H., Okamura, A., Moriguchi, K., Takiuchi, S., Ohishi, M., Suzuki, K., Higaki, J., and Ogihara, T. 1999. Angiotensin II type 1

receptor-mediated peroxide production in human macrophages.
Hypertension **33**:335-339.

93. Wang, H.D., Xu, S., Johns, D.G., Du, Y., Quinn, M.T., Cayatte, A.J., and Cohen, R.A. 2001. Role of NADPH oxidase in the vascular hypertrophic and oxidative stress response to angiotensin II in mice. *Circ. Res.* **88**:947-953.
94. Harrison, D.G. 1997. Cellular and molecular mechanisms of endothelial cell dysfunction. *J Clin. Invest.* **100**:2153-2157.
95. Warnholtz, A., Nickenig, G., Schulz, E., Macharzina, R., Brasen, J.H., Skatchkov, M., Heitzer, T., Stasch, J.P., Griendling, K.K., Harrison, D.G. et al. 1999. Increased NADH-oxidase-mediated superoxide production in the early stages of atherosclerosis: evidence for involvement of the renin-angiotensin system. *Circulation* **99**:2027-2033.
96. Prasad, A., Tupas-Habib, T., Schenke, W.H., Mincemoyer, R., Panza, J.A., Waclawin, M.A., Ellahham, S., and Quyyumi, A.A. 2000. Acute and chronic angiotensin-1 receptor antagonism reverses endothelial dysfunction in atherosclerosis. *Circulation* **101**:2349-2354.
97. Chen, X.L., Tummala, P.E., Olbrych, M.T., Alexander, R.W., and Medford, R.M. 1998. Angiotensin II induces monocyte chemoattractant protein-1 gene expression in rat vascular smooth muscle cells. *Circ. Res.* **83**:952-959.
98. Ruiz-Ortega, M., Lorenzo, O., Ruperez, M., Konig, S., Wittig, B., and Egido, J. 2000. Angiotensin II activates nuclear transcription factor kappaB through AT(1) and AT(2) in vascular smooth muscle cells: molecular mechanisms. *Circ. Res.* **86**:1266-1272.
99. Hernandez-Presa, M., Bustos, C., Ortego, M., Tunon, J., Renedo, G., Ruiz-Ortega, M., and Egido, J. 1997. Angiotensin-converting enzyme inhibition prevents arterial nuclear factor-kappa B activation, monocyte chemoattractant protein-1 expression, and macrophage infiltration in a rabbit model of early accelerated atherosclerosis. *Circulation* **95**:1532-1541.

100. Hernandez-Presa, M.A., Bustos, C., Ortego, M., Tunon, J., Ortega, L., and Egido, J. 1998. ACE inhibitor quinapril reduces the arterial expression of NF-kappaB-dependent proinflammatory factors but not of collagen I in a rabbit model of atherosclerosis. *Am. J Pathol.* **153**:1825-1837.
101. Soejima, H., Ogawa, H., Yasue, H., Kaikita, K., Takazoe, K., Nishiyama, K., Misumi, K., Miyamoto, S., Yoshimura, M., Kugiyama, K. et al. 1999. Angiotensin-converting enzyme inhibition reduces monocyte chemoattractant protein-1 and tissue factor levels in patients with myocardial infarction. *J Am. Coll. Cardiol.* **34**:983-988.
102. Yla-Herttuala, S., Lipton, B.A., Rosenfeld, M.E., Sarkioja, T., Yoshimura, T., Leonard, E.J., Witztum, J.L., and Steinberg, D. 1991. Expression of monocyte chemoattractant protein 1 in macrophage-rich areas of human and rabbit atherosclerotic lesions. *Proc. Natl. Acad. Sci U. S. A.* **88**:5252-5256.
103. Ortego, M., Bustos, C., Hernandez-Presa, M.A., Tunon, J., Diaz, C., Hernandez, G., and Egido, J. 1999. Atorvastatin reduces NF-kappaB activation and chemokine expression in vascular smooth muscle cells and mononuclear cells. *Atherosclerosis* **147**:253-261.
104. Pueyo, M.E., Gonzalez, W., Nicoletti, A., Savoie, F., Arnal, J.F., and Michel, J.B. 2000. Angiotensin II stimulates endothelial vascular cell adhesion molecule-1 via nuclear factor-kappaB activation induced by intracellular oxidative stress. *Arterioscler. Thromb. Vasc. Biol.* **20**:645-651.
105. Tummala, P.E., Chen, X.L., Sundell, C.L., Laursen, J.B., Hammes, C.P., Alexander, R.W., Harrison, D.G., and Medford, R.M. 1999. Angiotensin II induces vascular cell adhesion molecule-1 expression in rat vasculature: A potential link between the renin-angiotensin system and atherosclerosis. *Circulation* **100**:1223-1229.
106. Pastore, L., Tessitore, A., Martinotti, S., Toniato, E., Alesse, E., Bravi, M.C., Ferri, C., Desideri, G., Gulino, A., and Santucci, A. 1999. Angiotensin II stimulates intercellular adhesion molecule-1 (ICAM-1) expression by human vascular endothelial cells and increases soluble ICAM-1 release in vivo. *Circulation* **100**:1646-1652.

107. Grafe, M., uch-Schwelk, W., Zakrzewicz, A., Regitz-Zagrosek, V., Bartsch, P., Graf, K., Loebe, M., Gaetgens, P., and Fleck, E. 1997. Angiotensin II-induced leukocyte adhesion on human coronary endothelial cells is mediated by E-selectin. *Circ. Res.* **81**:804-811.
108. Han, Y., Runge, M.S., and Brasier, A.R. 1999. Angiotensin II induces interleukin-6 transcription in vascular smooth muscle cells through pleiotropic activation of nuclear factor-kappa B transcription factors. *Circ. Res.* **84**:695-703.
109. Cui, R., Tieu, B., Recinos, A., Tilton, R.G., and Brasier, A.R. 2006. RhoA mediates angiotensin II-induced phospho-Ser536 nuclear factor kappaB/RelA subunit exchange on the interleukin-6 promoter in VSMCs. *Circ. Res.* **99**:723-730.
110. bdAlla, S., Lothar, H., Langer, A., el, F.Y., and Quitterer, U. 2004. Factor XIIIa transglutaminase crosslinks AT1 receptor dimers of monocytes at the onset of atherosclerosis. *Cell* **119**:343-354.
111. Nakamura, A., Johns, E.J., Imaizumi, A., Yanagawa, Y., and Kohsaka, T. 1999. Effect of beta(2)-adrenoceptor activation and angiotensin II on tumour necrosis factor and interleukin 6 gene transcription in the rat renal resident macrophage cells. *Cytokine* **11**:759-765.
112. Daugherty, A., and Cassis, L. 1999. Chronic angiotensin II infusion promotes atherogenesis in low density lipoprotein receptor *-/-* mice. *Ann. N. Y. Acad. Sci.* **892**:108-118.
113. Daugherty, A., Manning, M.W., and Cassis, L.A. 2000. Angiotensin II promotes atherosclerotic lesions and aneurysms in apolipoprotein E-deficient mice. *J Clin. Invest.* **105**:1605-1612.
114. Manning, M.W., Cassis, L., Huang, J., Szilvassy, S., and Daugherty, A. 2002. Abdominal aortic aneurysms: fresh insights from a novel animal model of the disease. *Vasc. Med.* **7**:45-54.
115. Deng, G., Martin-McNulty, B., Sukovich, D.A., Freay, A., Halks-Miller, M., Thinnes, T., Loskutoff, D.J., Carmeliet, P., Dole, W.P., and Wang, Y.X.

2003. Urokinase-type plasminogen activator plays a critical role in angiotensin II-induced abdominal aortic aneurysm. *Circ. Res.* **92**:510-517.

116. Wang, Y.X., Martin-McNulty, B., Freay, A.D., Sukovich, D.A., Halks-Miller, M., Li, W.W., Vergona, R., Sullivan, M.E., Morser, J., Dole, W.P. et al. 2001. Angiotensin II increases urokinase-type plasminogen activator expression and induces aneurysm in the abdominal aorta of apolipoprotein E-deficient mice. *Am. J Pathol.* **159**:1455-1464.
117. Daugherty, A., Rateri, D.L., and Cassis, L.A. 2006. Role of the renin-angiotensin system in the development of abdominal aortic aneurysms in animals and humans. *Ann. N. Y. Acad. Sci.* **1085**:82-91.
118. Barisione, C., Charnigo, R., Howatt, D.A., Moorleggen, J.J., Rateri, D.L., and Daugherty, A. 2006. Rapid dilation of the abdominal aorta during infusion of angiotensin II detected by noninvasive high-frequency ultrasonography. *J Vasc. Surg.* **44**:372-376.
119. Lu, H., Rateri, D.L., Cassis, L.A., and Daugherty, A. 2008. The role of the renin-angiotensin system in aortic aneurysmal diseases. *Curr. Hypertens. Rep.* **10**:99-106.
120. Ayabe, N., Babaev, V.R., Tang, Y., Tanizawa, T., Fogo, A.B., Linton, M.F., Ichikawa, I., Fazio, S., and Kon, V. 2006. Transiently heightened angiotensin II has distinct effects on atherosclerosis and aneurysm formation in hyperlipidemic mice. *Atherosclerosis* **184**:312-321.
121. Daugherty, A., Manning, M.W., and Cassis, L.A. 2001. Antagonism of AT2 receptors augments angiotensin II-induced abdominal aortic aneurysms and atherosclerosis. *Br. J Pharmacol.* **134**:865-870.
122. Weiss, D., Kools, J.J., and Taylor, W.R. 2001. Angiotensin II-induced hypertension accelerates the development of atherosclerosis in apoE-deficient mice. *Circulation* **103**:448-454.
123. Recinos, A., III, LeJeune, W.S., Sun, H., Lee, C.Y., Tieu, B.C., Lu, M., Hou, T., Boldogh, I., Tilton, R.G., and Brasier, A.R. 2007. Angiotensin II induces

IL-6 expression and the Jak-STAT3 pathway in aortic adventitia of LDL receptor-deficient mice. *Atherosclerosis* **194**:125-133.

124. Saraff, K., Babamusta, F., Cassis, L.A., and Daugherty, A. 2003. Aortic dissection precedes formation of aneurysms and atherosclerosis in angiotensin II-infused, apolipoprotein E-deficient mice. *Arterioscler. Thromb. Vasc. Biol.* **23**:1621-1626.
125. Gavazzi, G., Deffert, C., Trocme, C., Schappi, M., Herrmann, F.R., and Krause, K.H. 2007. NOX1 deficiency protects from aortic dissection in response to angiotensin II. *Hypertension* **50**:189-196.
126. Ni, W., Kitamoto, S., Ishibashi, M., Usui, M., Inoue, S., Hiasa, K., Zhao, Q., Nishida, K., Takeshita, A., and Egashira, K. 2004. Monocyte chemoattractant protein-1 is an essential inflammatory mediator in angiotensin II-induced progression of established atherosclerosis in hypercholesterolemic mice. *Arterioscler. Thromb. Vasc. Biol.* **24**:534-539.
127. Ishibashi, M., Hiasa, K., Zhao, Q., Inoue, S., Ohtani, K., Kitamoto, S., Tsuchihashi, M., Sugaya, T., Charo, I.F., Kura, S. et al. 2004. Critical role of monocyte chemoattractant protein-1 receptor CCR2 on monocytes in hypertension-induced vascular inflammation and remodeling. *Circ. Res.* **94**:1203-1210.
128. Dol, F., Martin, G., Staels, B., Mares, A.M., Cazaubon, C., Nisato, D., Bidouard, J.P., Janiak, P., Schaeffer, P., and Herbert, J.M. 2001. Angiotensin AT1 receptor antagonist irbesartan decreases lesion size, chemokine expression, and macrophage accumulation in apolipoprotein E-deficient mice. *J Cardiovasc. Pharmacol.* **38**:395-405.
129. Gitlin, J.M., Trivedi, D.B., Langenbach, R., and Loftin, C.D. 2007. Genetic deficiency of cyclooxygenase-2 attenuates abdominal aortic aneurysm formation in mice. *Cardiovasc. Res.* **73**:227-236.
130. King, V.L., Trivedi, D.B., Gitlin, J.M., and Loftin, C.D. 2006. Selective cyclooxygenase-2 inhibition with celecoxib decreases angiotensin II-induced abdominal aortic aneurysm formation in mice. *Arterioscler. Thromb. Vasc. Biol.* **26**:1137-1143.

131. Ahluwalia, N., Lin, A.Y., Tager, A.M., Pruitt, I.E., Anderson, T.J., Kristo, F., Shen, D., Cruz, A.R., Aikawa, M., Luster, A.D. et al. 2007. Inhibited aortic aneurysm formation in BLT1-deficient mice. *J Immunol.* **179**:691-697.
132. Cao, R.Y., Adams, M.A., Habenicht, A.J., and Funk, C.D. 2007. Angiotensin II-induced abdominal aortic aneurysm occurs independently of the 5-lipoxygenase pathway in apolipoprotein E-deficient mice. *Prostaglandins Other Lipid Mediat.* **84**:34-42.
133. Eagleton, M.J., Ballard, N., Lynch, E., Srivastava, S.D., Upchurch, G.R., Jr., and Stanley, J.C. 2006. Early increased MT1-MMP expression and late MMP-2 and MMP-9 activity during Angiotensin II induced aneurysm formation. *J Surg Res.* **135**:345-351.
134. Manning, M.W., Cassis, L.A., and Daugherty, A. 2003. Differential effects of doxycycline, a broad-spectrum matrix metalloproteinase inhibitor, on angiotensin II-induced atherosclerosis and abdominal aortic aneurysms. *Arterioscler. Thromb. Vasc. Biol.* **23**:483-488.
135. Vinh, A., Gaspari, T.A., Liu, H.B., Dousha, L.F., Widdop, R.E., and Dear, A.E. 2008. A novel histone deacetylase inhibitor reduces abdominal aortic aneurysm formation in angiotensin II-infused apolipoprotein E-deficient mice. *J Vasc. Res.* **45**:143-152.
136. Bruemmer, D., Collins, A.R., Noh, G., Wang, W., Territo, M., rias-Magallona, S., Fishbein, M.C., Blaschke, F., Kintscher, U., Graf, K. et al. 2003. Angiotensin II-accelerated atherosclerosis and aneurysm formation is attenuated in osteopontin-deficient mice. *J Clin. Invest.* **112**:1318-1331.
137. Thomas, M., Gavrilu, D., McCormick, M.L., Miller, F.J., Jr., Daugherty, A., Cassis, L.A., Dellsperger, K.C., and Weintraub, N.L. 2006. Deletion of p47phox attenuates angiotensin II-induced abdominal aortic aneurysm formation in apolipoprotein E-deficient mice. *Circulation* **114**:404-413.
138. Wang, Y.X., Martin-McNulty, B., da, C., V, Vincelette, J., Lu, X., Feng, Q., Halks-Miller, M., Mahmoudi, M., Schroeder, M., Subramanyam, B. et al. 2005. Fasudil, a Rho-kinase inhibitor, attenuates angiotensin II-induced

abdominal aortic aneurysm in apolipoprotein E-deficient mice by inhibiting apoptosis and proteolysis. *Circulation* **111**:2219-2226.

139. Yoshimura, K., Aoki, H., Ikeda, Y., Fujii, K., Akiyama, N., Furutani, A., Hoshii, Y., Tanaka, N., Ricci, R., Ishihara, T. et al. 2005. Regression of abdominal aortic aneurysm by inhibition of c-Jun N-terminal kinase. *Nat. Med.* **11**:1330-1338.
140. Schecter, A.D., Berman, A.B., Yi, L., Ma, H., Daly, C.M., Soejima, K., Rollins, B.J., Charo, I.F., and Taubman, M.B. 2004. MCP-1-dependent signaling in CCR2(-/-) aortic smooth muscle cells. *J Leukoc. Biol.* **75**:1079-1085.
141. Spinetti, G., Wang, M., Monticone, R., Zhang, J., Zhao, D., and Lakatta, E.G. 2004. Rat aortic MCP-1 and its receptor CCR2 increase with age and alter vascular smooth muscle cell function. *Arterioscler. Thromb. Vasc. Biol.* **24**:1397-1402.
142. Taub, D.D., Proost, P., Murphy, W.J., Anver, M., Longo, D.L., van, D.J., and Oppenheim, J.J. 1995. Monocyte chemoattractant protein-1 (MCP-1), -2, and -3 are chemotactic for human T lymphocytes. *J Clin. Invest.* **95**:1370-1376.
143. Leonard, E.J., and Yoshimura, T. 1990. Human monocyte chemoattractant protein-1 (MCP-1). *Immunol. Today* **11**:97-101.
144. Nelken, N.A., Coughlin, S.R., Gordon, D., and Wilcox, J.N. 1991. Monocyte chemoattractant protein-1 in human atheromatous plaques. *J Clin. Invest.* **88**:1121-1127.
145. Ikeda, U., Matsui, K., Murakami, Y., and Shimada, K. 2002. Monocyte chemoattractant protein-1 and coronary artery disease. *Clin. Cardiol.* **25**:143-147.
146. Wilcox, J.N., Nelken, N.A., Coughlin, S.R., Gordon, D., and Schall, T.J. 1994. Local expression of inflammatory cytokines in human atherosclerotic plaques. *J Atheroscler. Thromb.* **1 Suppl 1**:S10-S13.

147. Chen, Y.L., Chang, Y.J., and Jiang, M.J. 1999. Monocyte chemotactic protein-1 gene and protein expression in atherogenesis of hypercholesterolemic rabbits. *Atherosclerosis* **143**:115-123.
148. Kowala, M.C., Recce, R., Beyer, S., Gu, C., and Valentine, M. 2000. Characterization of atherosclerosis in LDL receptor knockout mice: macrophage accumulation correlates with rapid and sustained expression of aortic MCP-1/JE. *Atherosclerosis* **149**:323-330.
149. Martin, G., Dol, F., Mares, A.M., Berezowski, V., Staels, B., Hum, D.W., Schaeffer, P., and Herbert, J.M. 2004. Lesion progression in apoE-deficient mice: implication of chemokines and effect of the AT1 angiotensin II receptor antagonist irbesartan. *J Cardiovasc. Pharmacol.* **43**:191-199.
150. Capers, Q., Alexander, R.W., Lou, P., De, L.H., Wilcox, J.N., Ishizaka, N., Howard, A.B., and Taylor, W.R. 1997. Monocyte chemoattractant protein-1 expression in aortic tissues of hypertensive rats. *Hypertension* **30**:1397-1402.
151. Swirski, F.K., Pittet, M.J., Kircher, M.F., Aikawa, E., Jaffer, F.A., Libby, P., and Weissleder, R. 2006. Monocyte accumulation in mouse atherogenesis is progressive and proportional to extent of disease. *Proc. Natl. Acad. Sci U. S. A.* **103**:10340-10345.
152. Swirski, F.K., Libby, P., Aikawa, E., Alcaide, P., Luscinskas, F.W., Weissleder, R., and Pittet, M.J. 2007. Ly-6Chi monocytes dominate hypercholesterolemia-associated monocytosis and give rise to macrophages in atheromata. *J Clin. Invest.* **117**:195-205.
153. Tacke, F., Alvarez, D., Kaplan, T.J., Jakubzick, C., Spanbroek, R., Llodra, J., Garin, A., Liu, J., Mack, M., van, R.N. et al. 2007. Monocyte subsets differentially employ CCR2, CCR5, and CX3CR1 to accumulate within atherosclerotic plaques. *J Clin. Invest.* **117**:185-194.
154. Namiki, M., Kawashima, S., Yamashita, T., Ozaki, M., Hirase, T., Ishida, T., Inoue, N., Hirata, K., Matsukawa, A., Morishita, R. et al. 2002. Local overexpression of monocyte chemoattractant protein-1 at vessel wall induces infiltration of macrophages and formation of atherosclerotic

lesion: synergism with hypercholesterolemia. *Arterioscler. Thromb. Vasc. Biol.* **22**:115-120.

155. Egashira, K. 2003. Molecular mechanisms mediating inflammation in vascular disease: special reference to monocyte chemoattractant protein-1. *Hypertension* **41**:834-841.
156. Gu, L., Okada, Y., Clinton, S.K., Gerard, C., Sukhova, G.K., Libby, P., and Rollins, B.J. 1998. Absence of monocyte chemoattractant protein-1 reduces atherosclerosis in low density lipoprotein receptor-deficient mice. *Mol. Cell* **2**:275-281.
157. Boring, L., Gosling, J., Cleary, M., and Charo, I.F. 1998. Decreased lesion formation in CCR2^{-/-} mice reveals a role for chemokines in the initiation of atherosclerosis. *Nature* **394**:894-897.
158. Guo, J., Van, E.M., Twisk, J., Maeda, N., Benson, G.M., Groot, P.H., and Van Berkel, T.J. 2003. Transplantation of monocyte CC-chemokine receptor 2-deficient bone marrow into ApoE3-Leiden mice inhibits atherogenesis. *Arterioscler. Thromb. Vasc. Biol.* **23**:447-453.
159. Guo, J., de, W., V, Van, E.M., Hildebrand, R.B., van Wanrooij, E.J., Kuiper, J., Maeda, N., Benson, G.M., Groot, P.H., and Van Berkel, T.J. 2005. Repopulation of apolipoprotein E knockout mice with CCR2-deficient bone marrow progenitor cells does not inhibit ongoing atherosclerotic lesion development. *Arterioscler. Thromb. Vasc. Biol.* **25**:1014-1019.
160. Boring, L., Gosling, J., Chensue, S.W., Kunkel, S.L., Farese, R.V., Jr., Broxmeyer, H.E., and Charo, I.F. 1997. Impaired monocyte migration and reduced type 1 (Th1) cytokine responses in C-C chemokine receptor 2 knockout mice. *J Clin. Invest.* **100**:2552-2561.
161. Kurihara, T., Warr, G., Loy, J., and Bravo, R. 1997. Defects in macrophage recruitment and host defense in mice lacking the CCR2 chemokine receptor. *J Exp. Med.* **186**:1757-1762.

162. MacTaggart, J.N., Xiong, W., Knispel, R., and Baxter, B.T. 2007. Deletion of CCR2 but not CCR5 or CXCR3 inhibits aortic aneurysm formation. *Surgery* **142**:284-288.
163. Bush, E., Maeda, N., Kuziel, W.A., Dawson, T.C., Wilcox, J.N., DeLeon, H., and Taylor, W.R. 2000. CC chemokine receptor 2 is required for macrophage infiltration and vascular hypertrophy in angiotensin II-induced hypertension. *Hypertension* **36**:360-363.
164. Ishibashi, M., Egashira, K., Zhao, Q., Hiasa, K., Ohtani, K., Ihara, Y., Charo, I.F., Kura, S., Tsuzuki, T., Takeshita, A. et al. 2004. Bone marrow-derived monocyte chemoattractant protein-1 receptor CCR2 is critical in angiotensin II-induced acceleration of atherosclerosis and aneurysm formation in hypercholesterolemic mice. *Arterioscler. Thromb. Vasc. Biol.* **24**:e174-e178.
165. Kishimoto, T. 2005. Interleukin-6: from basic science to medicine--40 years in immunology. *Annu. Rev. Immunol* **23**:1-21.
166. Kamimura, D., Ishihara, K., and Hirano, T. 2003. IL-6 signal transduction and its physiological roles: the signal orchestration model. *Rev. Physiol Biochem. Pharmacol.* **149**:1-38.
167. Kishimoto, T. 1989. The biology of interleukin-6. *Blood* **74**:1-10.
168. Hou, T, Tieu, B.C., Ray, S, Recinos, A., III, Cui, R, Tilton, R.G., and Brasier, A.R. 2008. Roles of IL-6-gp130 signaling in vascular inflammation. *Curr. Cardiol. Rev.* **4**:179-192.
169. Aznar, S., Valeron, P.F., del Rincon, S.V., Perez, L.F., Perona, R., and Lacal, J.C. 2001. Simultaneous tyrosine and serine phosphorylation of STAT3 transcription factor is involved in Rho A GTPase oncogenic transformation. *Mol. Biol. Cell* **12**:3282-3294.
170. Romano, M., Sironi, M., Toniatti, C., Polentarutti, N., Fruscella, P., Ghezzi, P., Faggioni, R., Luini, W., van, H., V, Sozzani, S. et al. 1997. Role of IL-6 and its soluble receptor in induction of chemokines and leukocyte recruitment. *Immunity.* **6**:315-325.

171. Biswas, P., Delfanti, F., Bernasconi, S., Mengozzi, M., Cota, M., Polentarutti, N., Mantovani, A., Lazzarin, A., Sozzani, S., and Poli, G. 1998. Interleukin-6 induces monocyte chemotactic protein-1 in peripheral blood mononuclear cells and in the U937 cell line. *Blood* **91**:258-265.
172. Watanabe, S., Mu, W., Kahn, A., Jing, N., Li, J.H., Lan, H.Y., Nakagawa, T., Ohashi, R., and Johnson, R.J. 2004. Role of JAK/STAT pathway in IL-6-induced activation of vascular smooth muscle cells. *Am. J Nephrol.* **24**:387-392.
173. Yang, X.P., Irani, K., Mattagajasingh, S., Dipaula, A., Khanday, F., Ozaki, M., Fox-Talbot, K., Baldwin, W.M., III, and Becker, L.C. 2005. Signal transducer and activator of transcription 3alpha and specificity protein 1 interact to upregulate intercellular adhesion molecule-1 in ischemic-reperfused myocardium and vascular endothelium. *Arterioscler. Thromb. Vasc. Biol.* **25**:1395-1400.
174. Coles, B., Fielding, C.A., Rose-John, S., Scheller, J., Jones, S.A., and O'Donnell, V.B. 2007. Classic interleukin-6 receptor signaling and interleukin-6 trans-signaling differentially control angiotensin II-dependent hypertension, cardiac signal transducer and activator of transcription-3 activation, and vascular hypertrophy in vivo. *Am. J Pathol.* **171**:315-325.
175. Rabe, B., Chalaris, A., May, U., Waetzig, G.H., Seegert, D., Williams, A.S., Jones, S.A., Rose-John, S., and Scheller, J. 2008. Transgenic blockade of interleukin 6 transsignaling abrogates inflammation. *Blood* **111**:1021-1028.
176. Guzik, T.J., Hoch, N.E., Brown, K.A., McCann, L.A., Rahman, A., Dikalov, S., Goronzy, J., Weyand, C., and Harrison, D.G. 2007. Role of the T cell in the genesis of angiotensin II induced hypertension and vascular dysfunction. *J Exp. Med.* **204**:2449-2460.
177. Ikeda, U., Ikeda, M., Seino, Y., Takahashi, M., Kano, S., and Shimada, K. 1992. Interleukin 6 gene transcripts are expressed in atherosclerotic lesions of genetically hyperlipidemic rabbits. *Atherosclerosis* **92**:213-218.
178. Ikeda, U., Ito, T., and Shimada, K. 2001. Interleukin-6 and acute coronary syndrome. *Clin. Cardiol.* **24**:701-704.

179. Schieffer, B., Schieffer, E., Hilfiker-Kleiner, D., Hilfiker, A., Kovanen, P.T., Kaartinen, M., Nussberger, J., Harringer, W., and Drexler, H. 2000. Expression of angiotensin II and interleukin 6 in human coronary atherosclerotic plaques: potential implications for inflammation and plaque instability. *Circulation* **101**:1372-1378.
180. Miyao, Y., Yasue, H., Ogawa, H., Misumi, I., Masuda, T., Sakamoto, T., and Morita, E. 1993. Elevated plasma interleukin-6 levels in patients with acute myocardial infarction. *Am. Heart J* **126**:1299-1304.
181. Biasucci, L.M., Vitelli, A., Liuzzo, G., Altamura, S., Caligiuri, G., Monaco, C., Rebuffi, A.G., Ciliberto, G., and Maseri, A. 1996. Elevated levels of interleukin-6 in unstable angina. *Circulation* **94**:874-877.
182. Biasucci, L.M., Liuzzo, G., Fantuzzi, G., Caligiuri, G., Rebuffi, A.G., Ginnetti, F., Dinarello, C.A., and Maseri, A. 1999. Increasing levels of interleukin (IL)-1Ra and IL-6 during the first 2 days of hospitalization in unstable angina are associated with increased risk of in-hospital coronary events. *Circulation* **99**:2079-2084.
183. Harris, T.B., Ferrucci, L., Tracy, R.P., Corti, M.C., Wacholder, S., Ettinger, W.H., Jr., Heimovitz, H., Cohen, H.J., and Wallace, R. 1999. Associations of elevated interleukin-6 and C-reactive protein levels with mortality in the elderly. *Am. J Med.* **106**:506-512.
184. Ridker, P.M., Rifai, N., Stampfer, M.J., and Hennekens, C.H. 2000. Plasma concentration of interleukin-6 and the risk of future myocardial infarction among apparently healthy men. *Circulation* **101**:1767-1772.
185. Volpato, S., Guralnik, J.M., Ferrucci, L., Balfour, J., Chaves, P., Fried, L.P., and Harris, T.B. 2001. Cardiovascular disease, interleukin-6, and risk of mortality in older women: the women's health and aging study. *Circulation* **103**:947-953.
186. Ridker, P.M., Hennekens, C.H., Buring, J.E., and Rifai, N. 2000. C-reactive protein and other markers of inflammation in the prediction of cardiovascular disease in women. *N. Engl. J Med.* **342**:836-843.

187. Mendall, M.A., Strachan, D.P., Butland, B.K., Ballam, L., Morris, J., Sweetnam, P.M., and Elwood, P.C. 2000. C-reactive protein: relation to total mortality, cardiovascular mortality and cardiovascular risk factors in men. *Eur. Heart J* **21**:1584-1590.
188. Treska, V., Topolcan, O., and Pecen, L. 2000. Cytokines as plasma markers of abdominal aortic aneurysm. *Clin. Chem. Lab Med.* **38**:1161-1164.
189. Rohde, L.E., Arroyo, L.H., Rifai, N., Creager, M.A., Libby, P., Ridker, P.M., and Lee, R.T. 1999. Plasma concentrations of interleukin-6 and abdominal aortic diameter among subjects without aortic dilatation. *Arterioscler. Thromb. Vasc. Biol.* **19**:1695-1699.
190. Jones, K.G., Brull, D.J., Brown, L.C., Sian, M., Greenhalgh, R.M., Humphries, S.E., and Powell, J.T. 2001. Interleukin-6 (IL-6) and the prognosis of abdominal aortic aneurysms. *Circulation* **103**:2260-2265.
191. Cheuk, B.L., and Cheng, S.W. 2008. Can local secretion of prostaglandin E2, thromboxane B2, and interleukin-6 play a role in ruptured abdominal aortic aneurysm? *World J Surg.* **32**:55-61.
192. 1998. Mortality results for randomised controlled trial of early elective surgery or ultrasonographic surveillance for small abdominal aortic aneurysms. The UK Small Aneurysm Trial Participants. *Lancet* **352**:1649-1655.
193. Huber, S.A., Sakkinen, P., Conze, D., Hardin, N., and Tracy, R. 1999. Interleukin-6 exacerbates early atherosclerosis in mice. *Arterioscler. Thromb. Vasc. Biol.* **19**:2364-2367.
194. Schieffer, B., Selle, T., Hilfiker, A., Hilfiker-Kleiner, D., Grote, K., Tietge, U.J., Trautwein, C., Luchtefeld, M., Schmittkamp, C., Heeneman, S. et al. 2004. Impact of interleukin-6 on plaque development and morphology in experimental atherosclerosis. *Circulation* **110**:3493-3500.
195. Song, L., and Schindler, C. 2004. IL-6 and the acute phase response in murine atherosclerosis. *Atherosclerosis* **177**:43-51.

196. Thompson, R.W., Curci, J.A., Ennis, T.L., Mao, D., Pagano, M.B., and Pham, C.T. 2006. Pathophysiology of abdominal aortic aneurysms: insights from the elastase-induced model in mice with different genetic backgrounds. *Ann. N. Y. Acad. Sci.* **1085**:59-73.
197. Keidar, S., Heinrich, R., Kaplan, M., Hayek, T., and Aviram, M. 2001. Angiotensin II administration to atherosclerotic mice increases macrophage uptake of oxidized ldl: a possible role for interleukin-6. *Arterioscler. Thromb. Vasc. Biol.* **21**:1464-1469.
198. Moreno, P.R., Purushothaman, K.R., Fuster, V., and O'Connor, W.N. 2002. Intimomedial interface damage and adventitial inflammation is increased beneath disrupted atherosclerosis in the aorta: implications for plaque vulnerability. *Circulation* **105**:2504-2511.
199. Schwartz, C.J., and Mitchell, J.R. 1962. Cellular infiltration of the human arterial adventitia associated with atheromatous plaques. *Circulation* **26**:73-78.
200. Maiellaro, K., and Taylor, W.R. 2007. The role of the adventitia in vascular inflammation. *Cardiovasc. Res.* **75**:640-648.
201. Dettman, R.W., Denetclaw, W., Jr., Ordahl, C.P., and Bristow, J. 1998. Common epicardial origin of coronary vascular smooth muscle, perivascular fibroblasts, and intermyocardial fibroblasts in the avian heart. *Dev. Biol.* **193**:169-181.
202. Bergwerff, M., Verberne, M.E., DeRuiter, M.C., Poelmann, R.E., and Gittenberger-de Groot, A.C. 1998. Neural crest cell contribution to the developing circulatory system: implications for vascular morphology? *Circ. Res.* **82**:221-231.
203. Sartore, S., Chiavegato, A., Faggin, E., Franch, R., Puato, M., Ausoni, S., and Pauletto, P. 2001. Contribution of adventitial fibroblasts to neointima formation and vascular remodeling: from innocent bystander to active participant. *Circ. Res.* **89**:1111-1121.
204. Xu, F., Ji, J., Li, L., Chen, R., and Hu, W. 2007. Activation of adventitial fibroblasts contributes to the early development of atherosclerosis: a novel

hypothesis that complements the "Response-to-Injury Hypothesis" and the "Inflammation Hypothesis". *Med. Hypotheses* **69**:908-912.

205. Kim, D.-K., Huh, J.-E., Lee, S.-H., Hong, K.-P., Park, J., Seo, J.-D., and Lee, W. 1999. Angiotensin II stimulates proliferation of adventitial fibroblasts cultured from rat aortic explants. *J Korean Med Sci.* **14**:496.
206. Li, J.M., Cui, T.X., Shiuchi, T., Liu, H.W., Min, L.J., Okumura, M., Jinno, T., Wu, L., Iwai, M., and Horiuchi, M. 2004. Nicotine enhances angiotensin II-induced mitogenic response in vascular smooth muscle cells and fibroblasts. *Arterioscler. Thromb. Vasc. Biol.* **24**:80-84.
207. McEwan, P.E., Gray, G.A., Sherry, L., Webb, D.J., and Kenyon, C.J. 1998. Differential effects of angiotensin II on cardiac cell proliferation and intramyocardial perivascular fibrosis in vivo. *Circulation* **98**:2765-2773.
208. Shen, W.L., Gao, P.J., Che, Z.Q., Ji, K.D., Yin, M., Yan, C., Berk, B.C., and Zhu, D.L. 2006. NAD(P)H oxidase-derived reactive oxygen species regulate angiotensin-II induced adventitial fibroblast phenotypic differentiation. *Biochem. Biophys. Res. Commun.* **339**:337-343.
209. Shi, Y., O'Brien, J.E., Fard, A., Mannion, J.D., Wang, D., and Zalewski, A. 1996. Adventitial myofibroblasts contribute to neointimal formation in injured porcine coronary arteries. *Circulation* **94**:1655-1664.
210. Shi, Y., Pieniek, M., Fard, A., O'Brien, J., Mannion, J.D., and Zalewski, A. 1996. Adventitial remodeling after coronary arterial injury. *Circulation* **93**:340-348.
211. Scott, N.A., Cipolla, G.D., Ross, C.E., Dunn, B., Martin, F.H., Simonet, L., and Wilcox, J.N. 1996. Identification of a potential role for the adventitia in vascular lesion formation after balloon overstretch injury of porcine coronary arteries. *Circulation* **93**:2178-2187.
212. Li, G., Chen, S.J., Oparil, S., Chen, Y.F., and Thompson, J.A. 2000. Direct in vivo evidence demonstrating neointimal migration of adventitial fibroblasts after balloon injury of rat carotid arteries. *Circulation* **101**:1362-1365.

213. Siow, R.C., Mallawaarachchi, C.M., and Weissberg, P.L. 2003. Migration of adventitial myofibroblasts following vascular balloon injury: insights from in vivo gene transfer to rat carotid arteries. *Cardiovasc. Res.* **59**:212-221.
214. Lee, S.J., Bae, S.S., Kim, K.H., Lee, W.S., Rhim, B.Y., Hong, K.W., and Kim, C.D. 2007. High glucose enhances MMP-2 production in the adventitial fibroblasts via Akt1-dependent NF- κ B pathway. *FEBS* **581**:4189-4194.
215. Tsuruda, T., Kato, J., Cao, Y.N., Hatakeyama, K., Masuyama, H., Imamura, T., Kitamura, K., Asada, Y., and Eto, T. 2004. Adrenomedullin induces matrix metalloproteinase-2 activity in rat aortic adventitial fibroblasts. *Biochem. Biophys. Res. Commun.* **325**:80-84.
216. Pagano, P.J., Ito, Y., Tornheim, K., Gallop, P.M., Tauber, A.I., and Cohen, R.A. 1995. An NADPH oxidase superoxide-generating system in the rabbit aorta. *Am. J Physiol.* **268**:H2274-H2280.
217. Pagano, P.J., Clark, J.K., Cifuentes-Pagano, M.E., Clark, S.M., Callis, G.M., and Quinn, M.T. 1997. Localization of a constitutively active, phagocyte-like NADPH oxidase in rabbit aortic adventitia: enhancement by angiotensin II. *Proc. Natl. Acad. Sci U. S. A.* **94**:14483-14488.
218. Xu, F., Ji, J., Li, L., Chen, R., and Hu W-C 2007. Adventitial fibroblasts are activated in the early stages of atherosclerosis in the apolipoprotein E knockout mouse. *Biochem. and Biophys. Res. Commun.* **352**:681-688.
219. Tilson, M.D., Fu, C., Xia, S.X., Syn, D., Yoon, Y., and McCaffrey, T. 2000. Expression of molecular messages for angiogenesis by fibroblasts from aneurysmal abdominal aorta versus dermal fibroblasts. *Int. J Surg Investig.* **1**:453-457.
220. da, C., V, Martin-McNulty, B., Vincelette, J., Zhang, L., Rutledge, J.C., Wilson, D.W., Vergona, R., Sullivan, M.E., and Wang, Y.X. 2006. Interaction between mild hypercholesterolemia, HDL-cholesterol levels, and angiotensin II in intimal hyperplasia in mice. *J Lipid Res.* **47**:476-483.
221. Libby, P. 2002. Inflammation in atherosclerosis. *Nature* **420**:868-874.

222. Busuttill, S., Hall, L., and Hines, G.L. 1993. Spontaneous dissection of the abdominal aorta: experience with five patients. *Ann. Vasc. Surg.* **7**:414-418.
223. Berk, B.C., Haendeler, J., and Sottile, J. 2000. Angiotensin II, atherosclerosis, and aortic aneurysms. *J Clin. Invest.* **105**:1525-1526.
224. Gordon, S. 2007. The macrophage: past, present and future. *Eur. J Immunol.* **37** Suppl 1:S9-17.
225. Weber, C., Zernecke, A., and Libby, P. 2008. The multifaceted contributions of leukocyte subsets to atherosclerosis: lessons from mouse models. *Nat. Rev. Immunol.* **8**:802-815.
226. Watt, S.M., Burgess, A.W., Metcalf, D., and Batty, F.L. 1980. Isolation of mouse bone marrow neutrophils by light scatter and autofluorescence. *The J of Histochem. and Cytochem.* **28**:934-946.
227. Fleisher, T.A., and Marti, G.E. 1993. Immunologic studies in humans: Unit 7.9 Detection of unseparated human lymphocytes by flow cytometry. In *Curr. Protoc. in Immunol.* J.E.Coligan, Bierer, B.E., Margulies, D.H., Shevach, E.M., Strober, W., and Coico, R., editors. John Wiley & Sons, Inc. United States. 7.9.1-7.9.7.
228. Fearn, C., Kravchenko, V.V., Ulevitch, R.J., and Loskutoff, D.J. 1995. Murine CD14 gene expression in vivo: extramyeloid synthesis and regulation by lipopolysaccharide. *J Exp. Med.* **181**:857-866.
229. Ziegler-Heitbrock, H.W., and Ulevitch, R.J. 1993. CD14: cell surface receptor and differentiation marker. *Immunol. Today* **14**:121-125.
230. Rodeberg, D.A., Morris, R.E., and Babcock, G.F. 1997. Azurophilic granules of human neutrophils contain CD14. *Infect. Immun.* **65**:4747-4753.
231. Araki, H., Katayama, N., Yamashita, Y., Mano, H., Fujieda, A., Usui, E., Mitani, H., Ohishi, K., Nishii, K., Masuya, M. et al. 2004. Reprogramming of human postmitotic neutrophils into macrophages by growth factors. *Blood* **103**:2973-2980.

232. Lagasse, E., and Weissman, I.L. 1996. Flow cytometric identification of murine neutrophils and monocytes. *J Immunol Methods* **197**:139-150.
233. Jiang, Y., Beller, D.I., Frenzl, G., and Graves, D.T. 1992. Monocyte chemoattractant protein-1 regulates adhesion molecule expression and cytokine production in human monocytes. *J Immunol.* **148**:2423-2428.
234. Arnaout, M.A. 1990. Structure and function of the leukocyte adhesion molecules CD11/CD18. *Blood* **75**:1037-1050.
235. Ross, G.D. 2002. Role of the lectin domain of Mac-1/CR3 (CD11b/CD18) in regulating intercellular adhesion. *Immunol Res.* **25**:219-227.
236. Boschmann, M., Engeli, S., Adams, F., Gorzelniak, K., Franke, G., Klaua, S., Kreuzberg, U., Luedtke, S., Kettritz, R., Sharma, A.M. et al. 2005. Adipose tissue metabolism and CD11b expression on monocytes in obese hypertensives. *Hypertension* **46**:130-136.
237. Ezekowitz, R.A., and Gordon, S. 1982. Down-regulation of mannosyl receptor-mediated endocytosis and antigen F4/80 in bacillus Calmette-Guerin-activated mouse macrophages. Role of T lymphocytes and lymphokines. *J Exp. Med.* **155**:1623-1637.
238. Ezekowitz, R.A., Austyn, J., Stahl, P.D., and Gordon, S. 1981. Surface properties of bacillus Calmette-Guerin-activated mouse macrophages. Reduced expression of mannose-specific endocytosis, Fc receptors, and antigen F4/80 accompanies induction of Ia. *J Exp. Med.* **154**:60-76.
239. Rogers, H.W., and Unanue, E.R. 1993. Neutrophils are involved in acute, nonspecific resistance to *Listeria monocytogenes* in mice. *Infect. Immun.* **61**:5090-5096.
240. Li, H., and Wong, W.S. 2000. Mechanisms of pertussis toxin-induced myelomonocytic cell adhesion: role of CD14 and urokinase receptor. *Immunology* **100**:502-509.
241. Moulton, K.S., Vakili, K., Zurakowski, D., Soliman, M., Butterfield, C., Sylvin, E., Lo, K.M., Gillies, S., Javaherian, K., and Folkman, J. 2003. Inhibition

of plaque neovascularization reduces macrophage accumulation and progression of advanced atherosclerosis. *Proc. Natl. Acad. Sci U. S. A.* **100**:4736-4741.

242. Oritani, K., Kaisho, T., Nakajima, K., and Hirano, T. 1992. Retinoic acid inhibits interleukin-6-induced macrophage differentiation and apoptosis in a murine hematopoietic cell line, Y6. *Blood* **80**:2298-2305.
243. Matas, D., Milyavsky, M., Shats, I., Nissim, L., Goldfinger, N., and Rotter, V. 2004. p53 is a regulator of macrophage differentiation. *Cell Death. Differ.* **11**:458-467.
244. Tanaka, H., Matsumura, I., Nakajima, K., Daino, H., Sonoyama, J., Yoshida, H., Oritani, K., Machii, T., Yamamoto, M., Hirano, T. et al. 2000. GATA-1 blocks IL-6-induced macrophage differentiation and apoptosis through the sustained expression of cyclin D1 and bcl-2 in a murine myeloid cell line M1. *Blood* **95**:1264-1273.
245. Krishnaraju, K., Hoffman, B., and Liebermann, D.A. 1998. The zinc finger transcription factor Egr-1 activates macrophage differentiation in M1 myeloblastic leukemia cells. *Blood* **92**:1957-1966.
246. Minami, M., Inoue, M., Wei, S., Takeda, K., Matsumoto, M., Kishimoto, T., and Akira, S. 1996. STAT3 activation is a critical step in gp130-mediated terminal differentiation and growth arrest of a myeloid cell line. *Proc. Natl. Acad. Sci. U. S. A.* **93**:3963-3966.
247. Yamanaka, Y., Nakajima, K., Fukada, T., Hibi, M., and Hirano, T. 1996. Differentiation and growth arrest signals are generated through the cytoplasmic region of gp130 that is essential for Stat3 activation. *EMBO J.* **15**:1557-1565.
248. Oritani, K., Kaisho, T., Nakajima, K., and Hirano, T. 1992. Retinoic acid inhibits interleukin-6-induced macrophage differentiation and apoptosis in a murine hematopoietic cell line, Y6. *Blood* **80**:2298-2305.
249. Miyaura, C., Onozaki, K., Akiyama, Y., Taniyama, T., Hirano, T., Kishimoto, T., and Suda, T. 1988. Recombinant human interleukin 6 (B-cell stimulatory

factor 2) is a potent inducer of differentiation of mouse myeloid leukemia cells (M1). *FEBS Lett.* **234**:17-21.

250. Chiu, C.P., and Lee, F. 1989. IL-6 is a differentiation factor for M1 and WEHI-3B myeloid leukemic cells. *J Immunol.* **142**:1909-1915.
251. Shabo, Y., Lotem, J., Rubinstein, M., Revel, M., Clark, S.C., Wolf, S.F., Kamen, R., and Sachs, L. 1988. The myeloid blood cell differentiation-inducing protein MGI-2A is interleukin-6. *Blood* **72**:2070-2073.
252. Tanaka, H., Matsumura, I., Nakajima, K., Daino, H., Sonoyama, J., Yoshida, H., Oritani, K., Machii, T., Yamamoto, M., Hirano, T. et al. 2000. GATA-1 blocks IL-6-induced macrophage differentiation and apoptosis through the sustained expression of cyclin D1 and bcl-2 in a murine myeloid cell line M1. *Blood* **95**:1264-1273.
253. Oritani, K., Kaisho, T., Nakajima, K., and Hirano, T. 1992. Retinoic acid inhibits interleukin-6-induced macrophage differentiation and apoptosis in a murine hematopoietic cell line, Y6. *Blood* **80**:2298-2305.
254. Haviernik, P., Lahoda, C., Bradley, H.L., Hawley, T.S., Ramezani, A., Hawley, R.G., Stetler-Stevenson, M., Stetler-Stevenson, W.G., and Bunting, K.D. 2004. Tissue inhibitor of matrix metalloproteinase-1 overexpression in M1 myeloblasts impairs IL-6-induced differentiation. *Oncogene* **23**:9212-9219.
255. Matas, D., Milyavsky, M., Shats, I., Nissim, L., Goldfinger, N., and Rotter, V. 2004. p53 is a regulator of macrophage differentiation. *Cell Death. Differ.* **11**:458-467.
256. Krishnaraju, K., Hoffman, B., and Liebermann, D.A. 1998. The zinc finger transcription factor Egr-1 activates macrophage differentiation in M1 myeloblastic leukemia cells. *Blood* **92**:1957-1966.
257. Oritani, K., Kaisho, T., Nakajima, K., and Hirano, T. 1992. Retinoic acid inhibits interleukin-6-induced macrophage differentiation and apoptosis in a murine hematopoietic cell line, Y6. *Blood* **80**:2298-2305.

258. Krishnaraju, K., Hoffman, B., and Liebermann, D.A. 1998. The zinc finger transcription factor Egr-1 activates macrophage differentiation in M1 myeloblastic leukemia cells. *Blood* **92**:1957-1966.
259. Tanaka, H., Matsumura, I., Nakajima, K., Daino, H., Sonoyama, J., Yoshida, H., Oritani, K., Machii, T., Yamamoto, M., Hirano, T. et al. 2000. GATA-1 blocks IL-6-induced macrophage differentiation and apoptosis through the sustained expression of cyclin D1 and bcl-2 in a murine myeloid cell line M1. *Blood* **95**:1264-1273.
260. Chomarat, P., Banchereau, J., Davoust, J., and Palucka, A.K. 2000. IL-6 switches the differentiation of monocytes from dendritic cells to macrophages. *Nat. Immunol.* **1**:510-514.
261. Keidar, S., Heinrich, R., Kaplan, M., Hayek, T., and Aviram, M. 2001. Angiotensin II administration to atherosclerotic mice increases macrophage uptake of oxidized ldl: a possible role for interleukin-6. *Arterioscler. Thromb. Vasc. Biol.* **21**:1464-1469.
262. Liao, H.S., Matsumoto, A., Itakura, H., Doi, T., Honda, M., Kodama, T., and Geng, Y.J. 1999. Transcriptional inhibition by interleukin-6 of the class A macrophage scavenger receptor in macrophages derived from human peripheral monocytes and the THP-1 monocytic cell line. *Arterioscler. Thromb. Vasc. Biol.* **19**:1872-1880.
263. Oritani, K., Kaisho, T., Nakajima, K., and Hirano, T. 1992. Retinoic acid inhibits interleukin-6-induced macrophage differentiation and apoptosis in a murine hematopoietic cell line, Y6. *Blood* **80**:2298-2305.
264. Tanaka, H., Matsumura, I., Nakajima, K., Daino, H., Sonoyama, J., Yoshida, H., Oritani, K., Machii, T., Yamamoto, M., Hirano, T. et al. 2000. GATA-1 blocks IL-6-induced macrophage differentiation and apoptosis through the sustained expression of cyclin D1 and bcl-2 in a murine myeloid cell line M1. *Blood* **95**:1264-1273.
265. Yamanaka, Y., Nakajima, K., Fukada, T., Hibi, M., and Hirano, T. 1996. Differentiation and growth arrest signals are generated through the cytoplasmic region of gp130 that is essential for Stat3 activation. *EMBO J.* **15**:1557-1565.

266. Krishnaraju, K., Hoffman, B., and Liebermann, D.A. 1998. The zinc finger transcription factor Egr-1 activates macrophage differentiation in M1 myeloblastic leukemia cells. *Blood* **92**:1957-1966.
267. Oritani, K., Kaisho, T., Nakajima, K., and Hirano, T. 1992. Retinoic acid inhibits interleukin-6-induced macrophage differentiation and apoptosis in a murine hematopoietic cell line, Y6. *Blood* **80**:2298-2305.
268. Krishnaraju, K., Hoffman, B., and Liebermann, D.A. 1998. The zinc finger transcription factor Egr-1 activates macrophage differentiation in M1 myeloblastic leukemia cells. *Blood* **92**:1957-1966.
269. Yamanaka, Y., Nakajima, K., Fukada, T., Hibi, M., and Hirano, T. 1996. Differentiation and growth arrest signals are generated through the cytoplasmic region of gp130 that is essential for Stat3 activation. *EMBO J.* **15**:1557-1565.
270. Minami, M., Inoue, M., Wei, S., Takeda, K., Matsumoto, M., Kishimoto, T., and Akira, S. 1996. STAT3 activation is a critical step in gp130-mediated terminal differentiation and growth arrest of a myeloid cell line. *Proc. Natl. Acad. Sci. U. S. A.* **93**:3963-3966.
271. Tanaka, H., Matsumura, I., Nakajima, K., Daino, H., Sonoyama, J., Yoshida, H., Oritani, K., Machii, T., Yamamoto, M., Hirano, T. et al. 2000. GATA-1 blocks IL-6-induced macrophage differentiation and apoptosis through the sustained expression of cyclin D1 and bcl-2 in a murine myeloid cell line M1. *Blood* **95**:1264-1273.
272. Oritani, K., Tomiyama, Y., Kincade, P.W., Aoyama, K., Yokota, T., Matsumura, I., Kanakura, Y., Nakajima, K., Hirano, T., and Matsuzawa, Y. 1999. Both Stat3-activation and Stat3-independent BCL2 downregulation are important for interleukin-6-induced apoptosis of 1A9-M cells. *Blood* **93**:1346-1354.
273. Minami, M., Inoue, M., Wei, S., Takeda, K., Matsumoto, M., Kishimoto, T., and Akira, S. 1996. STAT3 activation is a critical step in gp130-mediated terminal differentiation and growth arrest of a myeloid cell line. *Proc. Natl. Acad. Sci. U. S. A.* **93**:3963-3966.

274. Krishnaraju, K., Hoffman, B., and Liebermann, D.A. 1998. The zinc finger transcription factor Egr-1 activates macrophage differentiation in M1 myeloblastic leukemia cells. *Blood* **92**:1957-1966.
275. Biswas, P., Delfanti, F., Bernasconi, S., Mengozzi, M., Cota, M., Polentarutti, N., Mantovani, A., Lazzarin, A., Sozzani, S., and Poli, G. 1998. Interleukin-6 induces monocyte chemotactic protein-1 in peripheral blood mononuclear cells and in the U937 cell line. *Blood* **91**:258-265.
276. Biswas, P., Delfanti, F., Bernasconi, S., Mengozzi, M., Cota, M., Polentarutti, N., Mantovani, A., Lazzarin, A., Sozzani, S., and Poli, G. 1998. Interleukin-6 induces monocyte chemotactic protein-1 in peripheral blood mononuclear cells and in the U937 cell line. *Blood* **91**:258-265.
277. Rott, D., Zhu, J., Zhou, Y.F., Burnett, M.S., Zalles-Ganley, A., and Epstein, S.E. 2003. IL-6 is produced by splenocytes derived from CMV-infected mice in response to CMV antigens, and induces MCP-1 production by endothelial cells: a new mechanistic paradigm for infection-induced atherogenesis. *Atherosclerosis* **170**:223-228.
278. Yamanaka, Y., Nakajima, K., Fukada, T., Hibi, M., and Hirano, T. 1996. Differentiation and growth arrest signals are generated through the cytoplasmic region of gp130 that is essential for Stat3 activation. *EMBO J.* **15**:1557-1565.
279. Nakajima, K., Yamanaka, Y., Nakae, K., Kojima, H., Ichiba, M., Kiuchi, N., Kitaoka, T., Fukada, T., Hibi, M., and Hirano, T. 1996. A central role for Stat3 in IL-6-induced regulation of growth and differentiation in M1 leukemia cells. *EMBO J.* **15**:3651-3658.
280. Minami, M., Inoue, M., Wei, S., Takeda, K., Matsumoto, M., Kishimoto, T., and Akira, S. 1996. STAT3 activation is a critical step in gp130-mediated terminal differentiation and growth arrest of a myeloid cell line. *Proc. Natl. Acad. Sci. U. S. A.* **93**:3963-3966.
281. Minami, M., Inoue, M., Wei, S., Takeda, K., Matsumoto, M., Kishimoto, T., and Akira, S. 1996. STAT3 activation is a critical step in gp130-mediated terminal differentiation and growth arrest of a myeloid cell line. *Proc. Natl. Acad. Sci. U. S. A.* **93**:3963-3966.

282. Mangan, J.K., Rane, S.G., Kang, A.D., Amanullah, A., Wong, B.C., and Reddy, E.P. 2004. Mechanisms associated with IL-6-induced up-regulation of Jak3 and its role in monocytic differentiation. *Blood* **103**:4093-4101.
283. Recinos, A., III, LeJeune, W.S., Sun, H., Lee, C.Y., Tieu, B.C., Lu, M., Hou, T., Boldogh, I., Tilton, R.G., and Brasier, A.R. 2007. Angiotensin II induces IL-6 expression and the Jak-STAT3 pathway in aortic adventitia of LDL receptor-deficient mice. *Atherosclerosis* **194**:125-133.
284. Proost, P., Struyf, S., Couvreur, M., Lenaerts, J.P., Conings, R., Menten, P., Verhaert, P., Wuyts, A., and van, D.J. 1998. Posttranslational modifications affect the activity of the human monocyte chemotactic proteins MCP-1 and MCP-2: identification of MCP-2(6-76) as a natural chemokine inhibitor. *J Immunol.* **160**:4034-4041.
285. Park, S.G., Shin, H., Shin, Y.K., Lee, Y., Choi, E.C., Park, B.J., and Kim, S. 2005. The novel cytokine p43 stimulates dermal fibroblast proliferation and wound repair. *Am. J Pathol.* **166**:387-398.
286. Austgulen, R., Hammerstrom, J., and Nissen-Meyer, J. 1987. In vitro cultured human monocytes release fibroblast proliferation factor(s) different from interleukin 1. *J Leukoc. Biol.* **42**:1-8.
287. Chomarat, P., Banchereau, J., Davoust, J., and Palucka, A.K. 2000. IL-6 switches the differentiation of monocytes from dendritic cells to macrophages. *Nat. Immunol.* **1**:510-514.
288. Liu, E., Tu, W., Law, H.K., and Lau, Y.L. 2001. Changes of CD14 and CD1a expression in response to IL-4 and granulocyte-macrophage colony-stimulating factor are different in cord blood and adult blood monocytes. *Pediatr. Res.* **50**:184-189.
289. Chapuis, F., Rosenzweig, M., Yagello, M., Ekman, M., Biberfeld, P., and Gluckman, J.C. 1997. Differentiation of human dendritic cells from monocytes in vitro. *Eur. J Immunol.* **27**:431-441.
290. Rogers, C., Edelman, E.R., and Simon, D.I. 1998. A mAb to the beta2-leukocyte integrin Mac-1 (CD11b/CD18) reduces intimal thickening after

angioplasty or stent implantation in rabbits. *Proc. Natl. Acad. Sci U. S. A.* **95**:10134-10139.

291. Shi, C., Zhang, X., Chen, Z., Sulaiman, K., Feinberg, M.W., Ballantyne, C.M., Jain, M.K., and Simon, D.I. 2004. Integrin engagement regulates monocyte differentiation through the forkhead transcription factor Foxp1. *J Clin. Invest.* **114**:408-418.
292. Simpson, P.J., Todd, R.F., III, Fantone, J.C., Mickelson, J.K., Griffin, J.D., and Lucchesi, B.R. 1988. Reduction of experimental canine myocardial reperfusion injury by a monoclonal antibody (anti-Mo1, anti-CD11b) that inhibits leukocyte adhesion. *J Clin. Invest.* **81**:624-629.
293. Noda-Heiny, H., Daugherty, A., and Sobel, B.E. 1995. Augmented urokinase receptor expression in atheroma. *Arterioscler. Thromb. Vasc. Biol.* **15**:37-43.
294. Xue, W., Kindzelskii, A.L., Todd, R.F., III, and Petty, H.R. 1994. Physical association of complement receptor type 3 and urokinase-type plasminogen activator receptor in neutrophil membranes. *J Immunol.* **152**:4630-4640.
295. Wong, W.S., Simon, D.I., Rosoff, P.M., Rao, N.K., and Chapman, H.A. 1996. Mechanisms of pertussis toxin-induced myelomonocytic cell adhesion: role of Mac-1 (CD11b/CD18) and urokinase receptor (CD87). *Immunology* **88**:90-97.
296. Sitrin, R.G., Todd, R.F., III, Albrecht, E., and Gyetko, M.R. 1996. The urokinase receptor (CD87) facilitates CD11b/CD18-mediated adhesion of human monocytes. *J Clin. Invest.* **97**:1942-1951.
297. Gyetko, M.R., Todd, R.F., III, Wilkinson, C.C., and Sitrin, R.G. 1994. The urokinase receptor is required for human monocyte chemotaxis in vitro. *J Clin. Invest.* **93**:1380-1387.
298. Simon, D.I., Rao, N.K., Xu, H., Wei, Y., Majdic, O., Ronne, E., Kobzik, L., and Chapman, H.A. 1996. Mac-1 (CD11b/CD18) and the urokinase receptor (CD87) form a functional unit on monocytic cells. *Blood* **88**:3185-3194.

299. Pluskota, E., Soloviev, D.A., and Plow, E.F. 2003. Convergence of the adhesive and fibrinolytic systems: recognition of urokinase by integrin alpha Mbeta 2 as well as by the urokinase receptor regulates cell adhesion and migration. *Blood* **101**:1582-1590.
300. Gu, J.M., Johns, A., Morser, J., Dole, W.P., Greaves, D.R., and Deng, G.G. 2005. Urokinase plasminogen activator receptor promotes macrophage infiltration into the vascular wall of ApoE deficient mice. *J Cell Physiol.* **204**:73-82.
301. Moos, M.P., John, N., Grabner, R., Nossmann, S., Gunther, B., Vollandt, R., Funk, C.D., Kaiser, B., and Habenicht, A.J. 2005. The lamina adventitia is the major site of immune cell accumulation in standard chow-fed apolipoprotein E-deficient mice. *Arterioscler. Thromb. Vasc. Biol.* **25**:2386-2391.
302. Rayner, K., Van, E.S., Groot, P.H., and Reape, T.J. 2000. Localisation of mRNA for JE/MCP-1 and its receptor CCR2 in atherosclerotic lesions of the ApoE knockout mouse. *J Vasc. Res.* **37**:93-102.
303. Miyata, K., Shimokawa, H., Kandabashi, T., Higo, T., Morishige, K., Eto, Y., Egashira, K., Kaibuchi, K., and Takeshita, A. 2000. Rho-kinase is involved in macrophage-mediated formation of coronary vascular lesions in pigs in vivo. *Arterioscler. Thromb. Vasc. Biol.* **20**:2351-2358.
304. Daugherty, A., and Cassis, L. 2004. Angiotensin II-mediated development of vascular diseases. *Trends Cardiovasc. Med.* **14**:117-120.

VITA

Brian Cuong Tieu

Brian Cuong Tieu was born in Kowloon, Hong Kong on September 15, 1979 to Rose and Tom Tieu. He was raised in Beaumont, TX along with one older sister, Julie Tieu, PharmD. Brian attended the University of Texas at Austin where he performed research with professor Austen Riggs, PhD, studying chicken hemoglobin protein structure and function. In 2002, he graduated with highest honors and was distinguished as a Dean's Honored Graduate. Following graduation, he enrolled in the MD-PhD program at UTMB where he performed dissertation research under the guidance of professors Allan R. Brasier, MD and Ronald G. Tilton, PhD. He married a medical school classmate, Carolyn Cushing, MD, on November 24, 2007.

Education

High School Diploma, May 1998, West Brook High School, Beaumont, Texas
B.A. May 2002, University of Texas Austin, Austin, Texas

Publications

Cui R, Tieu BC, Recinos A, Tilton RG, and Brasier AR. RhoA mediates angiotensin II-induced phospho-Ser536 Nuclear Factor- κ B/RelA subunit exchange on the interleukin-6 promoter in VSMCs. *Circ Research*, 2006; 99: 723-730.

Starkey JM, Haidacher SJ, LeJeune WS, Zhang X, Tieu BC, Choudhary S, Allan R. Brasier AR, Denner LA, and Tilton RG. Diabetes-induced activation of canonical and noncanonical Nuclear Factor- κ B pathways in renal cortex. *Diabetes*, 2006; 55: 1252-1259.

Recinos A III, LeJeune WS, Sun H, Lee CY, Tieu BC, Lu M, Hou T, Boldogh I, Tilton RG, Brasier AR. Angiotensin II induces IL-6 expression and the Jak-STAT3 pathway in aortic adventitia of LDL receptor-deficient mice. *Atherosclerosis*, 2007; 194: 125-133.

Hou T, Tieu BC, Ray S, Recinos A, Cui R, Tilton RG, Brasier AR. Roles of IL-6-gp130 signaling in vascular inflammation. *Current Cardiology Reviews*, 2008; 4: 179-192.

Ye Y, Lin Y, Manickavasagam S, Perez-Polo J, Tieu BC, Birnbaum Y. Pioglitazone protects the myocardium against ischemia-reperfusion injury in eNOS- and iNOS-knockout mice. *American Journal of Physiology: Heart and Circulatory Physiology*, 2008; Epub ahead of print

Ye Y, Manickavasagam S, Lin Y, Perez-Polo J, Uretsky BR, Ye Zaiming, Lui CY, Tieu BC, Birnbaum Y. Phosphorylation of 5-lipoxygenase at Ser523 by protein kinase A

(PKA) determines whether pioglitazone and atorvastatin induce pro-inflammatory leukotriene B4 or anti-inflammatory 15-epi-lipoxin A4 production. *Journal of Immunology*, 2008; 181 (5):3515-3523.

Tieu BC, Lee CY, Sun H, LeJeune WS, Recinos A III, Brasier A.R., Tilton RG. Cytokine production, proliferation, and responses to angiotensin II by aortic adventitial fibroblasts. To be submitted.

Tieu BC, Lee CY, Sun H, LeJeune WS, Recinos A III, Guo D-C, Milewicz D, Tilton RG, Brasier AR. IL-6 in the adventitia accelerates macrophage-mediated vascular inflammation leading to aortic dissection. Submitted to *Journal of Clinical Investigations*.

Abstracts

Tieu BC, Wang R, and Shih C. HBV Propagation: Evidence supporting transdifferentiation of pancreas to liver. Texas Academy of Internal Medicine Scientific Meeting Nov. 2003.

Tieu BC, Tilton R, Recinos A, and Brasier AR. A mechanism of vascular inflammation in diabetes. McLaughlin Colloquium Jan. 2006-Best Graduate Poster Award and Endocrine Society Annual Meeting Jun. 2006.

Tieu BC, LeJeune SW, Sun H, Lee CY, Lu M, Boldogh I, Tilton RG, Recinos A III, Brasier AR. Angiotensin II induces IL-6 expression and the Jak-STAT3 pathway in aortic adventitia of LDL receptor-deficient mice. Science Forum Jun. 2006-Best Graduate Poster Award.

Recinos A III, LeJeune SW, Sun H, Lee CY, Tieu BC, Lu M, Boldogh I, Tilton RG, Brasier AR. Angiotensin II induces IL-6 expression and the Jak-STAT3 pathway in aortic adventitia of LDL receptor-deficient mice. AHA National Meeting Oct. 2006.

Tieu BC, Tilton RG, Recinos A III, and Brasier AR. Role of adventitial fibroblasts in vascular inflammation. McLaughlin Colloquium Mar. 2007.

Uhegwu LN, Tieu BC, Sun H, Lee CY, Vergara LA, Brasier AR, Recinos A III. Angiotensin II-induced adventitial vascular inflammation in a mouse model of aortic aneurysm formation. Summer Medical Student Research Poster Session UTMB. Jun. 2007.

Tieu BC, Lee CY, Sun H, LeJeune WS, Recinos A III, Tilton RG, Brasier AR. Production of IL-6 in the angiotensin II-infusion mouse model of atherosclerosis and aneurysm. BMB orientation poster session. Sept. 2007.

Evans S, Tieu BC, Sun H, Lee CY, LeJeune WS, Brasier AR, Recinos A III.
Preliminary studies of NFκB transcriptional inactivation in a mouse model of angiotensin II-induced development of aortic aneurysms. Summer Undergraduate Research Program Poster Session. Aug. 2008. S. Evans-Best Poster Presentation Award.